BEST AVAILABLE IMAGES

Defective images within this document are accurate representations of the original documents submitted by the applicant.

Defects in the images may include (but are not limited to):

- BLACK BORDERS
- TEXT CUT OFF AT TOP, BOTTOM OR SIDES
- FADED TEXT
- ILLEGIBLE TEXT
- SKEWED/SLANTED IMAGES
- COLORED PHOTOS
- BLACK OR VERY BLACK AND WHITE DARK PHOTOS
- GRAY SCALE DOCUMENTS

IMAGES ARE BEST AVAILABLE COPY.

As rescanning documents *will not* correct images, please do not report the images to the Image Problem Mailbox.

Receipt is hereby acknowledged of the following:

(2)

Applicant: CORNETT, *et al.*
Serial No.: 09/783,580 **Docket No.** 023533/0113 -2
Filing Date: February 15, 2001
For: Recombinant β_2-Adrenergic Receptor Delivery and Use in Treating Airway and Vascular Diseases

1. Request for Continued Examination (RCE) Transmittal
2. Request for Reconsideration
3. Declaration with Exhibits A-C
4. Information Disclosure Statement
5. PTO SB/08
6. 8 References
7. Check # 31909 in the amount of $595.00

FILE IN MAILROOM

Date Due: 10/18/03
Today's Date: 10/18/03

Return to: JAHU/adm
Inspected by:

IN THE UNITED STATES PATENT AND TRADEMARK OFFICE

Attorney Docket No. 023533/0113

In re patent application of

CORNETT *et al.*

Serial No. 09/783,580

Filed: February 15, 2001

Group Art Unit: 1632

Examiner: Scott David Priebe

For: RECOMBINANT BETA2-ADRENERGIC RECEPTOR DELIVERY AND USE IN TREATING AIRWAY AND VASCULAR DISEASES

DECLARATION UNDER 37 CFR § 1.132

Commissioner for Patents
PO Box 1450
Alexandria, Virginia 22313-1450

I, Lawrence E. Cornett, hereby declare:

1. I am an inventor of the captioned application. I have worked in the field of adrenergic receptor structure and function, including how adrenergic receptor gene expression is regulated in mammalian tissues that are responsive to circulating catecholamines since 1977. I have published over 32 papers in this field. My curriculum vitae is of record in this application as it has been submitted with my previous declarations.

2. I have read and understood the Office Action dated December 22, 2003, and particularly the Examiner's comments on pages 3 and 4, regarding the alleged insufficiency of my previous declaration filed under 37 CFR 1.132 on October 16, 2003 for overcoming the lack of an enabling disclosure based on the Examiner's position in the Office Action dated January 15, 2003, and maintained in the Advisory Action dated May 22, 2003, in the above-identified application.

3. The Examiner states that my previous declaration dated October 16, 2003 did not contain Figure 1, cited as Exhibit B, which was discussed in my declaration. From a fair reading of my previous declaration, it is evident that Figure 1 (Exhibit B) was submitted with my declaration dated October 16, 2003. I herewith provide a copy of Figure 1, as Attachment 1, and assure the

Examiner that attached Figure 1 is the same as Figure 1 referenced as Exhibit B in my previous declaration.

4. In response to the Examiner's comments that the evidence presented in my previous declaration dated October 16, 2003, is only peripherally related to "...whether the claimed method can be used to treat asthma or some other undisclosed airway disease," I would like to provide further explanation and clarification of the experimental data depicted in Figure 1 and provide additional data and comments to support my position that the claimed method can be used to introduce the β_2AR gene into airway cells which is expressed.

5. I refer you to my declaration dated October 16, 2003, ¶3 but as a courtesy, I again provide my previous statement regarding experimental data not provided and data provided in Figure 1 below:

> Twenty, adult Sprague Dawley rats at stable weights of ~400g were divided into 5 groups (n = 4 per group) based on treatment: Group 1 - saline treatment via endotracheal bolus; Group 2 - AAV2 treatment via endotracheal bolus; Group 3 - AAV2 treatment via endotracheal nebulization; Group 4 - AAV1 treatment via endotracheal bolus; and Group 5 - AAV1 treatment via endotracheal nebulization. AAV1 and AAV2 represent two different serotypes of AAV and, currently there are six known AAV serotypes. Nebulization was performed in-line with the ventilator using the Aeroneb Lab device (provided by Aerogen, Inc.). A total of 240 µl of vector containing the human -β_2AR gene (AAV-β_2AR/EGFP) or saline was delivered to the airway in 80 µl aliquots followed by ventilation for 5 minutes and rotation of the animal between each delivery to maximize distribution. Eighteen animals completed the study. One saline control animal expired after baseline measurement due to tracheal puncture, and one AAV1 animal was eliminated due to anesthesia issues at follow-up. All other animals were recovered after the first data collection and completed second data collection. Mean body weight was 421g at baseline and was 455g 4 weeks after treatment, representing a 9% change in body weight over the 4 week study period.
>
> Respiratory function was measured, using the FlexiVent System (SCIREO, Montreal, Quebec, Canada) before, and at 4 weeks after gene delivery for changes in lung function, including change in airway dynamic resistance (representing total airway resistance)

> and for change in Newtonian resistance (a measure of central airway resistance). Because it minimizes ventilator dead space, the FlexiVent System is a superior method to obtaining flow measurements in small animals compared to the more traditional methods using pneumotachographs. After 4 weeks, all treatment groups showed a modest fall in dynamic airway resistance (data not shown), but with no statistically significant differences between treatment groups. The modest drop in airway dynamic resistance likely reflects the modest change in airway size with slight increase in weight and airway diameter. The central airway resistance measurements in AAV-β_2AR treated rats and control-rats are presented in Figure 1 (Exhibit B). Both the AAV2 nebulization group (Group 3) and AAV1 nebulization group (Group 5) demonstrate a fall in Newtonian resistance in 3 of 4 rats in Group 3 (See Figure 1, *Panel B*) and in 3 of 3 rats in Group 5. (See Figure 1, *Panel C*). In the 3 control animals, there was no consistent change in Newtonian resistance over the 4 week period of the study (See Figure 1, *Panel A*). Animals treated with AAV1 or AAV2 via bolus showed no significant change in resistance (data not shown).

6. In particular the Examiner's criticisms of the data presented in ¶3 in my October 16, 2003 declaration, appear to be concerned with the fact the summary of the results are based on the administration of AAV-β_2AR to normal rats and that "...only a 'modest fall in dynamic airway resistance' was observed..." I wish to clarify the summarized data that was not shown in Figure 1 by that was characterized as "modest"by firstly stating that two different measurements of airway resistance were assessed and summarized above. Specifically, the rats' respiratory function was measured using the FlexiVent System before and at 4 weeks after gene delivery for (1) change in lung function, including change in airway dynamic resistance (representing total airway resistance including the trachea down to the smallest airways), and (2) change in Newtonian resistance (representing a measure of central airway resistance). In my previous declaration, I stated that:

> [a]fter 4 weeks, all treatment groups showed a modest fall in dynamic airway resistance (data not shown), but with no statistically significant differences between treatment groups. The modest drop in airway dynamic resistance likely reflects the modest change in airway size with slight increase in weight and airway diameter.

This summary reflects measurements of the dynamic airway resistance, which includes the component of resistance due to elastic forces within the tissue. Dynamic airway resistance quantitatively assesses the level of constriction in the lungs and is based on the Linear First-Order Single Compartment Model, which is a standard model of respiratory mechanics. However, using the Constant Phase Model, which is an advanced model of respiratory mechanics, it is possible to distinguish between central and peripheral respiratory mechanics. The Newtonian resistance parameter, also measured in our study, represents the resistance of the central airways, with the tissue component removed. It is well known that the central airways, as opposed to smaller, peripheral airways are of more significance in determining overall airway resistance in both non-asthmatic as well as the asthmatic lung (See Attachment 2 - Leff, AR and Schumacker, PT. Respiratory Physiology: Basics and Applications, W.B. Saunders Company, Philadelphia, 1993, pp. 24-46), and therefore are the more important targets for asthma treatments that relieve bronchoconstriction. Further, this latter measurement more directly reflects airway diameter. So, it is my opinion that the Newtonian resistance is the preferred measurement since it more directly reflects airway diameter because the tissue component of lung resistance is fairly constant except in certain diseases (fibrosis) where the lung becomes "stiff" and consequently difficult to move. Asthma is an obstructive airway disease manifested by airway narrowing. Newtonian resistance measures the resistance of the airways and consequently is the best measure of the status of the airways following delivery of medications that should benefit the asthmatic airway.

In my October 16, 2003 declaration, I summarized the Newtonian resistance measurements depicted in Figure 1 (herein Attachment 1) as follows:

> The central airway resistance measurements in AAV-β_2AR treated rats and control-rats are presented in Figure 1. Both the AAV2 nebulization group (Group 3) and AAV1 nebulization group (Group 5) demonstrate a fall in Newtonian resistance in 3 of 4 rats in Group 3 (See Figure 1, Panel B) and in 3 of 3 rats in Group 5. (See Figure 1, Panel C). In the 3 control animals, there was no consistent change in Newtonian resistance over the 4 week period of the study (See Figure 1, Panel A). Animals treated with AAV1 or AAV2 via bolus showed no significant change in resistance (data not shown).

Figure 1 provides data to support this summary and shows that the administration of the AAV-β_2AR to rats (Group 3 – Panel B and Group 5 – Panel C) as compared to control untreated rats (Panel A) results in decreased central airway resistance, thus showing an increase in central airway dilation In my opinion, this data demonstrates that the expression of AAV-β_2AR is responsible for the measured decreased central airway resistance and increased airway diameter.

7. It also is my opinion that rodents are reliable models to study human lung diseases. In support of my position, I provide a copy of Gomes *et al.*, as Attachment 3, which reports the results of studying the respiratory system mechanics of mice, rats, guinea pigs and rabbits and provides technical explanations for determining airway function in rodents. Gomes *et al.* concludes that the rodents that they "...studied had respiratory mechanics that scaled according to body weight (BW) in a similar fashion to that reported in other species"...and that .. "[t]his suggests that the lungs of the rodents that we studied differ from those of larger species essentially only in terms of scale, which supports their validity as general-purpose models of the human lung." (See 1st column on page 915).

8. In the Office Action of December 22, 2003, the Examiner accepts the data presented in previously submitted Figure 2, attached to my October 16, 2002 declaration, as evidence "that some airway cells had been transfected, and expressed the human β_2AR encoded by the AAV vectors." However, the Examiner criticizes the results presented in ¶4 of my October 16th declaration by stating that the data "simply verifies that some airway cells had been transfected, and expressed the human -β_2AR encoded by the AAV vectors.... and that there is no evidence that the 'modest' effect would be therapeutic in the treatment of asthma, and more importantly, that one would be able to transfect airway epithelium in asthmatics to produce even the 'modest' effect observed for the normal rats." I again refer to the results obtained with the immunohistochemistry experiments shown in Figure 2, previous Exhibit C as providing evidence that there is a distribution of target protein expression of both EGFP and human β_2AR between treatment groups, 4 weeks after treatment with AAV1 using nebulization (Figure 2, upper panels) and AAV2 using nebulization (Figure 2, center panels) of both EGFP and human β_2AR expression as compared to saline treated animals (Figure 2, bottom panels). Saline treated animals showed no EGFP or human β_2AR expression.

In regard to the Examiner's position that these results represent a modest effect, it is my opinion that for therapeutic effect it is not necessary to infect every airway epithelial cell. In support of my position, I direct the Examiner to the specification (p. 4 and Figure 2, also submitted with my previous declaration, herein Attachment 4), where the role of airway epithelial cells in mediating a relaxing effect on airway smooth muscle is discussed. Airway epithelial cells when stimulated by beta agonists are hypothesized to release a factor that acts on airway smooth muscle to cause relaxation. So, increased release of this relaxing factor by one airway epithelial cell would be expected to impact many airway smooth muscle cells in the immediate area.

9. In further support of the enablement of the claimed method to decrease airway resistance in an asthma model, I provide the results of another study which utilized allergen-sensitized Brown-Norway rats. Specifically to assess changes in β_2AR expression and airway responsiveness after AAV-β_2AR nebulization delivery, Brown-Norway rats were allergen sensitized and response to methacholine challenge was assessed at 4 weeks. Methacholine is an airway constrictor. Saline-treated controls (n=4) were compared to AAV-β_2AR (n=4) infected animals. Ovalbumin acts as an allergen and makes the rats' lungs asthma-like, e.g., constricted with inflammatory infiltrates. Evidence for allergen sensitization was confirmed during weekly ovalbumin aerosols in which animals developed dyspnea, retractions and gagging that resolved with aerosol cessation. The inflammatory response was assessed in adjacent sections stained with hematoxylin and eosin by a pathologist blinded to treatment. Two control and 3 AAV treated animals completed the study. One control expired during pre-treatment lung function, and another has persistent seizure activity induced by sedation, while one AAV rat expired during methacholine challenge. All three AAV-β_2AR treated animals showed decreased resistance and elastance when compared to the two controls during methacholine challenge dosing. As resistance falls at a constant ventilation pressure (PEEP), more gas flows to additional lung segments resulting in increased compliance due to over-distention.

Airway resistance is measured in ovalbumin-sensitized Brown-Norway rats treated with saline or infected with AAV-β2AR, and attached herewith as Figure 3 (Attachment 5) plots airway resistance during increasing methacholine challenge from one representative animal in each group (control, closed circles; AAV, open circles) beginning 4 weeks after infection

(baseline) and during methacholine challenge (0.325-6.25 mg/ml) to the end point of greater than 200% R. Point of recovery to 80% of baseline R is shown. The data show that the AAV-β_2AR treated animals were less responsive to methacholine suggesting that these animals' airways were dilated more compared to the control animals. Based on these results, it is my opinion that the observed increased dilation of the airways was due to overexpression of the AAV-β_2AR in these animals.

10. In further support of the validity of above allergen-induced bronchial hyperresponsiveness in sensitized Brown-Norway rats, I enclose a copy of Elwood *et al.*, (Attachment 6), discussed on page 34 of the present specification, and as noted therein, ...[t]he "sensitized Brown-Norway rat is considered a reasonable approximation of the state of airways in atopic asthma." This publication is one of many scientific publications that utilize an ovalbumin-sensitized Brown Norway rat as a model system to study the asthmatic lung. This publication also supports the use of a methacholine challenge to determine the state of the airways (e.g., airway diameter by measuring Newtonian resistance).

11. Additionally, a publication from McGraw *et al.* , 2000 (already of record in the application but provided here as a courtesy to the Examiner as Attachment 7) investigated lung function in transgenic mice that overexpress the β2AR and thereby shows a correlation between airway dilation and asthma therapy. This publication demonstrates using transgenic animals (the transgene is the β_2AR gene driven by a Clara cell promoter and the authors determined that the transgene was expressed at high levels in airway epithelial cells) that overexpression of the β_2AR in airway epithelial cells is protective against the constricting effect of methacholine on airways. This is the same result that we obtained using Brown-Norway rats in our Figure 3 (Attachment 5) that had been treated with the virus.

12. I also have considered the Examiner's comments that Orkin, Factor and Demoly raise issues that reporter gene studies are not predictive of therapeutic success and that studies of asthmatic lungs and the delivery of genes to them via vectors support the unpredictability of the outcome of treating airway diseases. The Examiner further states that the prior art represented by Orkin, Factor and Demoly disclose the unpredictability of the study of the asthmatic lung, and

thus uses this premise to criticize the data presented herein as not being indicative of therapeutic effect in treating asthma. In response to this position, I refer the Examiner to Gomes *et al.* (Attachment 2), discussed above, that provides a good discussion of measuring airway resistance in small animals. Again, the Examiner is directed to the last sentence of this publication in the 1st column on page 915 that concludes after performing the experiments that "...the lungs of the rodents that we studied differ from those of larger species essentially only in terms of scale, which supports their validity as general-purpose models of the human lung."

But an important consideration in regard to the "known issues" disclosed in Factor, Orkin and Demoly is that when these articles were written (and this still holds true today in large part), most scientists thought of gene therapy as providing cells/organisms that have a defective copy of an essential gene with a "good copy" of a that gene. This line of thinking requires that the defective gene be known since that is the only way one can provide a normal copy of the gene. This is the case for example, for cystic fibrosis, in which the defective gene is known as well as the precise mutations, e.g., the CFTR protein. Conceptually, it becomes straightforward to make a normal copy of the gene and deliver it to the afflicted cell/organism. Factor, Orkin and Demoly discuss using gene therapy strategies to treat asthma at a time when the "defective gene" underlying asthma was not known and it still is not known. So it is my opinion that this premise explains why these authors were so negative about the prospects of using gene therapy to treat asthma.

But what must be considered here is that while what the present invention is directed to is "gene therapy," it is not providing a normal copy of a gene to an organism that has a defective copy. But rather, what the present invention discloses is actually a "gene augmentation therapy" which provides a method to increase the amount of gene product (β2AR) that is a therapeutic target in asthma, and thereby increases the airway relaxing effect of both endogenous catecholamines and bronchodilator medicines.

In support of my position, Dr. Factor discloses in Factor (2001), page 518, paragraph bridging the 1st and 2nd columns, "another gene therapy approach to asthma" that may include the "development of supportive therapies that reduce airway resistance by either improved bronchodilation ..." Dr. Factor cites the McGraw publication (Attachment 7) discussed in paragraph 11, above, and describes his own preliminary data "...that adenoviral-mediated overexpression of a β2AR in the bronchial epithelium of normal mice attenuates methacholine-

induced bronchospasm by increasing sensitivity to endogenous catecholamines." Dr. Factor has published a review paper in 2003, Attachment 8, where he reiterates the information from his 2001 publication under the heading of "Supportive Approaches" and indicates that he has published his preliminary data showing that the overexpression of β2AR in normal mice attenuated methacholine-induced bronchospasm (see citation [26]). I therefore interpret Dr. Factor's comments as supporting the enablement of the claimed invention.

13. I hereby declare further that all statements made herein of my own knowledge are true and that all statements made on information and belief are believed to be true and further that these statements were made with the knowledge that willful false statements and the like so made are punishable by fine or imprisonment, or both, under Section 1001 of Title 18 of the United States Code and that such willful false statements may jeopardize the validity of the application or any patent issuing thereon.

By: _____ Date: 4/22/04
Lawrence E. Cornett, Ph.D.

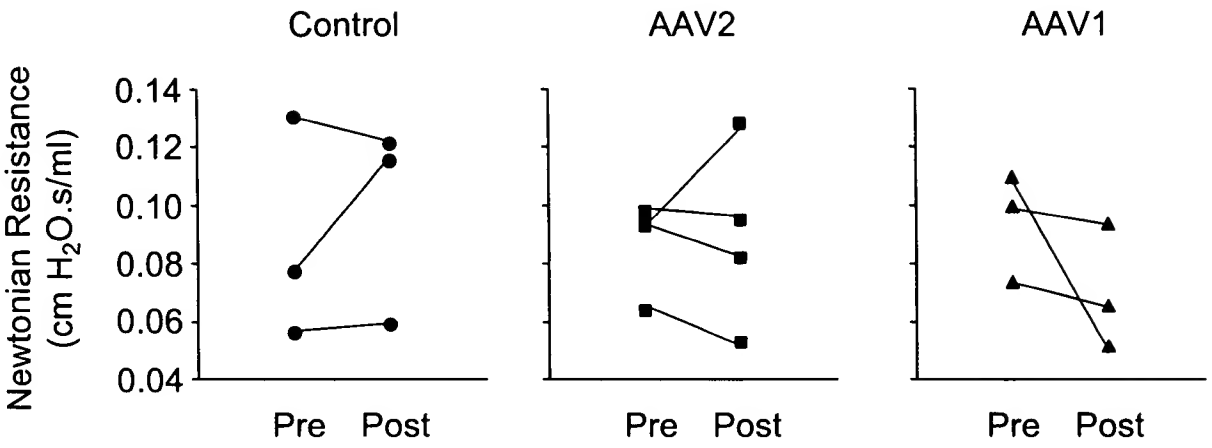

FIGURE 1

In: Leff AR and Schumacker PT Respiratory Physiology Basics and Applications W.B. Saunders Co. Philadelphia, 1993

Chapter 2

Lung Mechanics: Dynamics

Air is a fluid, and the principles that govern its movement in and out of the lung are those of *fluid dynamics*. Dynamics is that aspect of mechanics that studies physical systems in motion. By application of Newton's law of motion, the mechanisms that affect the flow of air into and out of the lung in health and in diseases are defined.

APPLICATIONS OF FLUID MECHANICS

Flow Regimens in Airways

Fluid flow will occur along a rigid tube when a hydrostatic pressure difference exists between one end of the tube and the other. In airways, gas flow will occur when a pressure difference exists between one point along the airway and another, as long as the airway is open and a free path for gas flow exists. When a fluid flows along a tube, the *average velocity* (speed, in cm/sec) can be calculated by dividing the overall flow rate (ml/sec) by the cross-sectional area of the tube (cm^2).

Fluid movement can be *laminar* or *turbulent* or may have characteristics intermediate between these two extremes (Figure 2–1). In laminar or stream-lined flow, the fluid traveling at the center of the tube moves most rapidly, while the fluid in direct contact with the tube wall remains stationary. If water flows down a pipe under laminar conditions, a small stream of ink injected at the center of the pipe will tend to stay at the center of the flow stream as it travels down the tube. Another stream of ink injected between the center of the pipe and the wall will also travel in a straight line but will move down the pipe more slowly. One way to imagine this is to think of the fluid as if it were composed of a series of concentric tubes sliding past

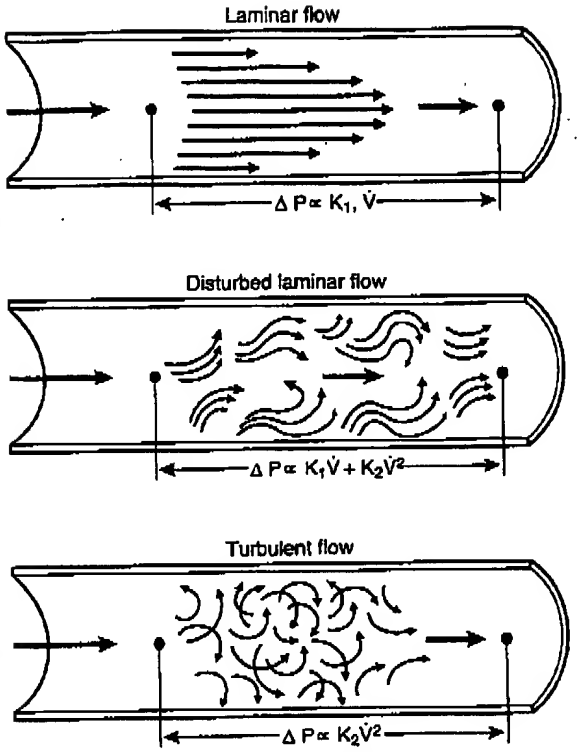

Figure 2–1. Laminar, disturbed, and turbulent flow conditions. All flow travels parallel to the axis of the tube under laminar flow conditions. Fluid at the center of the tube moves at a higher velocity than flow near the tube boundary. Eddies and vortices disrupt the flow pattern in turbulent flow states. Although net movement of fluid occurs along the tube, turbulent eddies generate flows perpendicular to the tube axis. This process consumes energy, causing a steeper drop in pressure along the tube than in laminar flow regimens. In disturbed laminar flow, characteristics of both laminar and turbulent flow are present.

each other, much like a radio aerial being pulled out. Because the fluid velocity decreases with the square of the radial distance away from the center of the tube, laminar flow is said to have a *parabolic* velocity profile. In laminar flow regimens, the *average* fluid velocity in the tube is half of the *peak* velocity seen at the center of the tube. Laminar flow does not begin at the entrance of the pipe, since the fluid must travel some distance down the pipe for laminar flow conditions to become fully established.

In *marginally laminar* or *disturbed* flow, characteristics of both laminar and turbulent flow can be seen. Flow is generally laminar, but eddies are generated at sites where the tube narrows or branches or changes dimensions or where irregularities in the tube surface are encountered. This flow regimen is similar to the pattern of eddies seen as water vapor rises above a cup of hot tea.

In *fully turbulent* flow, fluid movement occurs both in *radial* (i.e., perpendicular to the axis of the tube) and *axial* directions. Although fluid in contact with the tube wall still remains stationary, the velocity profile across the tube is much more blunt than the parabolic profile seen in laminar flow; there is less variation in fluid velocity as a function of radial position in the tube. Because fluid moving in a radial direction can impact on the tube wall, noise is often generated in turbulent flow states. Since energy is consumed in the process of generating the eddies and chaotic fluid movement, a higher driving pressure is required to support a given flow rate under turbulent as opposed to laminar flow conditions, other factors remaining the same.

Under laminar flow conditions, the pressure difference between two points along a tube is directly proportional to the flow rate:

$$\Delta P = k_1 \cdot \dot{V}$$

where ΔP is the pressure difference (cm H_2O), k_1 is a resistive constant for the system (cm $H_2O \cdot$ sec/ml) and $\dot{V}$ is flow rate (ml/sec). (Note that the dot above the $\dot{V}$ signifies *change in volume with respect to time*, i.e., flow rate). Stated alternatively, the driving pressure (ΔP) along a tube must be doubled to double the flow rate during laminar flow. In turbulent flow conditions, the pressure difference between two points along the tube increases with the square of the flow rate. Thus, doubling the flow under turbulent conditions requires more than a doubling of the driving pressure, since some of the fluid moves perpendicular to the axis of the tube. The relationship between driving pressure and flow for a turbulent system can be approximated by:

$$\Delta P = k_2 \cdot \dot{V}^2$$

where ΔP is the pressure difference, k_2 is a constant for the system, and $\dot{V}$ is flow. Thus, there is a linear relationship between pressure and flow under laminar conditions and a nonlinear relationship under turbulent conditions. Figure 2–2 shows this relationship graphically. During tidal breathing, fluid flow is highly turbulent in the trachea, is less turbu-

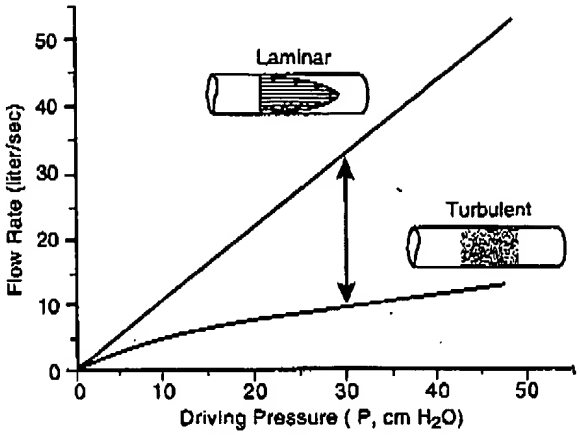

Figure 2–2. Relationship between driving pressure and flow through a pipe under laminar and turbulent flow conditions. During laminar flow, an increase in the driving pressure produces a proportionate increase in flow rate. In turbulent flow states, the same increase in pressure augments flow to a lesser degree, since some of the increase in driving pressure moves fluid in a direction perpendicular to the tube axis.

lent in smaller bronchi, and finally becomes laminar-like in the small peripheral airways. Therefore, the total pressure drop that occurs between alveoli and the mouth during inhalation includes some contribution from laminar-like flow plus some contribution from turbulent flow regimens. This can be approximated using the following relationship:

$$\Delta P \approx k_1 \cdot \dot{V} + k_2 \cdot \dot{V}^2$$

This equation states that the total pressure difference between an alveolus and the mouth (ΔP) is the sum of the pressure drop encountered in laminar flow regions (small airways) and in turbulent flow regions (larger airways).

Reynolds Number and Turbulent Flow

It is possible to predict whether flow in a system will tend to be laminar or turbulent by calculating the *Reynolds number* (Re).

$$Re = \frac{(D \cdot u \cdot \rho)}{\eta}$$

where ρ is the density of the fluid (g/ml), D is the diameter of the tube or airway (cm), u is the average velocity (cm/sec), and η is the viscosity of the fluid (g/[sec · cm]). Reynolds number is a dimensionless value because it expresses the ratio of two dimensionally equivalent terms (kinematic/viscous). For any fluid, flow generally tends to be turbulent when Re is greater than 2000 and laminar when Re is less than 2000, although this is only an approximation.

During normal tidal breathing, gas flows of 1 liter/sec are common at the mouth. In an adult trachea with a diameter of 3 cm, this will produce tracheal gas velocities of about 150 cm/sec. Since air has a density of about 0.0012 g/ml and a viscosity of 1.83×10^{-4} g/(sec · cm), the calculated Reynolds number in a trachea with diameter of 3 cm (more than 2000) indicates that flow in the trachea is highly turbulent even during quiet breathing. The open glottis and the vocal cords introduce mechanical obstructions that further promote the tendency to develop turbulence. However, since the total cross-sectional area of the airways expands enormously from the central to the peripheral regions of the lung, gas velocities decrease significantly in the more distal (i.e., toward the alveoli) airways. This greatly lessens the tendency for flow to be turbulent in the lung periphery, even during maximal ventilation. The increase in total cross-sectional area of the airways toward the lung periphery has been compared with the shape of a thumbtack (Figure 2–3). Because the individual airways decrease in diameter toward the lung periphery, the tendency for turbulent flow to occur is even further reduced. Therefore, the flow regimens in the lung are highly turbulent in the larger airways but never turbulent in the small distal airways.

RESISTANCE TO AIRFLOW

Pressure–Flow Relationships in Airways

When flow in a tube is laminar, there is a linear relationship between driving pressure and flow (see Figure 2–2). Flow is set both by the driving pressure applied and the *resistance* to flow in the system. Under laminar conditions:

$$\dot{V} = \frac{\Delta P}{R}$$

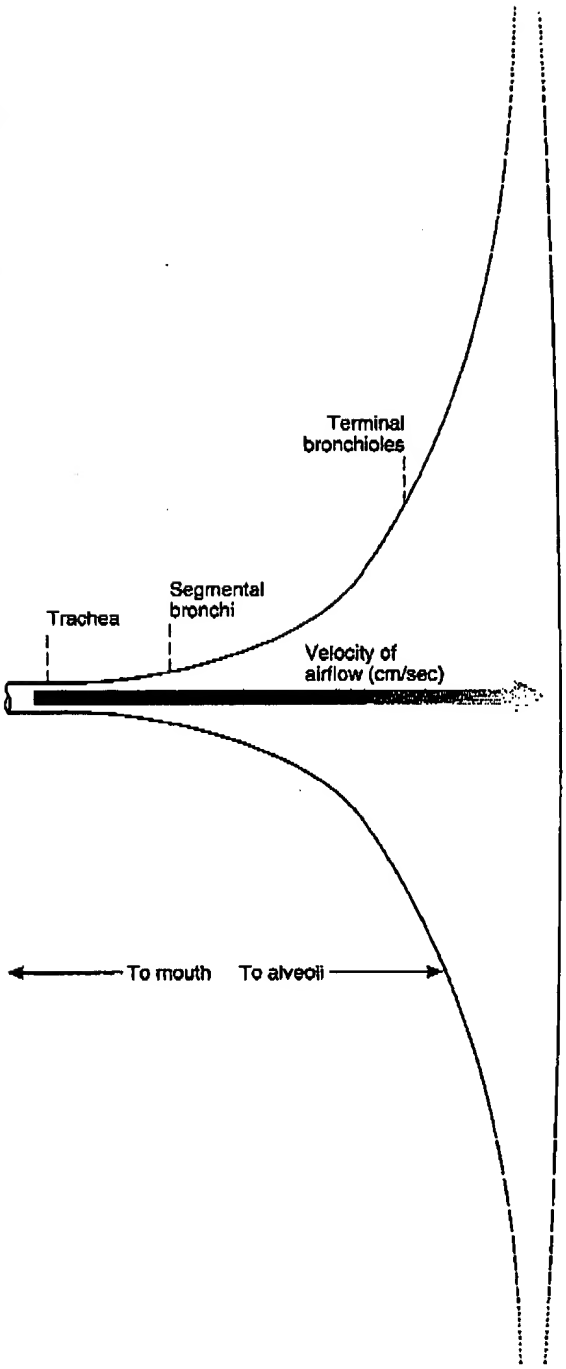

Figure 2-3. Total airway cross-sectional area as a function of distance into the lung. Although the diameters of individual airways become smaller toward the lung periphery, the number of airways increases dramatically. Accordingly, the total airway cross-sectional area increases markedly toward the alveoli and gas velocities decrease.

where $\dot{V}$ is flow, ΔP is driving pressure from one end of the system to other, and R is resistance over the same distance. As driving pressure increases, flow increases proportionally as long as resistance in the system remains constant. In other words, the resistance to flow is defined as the pressure difference required to maintain a given flow rate through a system.

Poiseuille's law defines the relationship between flow and pressure in a tube with fixed dimensions, under *laminar* flow conditions:

$$\dot{V} = \frac{(\Delta P \cdot \pi \cdot r^4)}{(8 \cdot \eta \cdot L)}$$

where ΔP is the pressure drop along a tube, $\dot{V}$ is the flow rate, η is the fluid viscosity, L is the length of the tube, and r is the tube radius. From the above equation, the resistance term is represented by the following equation:

$$\text{Resistance} = \frac{8 \cdot \eta \cdot L}{\pi \cdot r^4}$$

Note that for any given fluid, the pressure difference required to drive a given flow rate is directly proportional to the length of the tube but is inversely proportional to the fourth power of the radius of the tube. Thus for a given driving pressure difference, doubling the length of the tube will halve the flow rate, whereas halving the tube diameter will decrease the flow 16 times under laminar flow conditions. Stated differently, the resistance is inversely proportional to the radius raised to the fourth power but directly proportional to the length of the tube and the viscosity of the fluid. Clearly, the tube radius is the dominant factor in determining the resistance to flow.

Airflow Velocity

Flow in a tube possesses energy in two different forms. *Kinetic energy* is that part of the total energy associated with bulk movement of the fluid and is related to the density of the fluid (ρ, in g/ml) and the square of the average velocity (u^2):

$$\text{Kinetic energy} = \tfrac{1}{2}\, \rho u^2$$

The second form of energy is *potential energy*, and in airways the hydrostatic pressure is the major component of this. The *total energy* of the fluid flow is the sum of the potential and kinetic energy components. As fluid travels along a pipe, frictional resistance decreases the total energy of the flow. This is seen as a decrease in the pressure component of the total energy (i.e., the hydrostatic pressure decreases along the tube, reflecting frictional loss of pressure energy). If the velocity of the flow changes along the tube, then a greater proportion of the total energy is converted from potential (pressure) to kinetic energy. This concept is demonstrated in Figure 2–4, which illustrates the events that occur as a fluid flows along a tube whose diameter narrows. In this figure, a gas flow of 1 liter/sec travels down a tube with a diameter of 3 cm and a cross-sectional area of 7.06 cm^2. At a point along the tube, the diameter tapers to 2.1 cm, so that the area (3.53 cm^2) is half of the original area. Since the average velocity (cm/sec) of gas in the tube is calculated by dividing the flow rate (cm^3/sec) by the area of the tube (cm^2), the fluid must accelerate from 140 cm/sec to 280 cm/sec as it enters the narrow section. The energy used to accelerate the fluid comes from the potential (pressure) energy. Hence, the hydrostatic pressure falls within the narrow portion of the tube because the kinetic energy has increased at the expense of the pressure energy component. At the end of the narrow segment the fluid decelerates and the veloc-

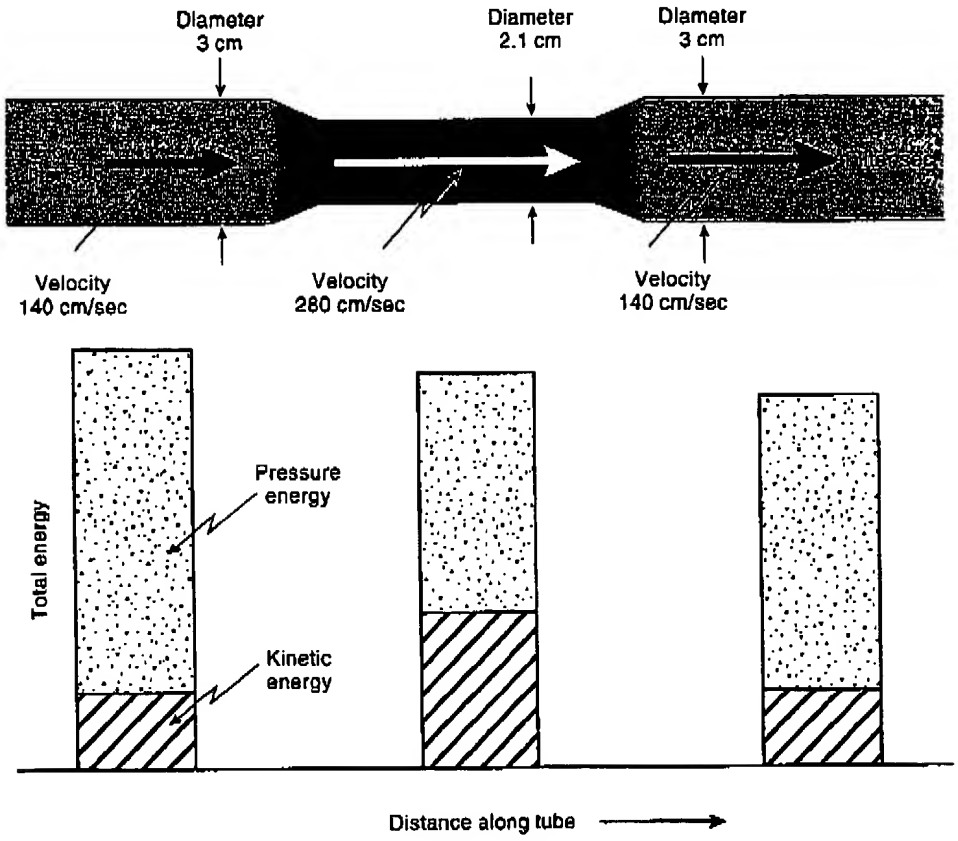

Figure 2–4. The Bernoulli principle. When a fluid moves through a tube at a constant flow rate, the total energy of the fluid (potential energy + kinetic energy) decreases because frictional losses convert some of the energy into heat. Increases in fluid velocity occur where the tube narrows, causing an increase in the kinetic energy component ($\frac{1}{2} \rho u^2$) at the expense of potential energy (pressure decreases). When the tube widens again, the fluid decelerates and kinetic energy is converted into pressure energy.

ity of flow decreases. The corresponding loss in kinetic energy is converted back to pressure energy, so the hydrostatic pressure rises. As all of this occurs, there is still a progressive loss in the total energy of the fluid along the tube, because resistive losses cause the conversion of some of the energy into heat. At the exit of the tube, the kinetic energy component is the same as was present at the start of the tube, because the velocities are the same. However, the total energy is reduced because the pressure component is smaller. The key point to remember is that when velocity speeds up because a tube narrows, the hydrostatic pressure decreases as a result. This phenomenon is referred to as the *Bernoulli effect*. Note from Figure 2–2 that during an exhalation, gas velocity must increase dramatically as flow travels toward the trachea, because the total airway area decreases. This causes the hydrostatic pressure to fall within the airways, an effect that becomes very important during forceful exhalations (discussed later).

The Respiratory Cycle

Exchange of oxygen and carbon dioxide between alveolar gas and pulmonary capillary blood occurs as these gases move passively (i.e., *diffuse*) from regions of higher *partial pressure* to regions of lower partial pressure. To maintain the partial pressure differences driving diffusion in the alveoli, the heart must continually pump blood through the pulmonary circulation and the respiratory system must continually deliver fresh gas to the alveoli. Moreover, blood flow and alveolar ventilation must be adjusted to accommodate a wide range of metabolic rates, ranging from resting states to maximal exercise.

The *minute ventilation* is the volume of gas breathed per minute. This involves the bulk (convective) movement of air into and out of the lungs. Ventilation is normally achieved by periodic breathing or *tidal ventilation*. During inhalation, the diaphragm and the inspiratory muscles of the chest wall shorten, causing the diaphragm to move downward and the chest wall to move upward and outward. This process lowers the hydrostatic pressure in the pleural space by expanding the chest volume. Since the lungs are not rigid structures, the decrease in pleural pressure is transmitted across the visceral pleural surface into the lungs, causing alveolar hydrostatic pressure to fall. When alveolar pressure becomes less than ambient pressure, gas flows into the lungs (assuming that the glottis and airways are open) until the alveolar hydrostatic pressure rises to the ambient pressure. At this point (end-inspiration), the hydrostatic pressure difference between alveolar gas and ambient air is zero, so inspiratory flow ceases. Note also that at end-inspiration the force generated by the contracting inspiratory muscles equals the elastic force generated by the lungs and chest wall. At the beginning of exhalation, the diaphragm and other inspiratory muscles relax. This causes the hydrostatic pressure in the pleural space to increase, as the elastic (potential) energy stored in the lung and chest wall and abdomen begin to compress the thoracic contents. Once again, the change in pleural hydrostatic pressure is transmitted across the visceral pleura to alveolar gas, causing its pressure to rise above the ambient pressure. If the airway remains open, gas flows out of the lung until alveolar pressure decreases to equal ambient atmospheric pressure.

Figure 2–5 details this sequence of events that occur during a single breath, assuming that the airway and glottis remain open throughout. First, consider the situation existing at the instant before the breath begins (point A in Figure 2–5). At this point, inspiratory and expiratory muscles are relaxed, so the lung is at end-expiratory volume (i.e., functional residual capacity [FRC]). At that point, airflow is absent because alveolar pressure is equal to ambient atmospheric pressure (i.e., no pressure gradient between alveoli and atmospheric exists). Pleural pressure is -7.5 cm H_2O at point A, so *transpulmonary pressure* (P_{tp}) (i.e., the transmural pressure for the lung, defined as alveolar [P_{alv}] minus pleural pressure [P_{pl}]) is:

$$P_{tp} = P_{alv} - P_{pl} = 0 - (-7.5)$$

$$= +7.5 \text{ cm } H_2O.$$

Transmural pressure for the chest wall at point A would then be:

$$P_{\text{trans-chest wall}} = P_{pl} - P_{\text{atmospheric}}$$

$$= (-7.5) - 0 = -7.5 \text{ cm } H_2O.$$

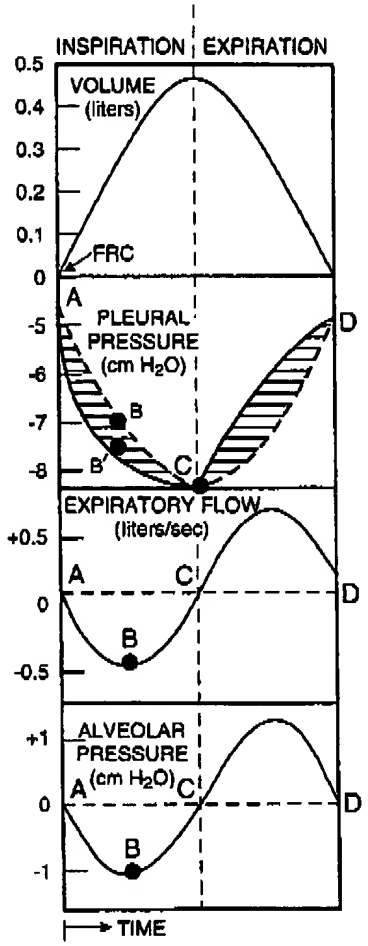

Figure 2–5. Changes in pleural and alveolar pressures during a tidal breath. Note that whenever lung volume is not changing with time, lung volume is determined by transpulmonary pressure. See text for further explanation. (Adapted and redrawn from West JB: Respiratory Physiology: The Essentials, 4th ed. © 1985, the Williams & Wilkins, Co., Baltimore.)

The positive transmural pressure for the lung indicates that the lung is being held open at FRC by a positive distending pressure. By contrast, the negative resting transmural pressure for the chest wall at FRC indicates that the chest wall is being pulled in by a negative distending pressure. The negative pleural pressure at FRC reflects a balance between this tendency for the lung to collapse toward a smaller volume and the tendency for the chest wall to spring out to a larger volume. Stated differently, FRC is defined as the lung volume at which the negative transmural pressure for the relaxed chest wall (-7.5 cm H_2O) matches the positive transmural pressure for the lung ($+7.5$ cm H_2O) (see Chapter 1). At these matching transmural pressures, both the lung and the relaxed chest wall have the same volume (an anatomical necessity).

At the start of inhalation, the diaphragm and other inspiratory muscles shorten, causing chest volume to expand and pleural pressure to decrease. The decrease in pleural pressure is transmitted through the lung visceral pleura to the alveolar space, causing alveolar pressure to decrease. Approximately halfway through inspiration (point B in Figure 2–5) the inspiratory flow rate is maximal because alveolar pressure is maximally negative. At end-inspiration (point C), alveolar pressure again rises to ambient pressure and so inspiratory flow ceases. At that instant, pleural pressure is about -11 cm H_2O, so transmural pressures are:

$$P_{tp} = P_{alv} - P_{pl} = 0 - (-11)$$

$$= +11 \text{ cm } H_2O.$$

This higher static transpulmonary pressure is associated with a lung volume that is about 500 ml above FRC. Transmural pressure for the chest wall at point A would then be:

$$P_{\text{trans-chest wall}} = P_{pl} - P_{\text{atmospheric}}$$

$$= (-11) - 0 = -11 \text{ cm } H_2O.$$

Note that the transmural pressure for the chest wall is more negative, yet the thoracic volume is larger! This occurs because the respiratory muscles are contracting, thereby dramatically altering the mechanical properties of the chest wall relative to its relaxed (i.e., passive) pressure–volume relationship.

During exhalation, the cycle is reversed and lung volume returns from end-inspiration to FRC. This is associated with a return of pleural pressure from -11 cm H_2O to -7.5 cm H_2O. At point D, the conditions of physiological equilibrium at FRC

again are established as at point A and the cycle is completed.

Lung Resistance

The pleural pressure curve AB'C (see Figure 2–5) represents the change in pleural pressure seen during tidal breathing. The dashed line ABC represents the pleural pressure curve that *would have been required* to inflate the same lung very slowly; that is, it reflects the pressure–volume relationship of the lung obtained under quasi-static conditions. Note that during a normal inspiration, pleural pressure transiently becomes more negative (AB'C) than it would during a very slow inflation (ABC). Likewise, during exhalation pleural pressure transiently rises above the level that would occur during a very slow exhalation.

The difference between curve ABC and curve AB'C represents the additional pressure necessary to overcome the resistance encountered while *changing* lung volume. This impedance to changing lung volume is termed *lung resistance.* Note that when lung volume is not changing with time (i.e., at end-inspiration or end-expiration), the transpulmonary pressure is identical to what would occur during a static lung inflation to that volume. While lung volume is changing, the additional pleural pressure required to overcome lung resistance depends on how fast the lung volume is changing. Thus, to decrease lung volume rapidly, a larger increment in pleural pressure is required than would be needed to decrease lung volume slowly. Two factors contribute to this lung resistance. Part of the lung resistance arises from the pressure drop created by gas flow in the airways, as gas enters or leaves the lung *(airways resistance).* One component of the airways resistance is due to *frictional resistance* to airflow. Another part is due to the *acceleration* (or deceleration) of gas to a higher (or lower) velocity as it moves away from (or toward) the lung periphery as a result of the changing total cross-sectional area (see Figure 2–2). The second factor contributing to lung resistance reflects the viscous impedance encountered in changing lung volume, separate and apart from the gas flow resistance *(viscous contribution).*

This situation is somewhat analogous to inflating and deflating an old fireplace bellows equipped with a spring (Figure 2–6). Inflating the bellows very slowly requires an increasing force to overcome the elastic pull of the spring (static lung recoil). Inflating the bellows more rapidly *requires an additional force at any given volume,* owing to the bellow's resistance to changing volume (analogous to lung resistance). Because of this resistance, the more rapidly the bellows is inflated the greater the force required. Part of the overall resistance arises from the intrinsic resistance of the bellows itself. This is the resistance to movement offered by the moving parts of the bellows, analogous to the viscous component of lung resistance. In effect, this is the resistance to movement that would be encountered if the spring were removed and the bellows was operated in a vacuum environment. Most of the bellow's resistance to movement is due to the impedance to airflow through the spout (airways resistance). Thus, narrowing the diameter of the spout will increase the force needed to inflate the bellows at a given rate (increased frictional and accelerative contributions). By analogy, airways resistance is the resistance encountered if the bellows were operated with the spring removed and the viscous component subtracted.

The *viscous* component of lung resistance (analo-

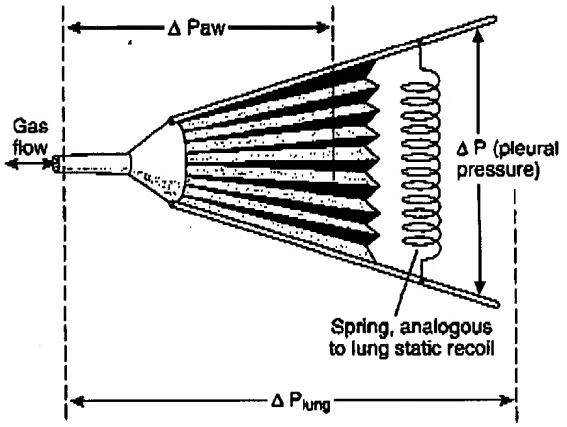

Figure 2–6. By analogy, respiratory system resistance is similar to the resistance encountered in operating a fireplace bellows (with the spring detached). Part of the resistance encountered is due to the work of driving flow through airways that narrow in total area from the alveolus toward the mouth (airways resistance). Another component relates to the resistance in moving the bellows itself, as would be encountered if operated in a vacuum (tissue viscous resistance). The spring represents the force that would be required to operate the bellows very slowly (static lung recoil).

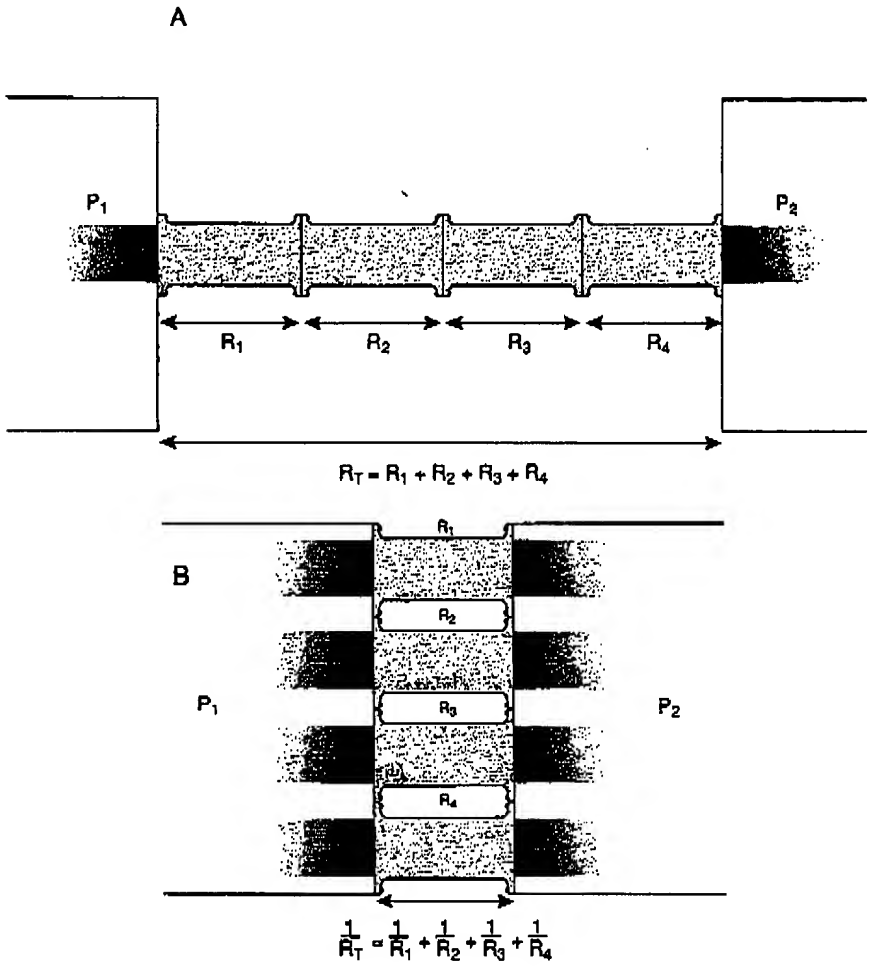

Figure 2–7. Resistance to fluid flow through four pipe segments, arranged sequentially in series (*A*) or in parallel (B). The total resistance (R_t) is the sum of individual resistances when arranged in series. When arranged in parallel, the total resistance is less than for any single segment because multiple separate pathways exist.

gous to the impedance offered by the moving parts of the bellows) varies with lung volume and can also be influenced by other factors. Sometimes called *tissue viscous resistance* or *lung viscance,* this component of lung resistance is generally small during normal tidal breathing. Airways resistance is the major component of lung resistance in the normal lung.

Lung resistance at a given lung volume can be measured during tidal breathing by subtracting the static lung transpulmonary pressure contribution from the total pressure difference between pleural pressure and the pressure at the airway opening. [In the fireplace bellows analogy, this is similar to measuring the resistance to operating the bellows while the spring is removed.] In practice, a balloon catheter is advanced down the esophagus to measure pleural pressure, as was used for determination of the static pressure–volume relationship described in Chapter 1. Because lung resistance decreases as lung volume increases, repeated measurements of lung resistance will differ unless the measurements are all made at the same lung volume. For this reason, repeated measurements are generally made at the same point in the ventilatory cycle (i.e., at mid-inspiration or mid-expiration). Referring to Figure 2–5, the pleural pressure at mid-inspiration (point B) is -7.5 cm H_2O. At that lung volume, the static pleural pressure would be -7.0 cm H_2O (point B'). Thus, the magnitude of the pleural pressure is 0.5

cm H_2O greater than would be seen with a static inflation at that lung volume. At point B, flow is 0.5 liter/sec. Recall that resistance is defined as a pressure difference divided by flow. The pressure difference created by the flow is therefore 0.5 cm H_2O minus the pressure at the airway opening (0 cm H_2O):

$$R = \frac{\Delta P}{\Delta \dot{V}}$$

$$R_L = \frac{0.5 \text{ cm } H_2O}{0.5 \text{ liter/sec}}$$

$$R_L = 1.0 \frac{\text{cm } H_2O}{\text{liter/sec}}$$

where R_L is the symbol for lung resistance (flow + viscous components) and cm H_2O/(liter/sec) is the unit of lung resistance. This lung resistance (1.0 cm H_2O/[liter/sec]) is typical of that which occurs in a normal adult human during inspiration.

Distribution of Lung Resistance

When laminar flow occurs through a branched system of tubes, the overall resistance across the system depends on the individual resistances in each pipe and the manner in which the pipes are connected. Figure 2–7 shows an arrangement of four pipe segments, each with a flow resistance of 1 torr/(liter/sec). When connected in series, the resistance of the network equals the sum of the individual resistances:

$$R_{Total} = R_1 + R_2 + R_3 + R_4$$

$$R_{Total} = 1 + 1 + 1 + 1 = 4$$

However, if the pipes are arranged in parallel (Figure 2–7*B*) the total resistance across the network will be less than the resistance of any single pipe. In this example, four simultaneous pathways exist, so the total resistance is only one-fourth of the resistance of any single segment. In general, the total resistance (R_{Total}) across a group of resistances arranged in parallel can be calculated using the relationship

$$\frac{1}{R_T} = \frac{1}{R_1} + \frac{1}{R_2} + \frac{1}{R_3} + \ldots$$

As airways travel from the trachea toward the alveoli, they branch successively into daughter airways. At each branch point, the daughter airways are described as belonging to the next *generation*. In general, airways of similar generation number tend to be about the same diameter. In moving from the trachea to the periphery of the lung the airways increase in number as they branch, but the individual bronchi become progressively smaller in diameter. The smaller diameter tends to increase the resistance offered by each bronchus, but the large increase in the number of parallel pathways tends to reduce the overall resistance encountered at each generation of branching. This can be described as a network of resistances, as shown in Figure 2–8. The collective resistance contributed by each generation reflects a balance between the number of airways in parallel and the radius of each. Figure 2–9 shows the relative resistances encountered at each airway generation. If the trachea is considered as generation 0, resistance increases slightly for the first few generations, reaching a peak near generations 3 to 6 (corresponding to segmental bronchi). Beyond this level, the increase in the number of parallel airways outweighs the decrease in diameter of each bronchus, causing the resistance at further generations to decrease progressively. At the level of the terminal bronchioles (generation 16), the airways resistance is a small fraction of the resistance in the segmental bronchi. During normal breathing, approximately 80% of the resistance to airflow at FRC is in airways whose diameters exceed 2 mm.

Measurement of Airways Resistance

By measuring pleural pressure and airflow simultaneously, lung resistance can be determined during tidal breathing if the static volume–pressure relationship of the lung is known. Theoretically, airways resistance could be calculated by subtracting the viscous component from the measured lung resistance. However, the viscous component of lung resistance is difficult to measure directly, so this approach is not practical. Moreover, lung resistance itself is difficult to measure in the clinical setting because it requires the placement of a balloon-tipped catheter at the correct position in the esophagus.

The direct measurement of airways resistance re-

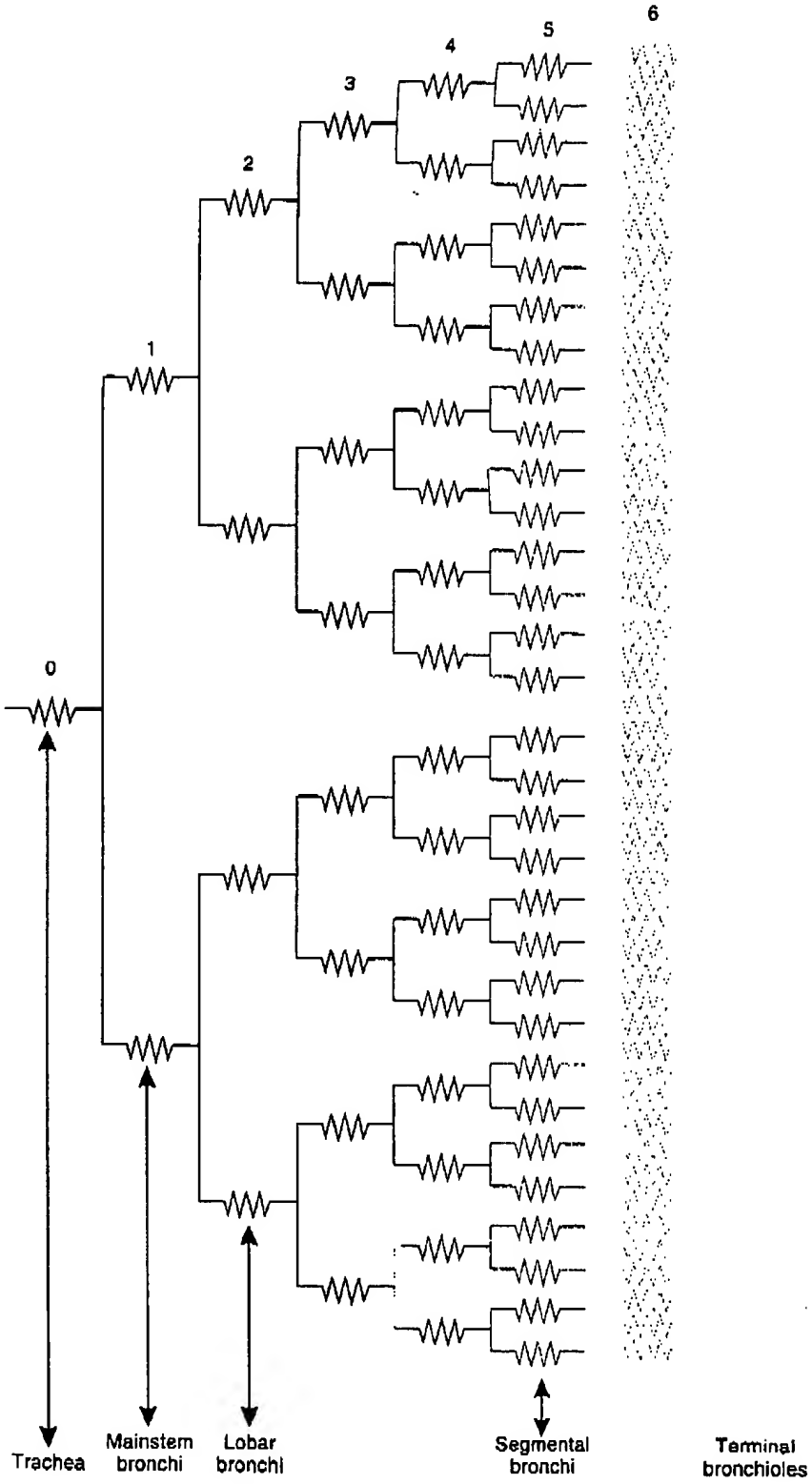

Figure 2–8. Airway resistance as a function of airway generation. The resistance contribution of any given airway generation (i.e., all the airways of that generation taken collectively) reflects a balance between the number of airways of that generation (arranged in parallel) and the individual resistance of each. Most of the overall airway resistance normally resides in generations 0 through 8. The contribution of resistance contributed by higher generations is relatively less because the number of smaller airways is large relative to their individual resistances.

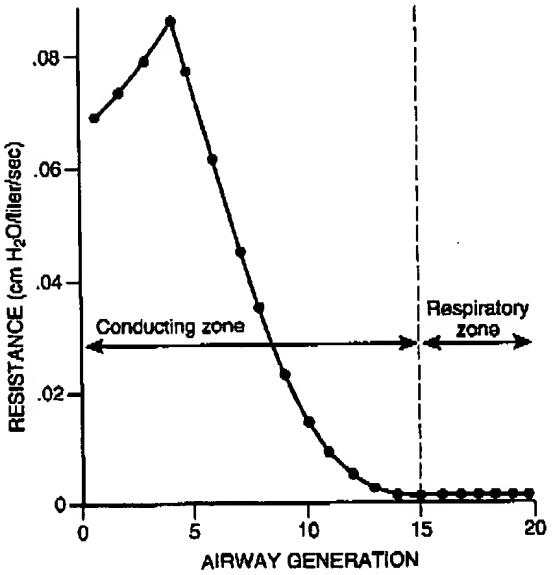

Figure 2–9. Airways resistance as a function of airway generation. In the normal lung, most of the resistance to airflow occurs in the first eight airway generations. (Redrawn from Pedley TJ et al: The prediction of pressure drop and variation of resistance within the human bronchial airways. Respir Physiol 9:387, 1970.)

quires that the alveolar-minus-mouth pressure difference be measured simultaneously with gas flow rate during a breath. This can be accomplished using a *body plethysmograph*, shown in Figure 2–10.

A subject fitted with a nose clip is seated inside a sealed body plethysmograph. The subject breathes air through a mouthpiece, equipped with an electrically operated occlusive shutter (normally open). A flow transducer attached to the mouthpiece measures the airflow rate as the subject breathes in and out. At the end of a passive exhalation (i.e., at FRC) the technologist closes the shutter to prevent airflow and asks the subject to pant rapidly against the closed shutter (see Figure 2–10*A*). When the shutter is closed, neither inspiration nor expiration can occur, so the pressure in the mouth is the same as alveolar pressure. This mouth pressure (P_M) is measured using a pressure transducer, as is the pressure in the box (P_B). When P_M is plotted as a function of P_B, a straight line is obtained with a slope of $\Delta P_M/\Delta P_B$. The airway shutter is then opened (see Figure 2–10*B*) and the subject is again asked to pant at FRC. During this procedure, the instantaneous flow at the mouth ($\dot{V}_M$) is measured, along with the pressure in the box (P_B). When $\dot{V}_M$ is plotted as a function of P_B, another straight line is obtained with a slope $\Delta\dot{V}_M/\Delta P_B$. From the closed shutter maneuver, the alveolar pressure corresponding to a given box pressure is known. Applying this to the open shutter, panting allows the alveolar pressure to be calculated from the measured box pressure. This calculation is made by dividing the slope of the $\Delta P_M/\Delta P_B$ line by the slope of the $\Delta\dot{V}_M/\Delta P_B$ line:

$$\frac{(\Delta P_M/\Delta P_B)}{(\Delta\dot{V}_M/\Delta P_B)} = \frac{\Delta P_M}{\Delta\dot{V}_M} = \text{Raw}$$

This yields a ratio of alveolar pressure to flow. Since the pressure at the mouth remains atmospheric during the open-shutter panting maneuver, this ratio is equal to the airways resistance, Raw.

The measurement of airways resistance with the body plethysmograph is relatively simple and can be combined with the measurement of FRC (see Chapter 1). Since panting with the shutter open only changes lung volume by about 50 ml, this measurement of Raw effectively avoids the changes in airway resistance that occur when lung volume changes (see later). This technique to assess Raw has become the standard for measuring resistance to airflow in clinical assessments of lung volume.

Airways Resistance and Lung Volume

Resistance to airflow changes markedly at different lung volumes. For this reason, measurements of lung resistance or airways resistance should always be made at a known lung volume. Since FRC is a volume that is easily reproducible, and since it is the volume at which persons normally breathe, measurements of resistance are usually made at FRC or some increment above FRC. Figure 2–11 shows how lung resistance varies as a function of lung volume in normal subjects. Lung resistance is highest at low lung volumes and lowest at high lung volumes. Two factors contribute to this volume dependence.

At higher lung volumes, the alveoli are more distended and the elastic tension in the alveolar walls is higher. Bronchi coursing through the lung parenchyma are surrounded by and attached to alveoli and are pulled open by the elastic tension in the

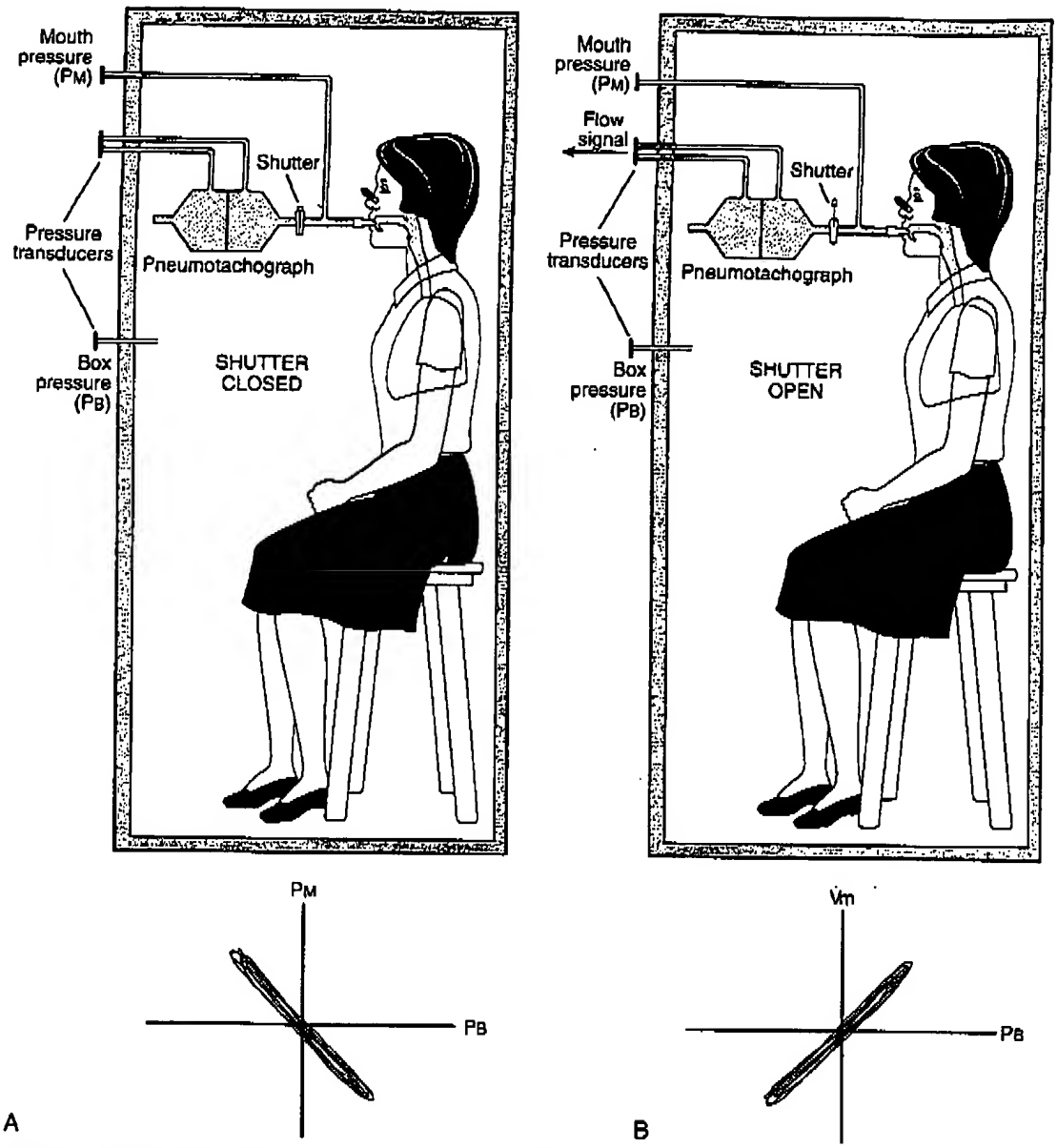

Figure 2–10. Measurement of airways resistance using a body plethysmograph. See text for further explanation.

alveolar walls. Because the bronchi have relatively distensible walls, their caliber (and therefore their resistance) is influenced to a great extent by this mechanical *tethering* effect. At low lung volumes approaching residual volume, tension in alveolar walls is less, so the tethering of the bronchi is reduced and airway resistance is increased. Moreover, some airways begin to close at these low lung volumes *(closing volume)*, further increasing the overall resistance to airflow.

The second factor contributing to the change in lung resistance at different lung volumes arises from changes in autonomic *parasympathetic nervous system* tone with lung volume. During inspiration, specialized neural mechanoreceptors *(stretch receptors)* within the smooth muscle layers in airway

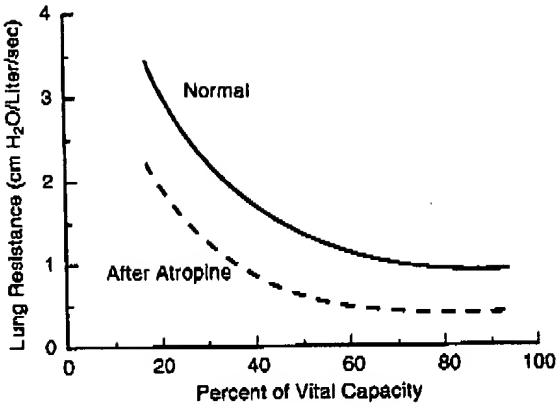

Figure 2–11. Lung resistance as a function of lung inflation. Airways resistance decreases as lung volume increases. At lung volumes above functional residual capacity the airways resistance decreases because (1) increased tension in alveolar septal walls is transmitted to adjacent airways, increasing their diameter, and (2) distention of airway stretch receptors elicits a reflex decrease in parasympathetic nervous system tone, causing a decrease in airway smooth muscle tension. Dashed line shows the effect of atropine (inhibiting parasympathetic effects) on airways resistance. (Redrawn from Vincent NJ, et al: J Appl Physiol 29:236–243, 1970.)

walls detect the increase in lung volume. Mechanical stretch of these receptors at higher lung volumes causes their neural rate of firing to increase. This afferent information is transmitted to the autonomic centers in the brain stem by way of the vagus nerve, and it elicits a reflex decrease in efferent parasympathetic tone (Chapter 12). Decreases in parasympathetic neural tone tend to reduce the active constriction of airway smooth muscle cells *(bronchomotor tone)*, thereby reducing airways resistance by increasing airway diameter. Conversely, during exhalation lung volume decreases and parasympathetic tone increases, causing a greater constriction of airway smooth muscle and a greater airflow resistance. Atropine, a drug that blocks the effects of the parasympathetic nervous system by inhibiting postganglionic parasympathetic receptors, diminishes the effects of lung volume on lung resistance (see Figure 2–11). However, atropine does not affect the change in resistance caused by the mechanical tethering of the airways.

DETERMINANTS OF MAXIMUM AIRFLOW

The respiratory system exhibits an enormous reserve capacity, relative to the demands faced at rest. For example, at rest, an adult human normally breathes 7 to 10 liters of air per minute (the *minute ventilation*). However, during strenuous exercise the minute ventilation can exceed 100 liters/min. In healthy young subjects asked to breathe as hard as possible for 15 seconds, a *maximal voluntary ventilation* (or *ventilation capacity*) of 200 liters/min may be achieved. This ability to augment greatly ventilation contributes to the wide physiological range of metabolic rates that a healthy subject can achieve. Because this reserve capacity of the respiratory system is so large, lung diseases can often progress to advanced stages without infringing on the ability of the respiratory system to meet resting needs. To detect advancing lung disease, several clinical pulmonary function measurements attempt to stress the capacity of the respiratory system. One such measurement is the forced exhalation test.

Flow During Maximal Expiration

Recall from Chapter 1 that a spirogram can be used to record changes in lung volume during quiet breathing, as well as during submaximal or maximal inspirations or expirations. The spirogram records changes in volume (ΔV, in liters, on the y-axis) as a function of time (Δt, in seconds, on the x-axis). Note that the slope of any line on a spirogram has units of $\Delta V/\Delta t$ (in liters/sec), which is equivalent to flow rate. Typically, the subject is asked to inhale to total

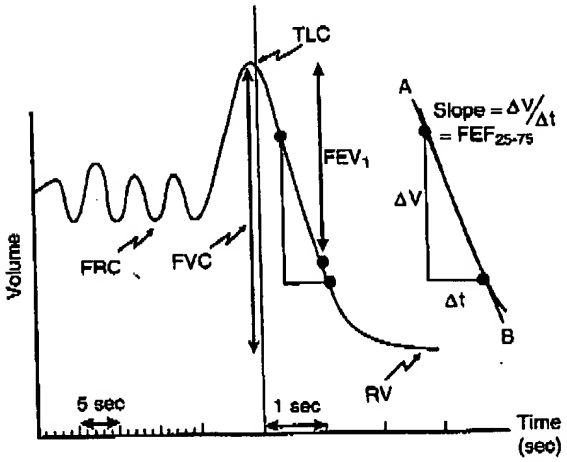

Figure 2–12. Tracing from a spirometer during measurement of a forced expiratory maneuver.

lung capacity (TLC) and then to exhale as forcefully as possible to residual volume (RV). [Horrific shrieks from the pulmonary function technologist usually help to provide incentive during the exhalation!] This creates a tracing like that shown in Figure 2–12. From the spirogram of the forced expiration maneuver one can see that the exhaled flow rate ($\Delta V/\Delta t$) is more rapid at the beginning of the exhalation than at the end, since the curve is steeper in the early part of the exhalation than the later.

It is useful to plot the instantaneous exhaled flow rate (liters/sec) as a function of exhaled volume. This is most easily done electronically, since the calculation of the slope by hand from the paper spirogram is tedious. Figure 2–13 is an example of such a plot of the instantaneous exhaled flow rate as a function of the volume of gas exhaled in a normal subject. Flows above the horizontal line are expiratory, while flows below the line are in an inspiratory direction. Lung volumes are greater toward the left side and lowest at the right side, since the volume being plotted on the x-axis is exhaled volume. The collection of small loops in the center was obtained during quiet tidal breathing. By inspection, the tidal volume in this subject averaged about 700 ml. During quiet breathing, the maximum flow encountered during inspiration or expiration was about 1 liter/sec, which is much lower than the maximum flow rates that the lung is capable of achieving. At the start of the maneuver, the subject inhaled

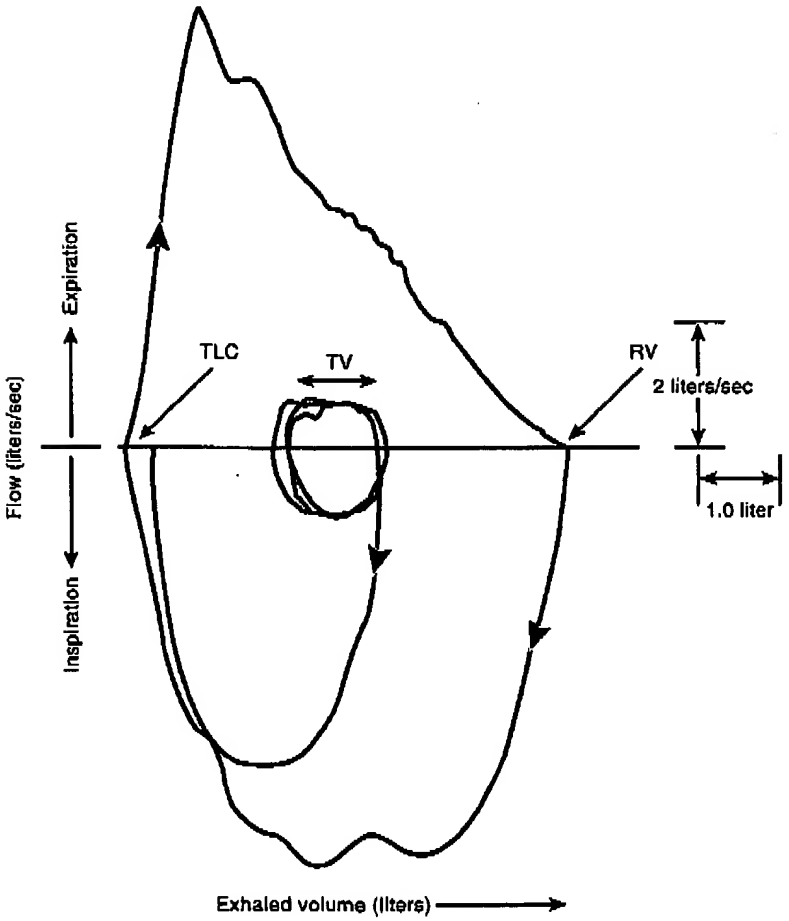

Figure 2–13. Air flow rate (on the ordinate) as a function of lung volume (on the abscissa) during a forced expiratory maneuver. Points above the horizontal axis represent expiratory flows; points below the line are inspiratory. Lung volumes are highest at the left and lowest at the right. See text for further explanation.

deeply and forcefully to TLC (large downward [inspiratory] flow beginning at FRC) and then immediately exhaled forcefully down to RV (large upward [expiratory] flow ending at RV). Several typical characteristics can be noted in this *flow-volume loop*.

First, note that the maximal inspiratory flow was about the same or greater than the maximal expiratory flow. The maximum inspiratory flow rate is influenced by several factors. On one hand, the maximum force that can be generated by the inspiratory muscles decreases as lung volume increases above RV. Hence, the inspiratory force decreases as inhalation proceeds. Second, the static recoil pressure of the lung increases as lung volume increases above RV. This opposes the inspiratory muscles and tends to reduce maximum inspiratory flow rate. On the other hand, airways resistance tends to decrease as lung volume increases because the caliber of the airways increases. Normally, the above factors combine to cause maximal inspiratory flow to occur about halfway between TLC and RV. During forced expiration the flow rate rises rapidly at the start of the exhalation and reaches its peak early in the exhalation while lung volume is still high. Thereafter, the flow rate decreases progressively toward the end of the exhalation.

Figure 2–14 shows three flow-volume curves superimposed on the same graph. To generate these curves a subject performed three forced expirations, each with progressively greater effort. As the effort increases, note that the peak flow early in the expiration also increases. However, in the later part of the expiration all three curves converge, indicating that the flow rate in the later part of expiration is *effort independent*. In that range, the expiratory rate is *flow-limited* by the lung, and no amount of additional effort can increase the flow rate beyond this limit. Thus, over much of a forced expiration the maximal flow rate is determined by a property of

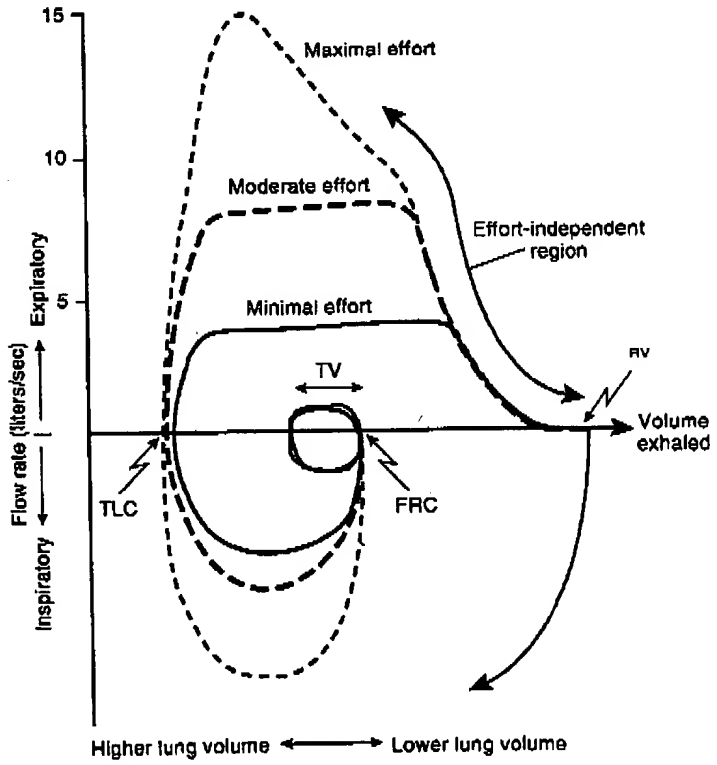

Figure 2–14. Three superimposed expiratory flow maneuvers, made with increasing effort. Note that peak inspiratory and expiratory flow rates are *effort dependent*, whereas expiratory flow rates later in expiration are *effort independent*.

the lungs and not by the effort expended by the subject. This measurement is highly reproducible in a single subject and is relatively sensitive to changes in lung properties caused by diseases. Accordingly, the forced expiratory flow–volume loop has become a common clinical test of pulmonary function.

Lung Volume and Maximal Expiratory Flow Rate

During a forced exhalation, flow rate rises rapidly to a peak early in the maneuver but then decreases progressively as lung volume diminishes. In the effort-independent portion of the flow–volume relationship, the *maximal* expiratory flow rate in any given subject is heavily influenced by *lung volume.* This concept is shown graphically in Figure 2–15*A*. To generate this graph, a subject with an esophageal balloon catheter (to measure pleural pressure) was asked to exhale several times, with increasing effort. The first few exhalations were made with mild effort, while the subsequent exhalations were made with increasing effort, up to a maximal effort. During forceful exhalations, pleural pressure increased significantly (to 40–60 cm H_2O), while during less forceful exhalations the rise in pleural pressure was less. During each exhalation, expiratory flow and exhaled volume were recorded *only when the lung volume passed through a predetermined level.* For example, consider the curve labeled 3 in Figure 2–15. This line represents the different flow rates measured during exhalations at different efforts, at the times that 70% of the vital capacity had been exhaled. Thus, the lung volumes corresponding to all of the points on curve 3 are identical. Similarly, the points on curve 4 represent the different expiratory flow rates that were obtained during exhalations of varying intensity, at the point where 90% of the vital capacity had been exhaled (i.e., lung volume = RV + 10% of VC). For curve 2, expiratory flow rate (at that lung volume) increases with increasing effort, until a maximal flow is reached. Further effort (higher pleural pressure) will not increase expiratory flow above the plateau value for that lung volume. Note that the maximal flow for curve 2 was greater than for curve 3, and the lung volume corresponding to 2 was greater than for 3. Thus, the maximum expiratory flow that can be achieved increases as the lung volume increases toward TLC. Another set of flows was collected at high lung volumes (90% of TLC) during various

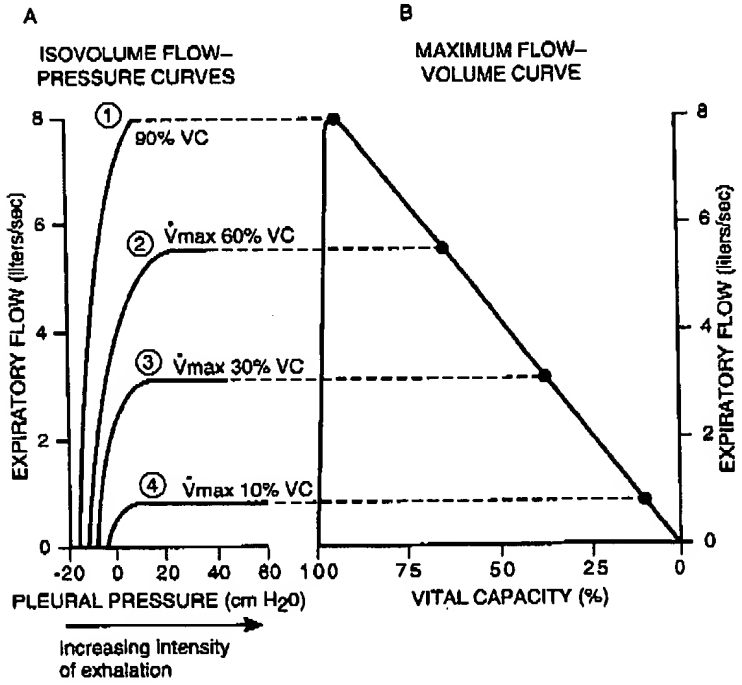

Figure 2–15. Greater levels of (effort-independent) expiratory flow rate can be achieved when lung volume is higher. Each curve represents the relationship between expiratory effort (pleural pressure) and expiratory flow rate *that would have been noted if lung volume could have remained constant.* At any given lung volume, expiratory flow rate increases with expiratory effort until an effort-independent expiratory flow rate is reached. Above this level, further increases in effort do not produce increases in flow rate. At total lung capacity in a normal subject, increases in effort always produce increases in flow rate. See text for further explanation. (Redrawn from Murray JF: The Normal Lung, 2nd ed. Philadelphia, WB Saunders, 1986.)

exhalations with varying effort (curve 1). Note that at this high lung inflation, expiratory flows continued to increase with increasing effort; that is, there was no clear limitation to flow other than effort. Since each of curves 1 through 4 correspond to specific lung volumes, these relationships are referred to as *isovolume pressure–flow curves.*

If the *maximal* values of expiratory flow (see Figure 2–15*B*) are plotted as a function of their respective lung volumes (volume below TLC), this yields a curve whose shape is identical to the descending portion of a single-breath forced-exhalation maneuver. Thus, the clinical measurement of a single forced exhalation provides (in the effort-independent region) a continuous plot of the maximal flow that can be achieved at lung volumes ranging from near TLC to RV.

Expiratory Flow Limitation Mechanism

As described previously, maximal expiratory flow rates are normally limited by factors other than effort after lung volume falls more than about 20% of the way from TLC toward RV. The reason for this is that airways are intrinsically floppy, distensible tubes that tend to become compressed when the pressure outside them exceeds the pressure inside. Stated more formally, airways become liable to collapse when their transmural pressure (defined as inside-minus-outside pressure difference) becomes negative. Expiratory flow-limitation occurs when highly localized events called *choke points* (not related to ordinary choking) occur at specific sites along the airways where negative transmural pressures cause a critical narrowing in the airway diameter. This is roughly analogous to the situation that occurs when attempting to drink water through a paper soda straw that has become saturated with water and is soggy and collapsible. If the subject draws too forcefully on the straw, the pressure inside becomes negative with respect to ambient pressure and the straw collapses. When this occurs, no amount of additional effort will cause the flow to increase. However, one can still draw water slowly through the straw without causing the flow limitation to occur.

Figure 2–16 shows the sequence of events that occur during expiratory flow limitation in a lung surrounded by the chest wall and the pleural space. Note that the airways are shown schematically as tapered tubes, because the total airway cross-sectional area narrows enormously in traveling from the alveoli to the trachea. Figure 2–16*A* shows the lung held at TLC while no airflow is occurring. In this state, alveolar pressure is zero (relative to atmospheric) and pleural pressure is -30 cm H_2O, so the lung transmural pressure (transpulmonary pressure) equals $+30$ cm H_2O. Since there is no flow, the pressure inside the airways is also zero. Since the pressure immediately outside the intrathoracic airways is the same as pleural pressure, the transmural pressure (pressure inside – pressure outside) for the airways is also $+30$ cm H_2O. This positive transmural pressure tends to hold the airways open, in the same way that a positive transpulmonary pressure holds the alveoli open.

Next, consider what happens at the instant a forced exhalation begins (see Figure 2–16*B*). As the inspiratory muscles relax and expiratory muscles contract, the chest volume decreases and pleural pressure rises rapidly to $+60$ cm H_2O. At that instant, alveolar pressure rises to 90 cm H_2O, because alveolar pressure exceeds pleural pressure by the static lung recoil pressure corresponding to that lung volume. Driven by a pressure difference between alveolus and the mouth of 90 cm H_2O, expiratory flow begins in earnest. As expiratory flow begins, a gradient in pressure develops inside the airways between the alveoli and the mouth, as shown in Figure 2–16*B*. This reduces the transmural pressure for the airways, because it lowers the pressure in the lumen relative to the pressure outside the bronchi (pleural pressure). Two major factors contribute to the fall in intra-airway pressure between the alveoli and the mouth. First, there is a resistive pressure drop caused by the frictional pressure loss associated with the flow. This resistive loss becomes greater toward the trachea, because the number of parallel airways decreases more rapidly than the diameter of the individual airways increase (see Figure 2–3). The second factor lowering the pressure inside the airways is caused by the fact that the gas velocity increases toward the trachea, because the total cross-sectional area of the airways decreases. This acceleration of gas flow further decreases the pressure, due to the Bernoulli effect (see Figure 2–4). Both contributions tend to lower the airway transmural pressure, thereby decreasing the diameter of the airways. During the exhalation, lung volume decreases so the static re-

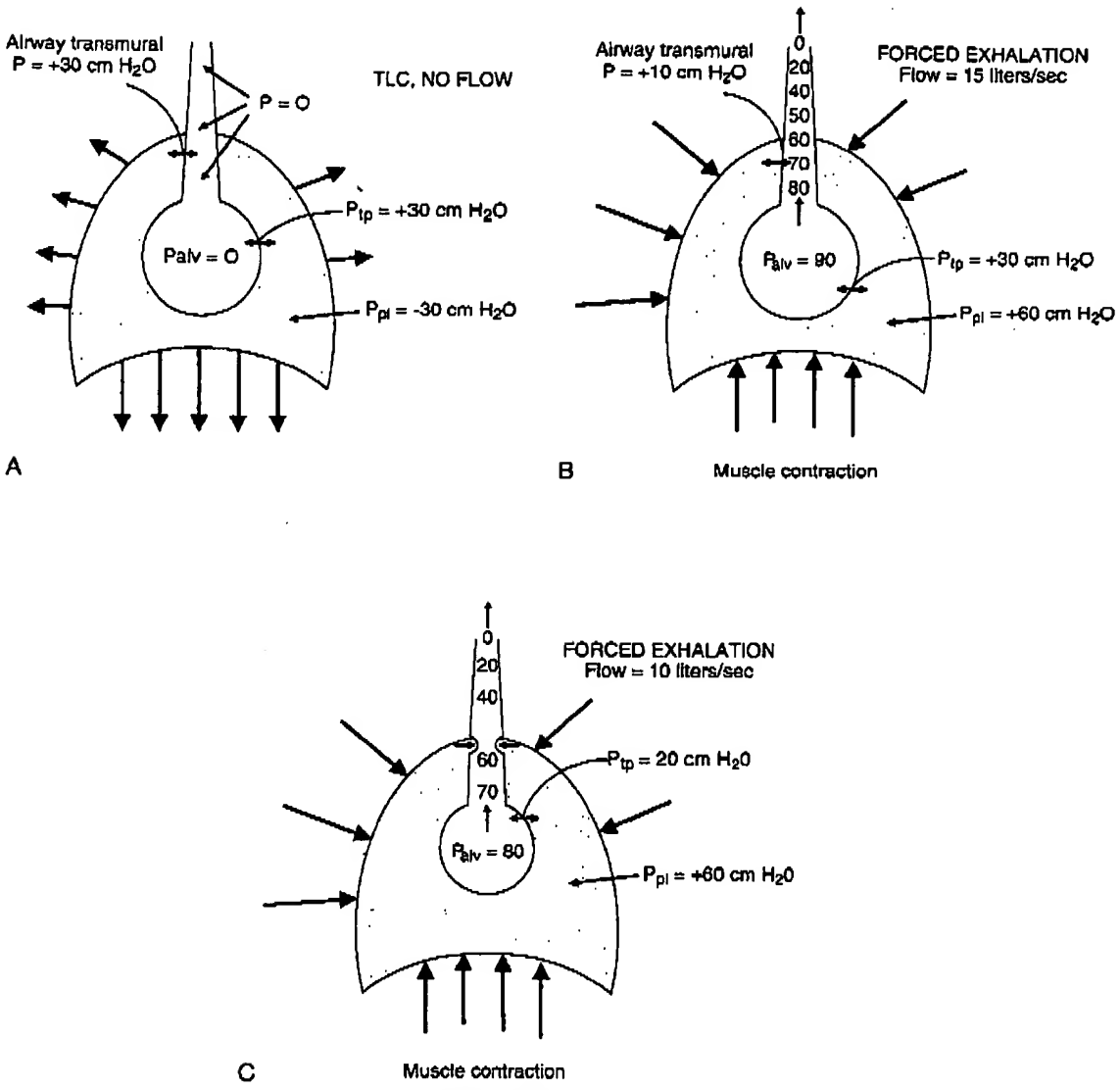

Figure 2–16. *A*, End inspiration, before the start of exhalation. *B*, At the start of a forced exhalation. *C*, Expiratory flow limitation later in a forced exhalation. Expiratory flow limitation occurs at locations where airway diameter is narrowed as a result of a negative transmural pressure. See text for further explanation.

coil pressure decreases. This lowers the difference between pleural pressure and alveolar pressure, thereby decreasing a major factor contributing to airway transmural pressure. In addition, the mechanical tethering (Figure 2–17) that helps to hold the airways open at high lung volumes becomes less as lung volume decreases. Moreover, the mainstem bronchi and the trachea are not surrounded by alveoli and therefore do not benefit from this support.

Figure 2–16C shows the balance of forces acting during expiratory flow-limitation. At this point, pleural pressure is still at 60 cm H_2O and lung volume has decreased by 20% from TLC. Lung static recoil pressure at this volume is +20 cm H_2O, so alveolar pressure is 20 + 60 = 80 cm H_2O. Expiratory flow is 10 liters/sec, and the pressure inside the airways decreases from 80 cm H_2O (at the alveoli) to 0 cm H_2O (at the mouth). At the point where the

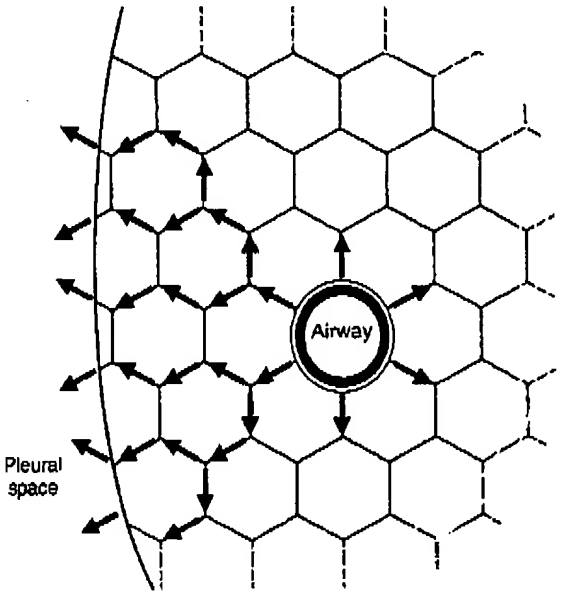

Figure 2–17. Airway tethering by the surrounding alveoli. At higher lung volumes there is more tension in the alveolar septal walls. This tension is transmitted to the airways passing through the lung parenchyma, tending to increase their diameter and prevent their collapse *(mechanical tethering)*. Hence, higher expiratory flows can be achieved at high lung volumes.

pressure inside the airways has decreased to less than 60 cm H_2O (somewhere between the alveoli and the mouth), the pressure outside the airways becomes greater than the pressure inside. This negative airway transmural pressure causes the airway to narrow, as a choke point forms. For this reason, a greater expiratory effort (higher pleural pressure) cannot increase the flow further because the higher pleural pressure will tend to collapse the airway at the choke point just as much as it tends to increase the driving gradient for flow. This is why effort-independent expiratory flow limitation occurs in forced exhalation.

As expiration continues, lung static recoil pressure continues to decrease because lung volume decreases. The fall in static recoil pressure decreases the transmural pressure tending to hold the airways open, facilitating the development of a choke point. Airway resistance also increases at lower lung volumes, accentuating the resistive drop in pressure along the airways. Finally, mechanical tethering of the airways becomes less at lower lung volumes, thus promoting the collapse at a choke point. These factors contribute to the lessened maximal expiratory flow that occurs later in a forced exhalation.

In summary, flow limitation occurs at specific sites of narrowing (choke points) along the airway, which are likely to form at locations where the airway transmural pressure becomes negative. The major factor contributing to a positive airway transmural pressure is a high lung static recoil pressure (high lung volume), because this contributes to a greater pressure within the airspaces relative to pleural pressure. Factors that tend to reduce airway transmural pressure during expiration (thus promoting flow-limitation) are (1) the resistive drop in pressure due to airflow from alveoli toward the mouth; (2) the Bernoulli reduction of intra-airway pressure caused by the acceleration of flow as the total airway cross-sectional area decreases toward the mouth; and (3) loss of mechanical tethering of central airways as they exit from the lung.

Tests of Expiratory Flow Limitation in Lung Diseases

The *vital capacity* (VC) measured as the change in volume from TLC to RV during a forced expiration is called the *forced vital capacity* (FVC). Line AB in the inset of Figure 2–12 connects the points on the FVC curve at 25% of VC and 75% of VC. This provides an "average slope" (liters/sec) in the middle of the forced expiration and is termed FEF_{25-75} (forced expiratory flow between 25% and 75% of FVC). This provides an index of the forced expiratory flow within the effort-independent (flow-limited) range. However, in practice there is considerable variability in this measurement among individuals. A more reproducible number is the volume of air (in liters) exhaled during the first second of the forced exhalation. This volume is termed the *forced expiratory volume in 1 second* (FEV_1). Typically, the FEV_1 is normalized by dividing it by the FVC and expressing the result as a percentage. Note that the FEV_1/FVC ratio is dimensionless, since it is the ratio of two dimensionally similar terms. In healthy persons between the ages of 25 and 50 the FEV_1/FVC is usually between 75% and 85%.

Acute and chronic lung diseases can change the expiratory flow–volume relationship by virtue of the changes they cause in (1) static lung recoil pressures; (2) airways resistance and the distribution of resistance along the airways; (3) loss of mechanical tethering of intraparenchymal airways; (4) changes

in the stiffness or mechanical properties of the airways; and (5) regional differences in the severity of the above changes among lung regions.

Abnormally low values of FEV_1, FEF_{25-75}, and FEV_1/FVC are the hallmark of *obstructive lung diseases.* Diseases in this category include emphysema, asthma, chronic bronchitis, and cystic fibrosis. The common observation among these diverse diseases is that expiratory flow becomes limited at relatively low flow rates (hence the term *obstructive*), although the mechanism responsible varies among the diseases. In *asthma,* flow limitation occurs primarily as a result of decreased airway caliber caused by abnormally increased bronchial smooth muscle tone and swelling of the mucosal layer lining the airways. In *chronic bronchitis* and *cystic fibrosis,* the accumulation of excessive bronchial secretions hinders normal air flow. In *emphysema,* the decreased static lung recoil (increased lung compliance) resulting from the destruction of alveolar septal walls tends to promote the development of flow-limitation (choke points) at much lower flow rates than for normal persons. The loss in static recoil pressure also causes TLC to be increased, as is FRC. Accordingly, emphysematous patients often breathe at higher lung volumes than do normal subjects. Finally, the loss in elastic tethering of intraparenchymal airways further promotes the development of choke points during exhalation.

Figure 2–18 shows an expiratory flow–volume loop in a patient with emphysema. Compared with the normal subject, TLC and FRC are both increased. Note that during quiet tidal breathing, the emphysematous patient's expiratory curve intersects the maximal expiratory curve, indicating that resting exhalations in this patient are already flow limited! Note also that the shape of the expiratory curve is deeply convex owing to the severe flow limitation at lower lung volumes. By contrast, inspiratory flows are relatively normal, since the negative pleural pressure during inspiration tends to promote airway opening by increasing airway transmural pressures. Consequently, rapid inspiration is not a problem for these patients whereas exhalation is a slow and extended process.

Another class of lung diseases are termed *restrictive diseases,* because they restrict the extent of lung inflation. Decreased TLC is the hallmark of restrictive diseases, which generally arise from three different causes: (1) diseases causing increased static lung recoil such as *interstitial fibrosis;* (2) diseases limiting chest wall movement such as *kyphoscoliosis* or (more commonly) *obesity;* and (3) muscular weakness, such as in *myasthenia gravis.* The effect of restrictive disease on lung statics and dynamics varies with the cause and the extent of the disease.

Restrictive disease associated with an increased lung static recoil often occurs in pulmonary interstitial fibrosis. Compared with a normal subject, TLC and RV are both reduced, owing to the increased static lung recoil. Although maximal expiratory flows may appear to be increased in these patients (FEV_1/FVC ratio is elevated), the FEV_1 may be normal or even reduced, while FVC is significantly reduced. Thus, expiratory flows would not be elevated if plotted as a function of pleural pressure.

Features characteristic of restrictive lung disease are also associated with diseases involving muscle weakness. In these patients, TLC is low because there is insufficient strength to overcome the static recoil of the lungs and chest wall associated with a normal TLC. Likewise, RV may be high because there is insufficient strength to reach a normal RV. However, static lung recoil can be normal, so the expiratory flows are not elevated above normal.

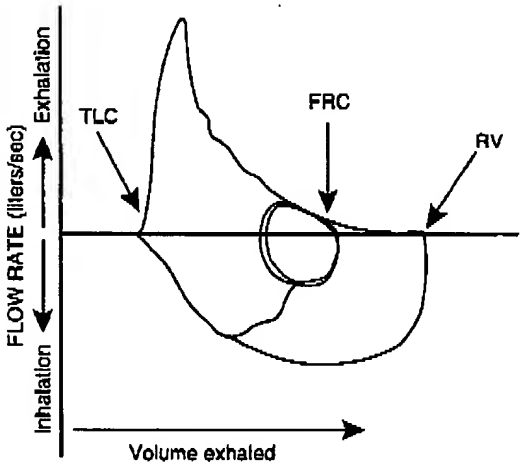

Figure 2–18. Severe expiratory flow limitation can occur in a patient with emphysema. This flow–volume loop shows that expiratory flow rate falls sharply after the start of expiration. The remainder of expiration is prolonged, owing to the slow rate of flow-limited exhalation. Note also the increased total lung capacity and increased functional residual capacity, caused by the increased lung compliance in this patient.

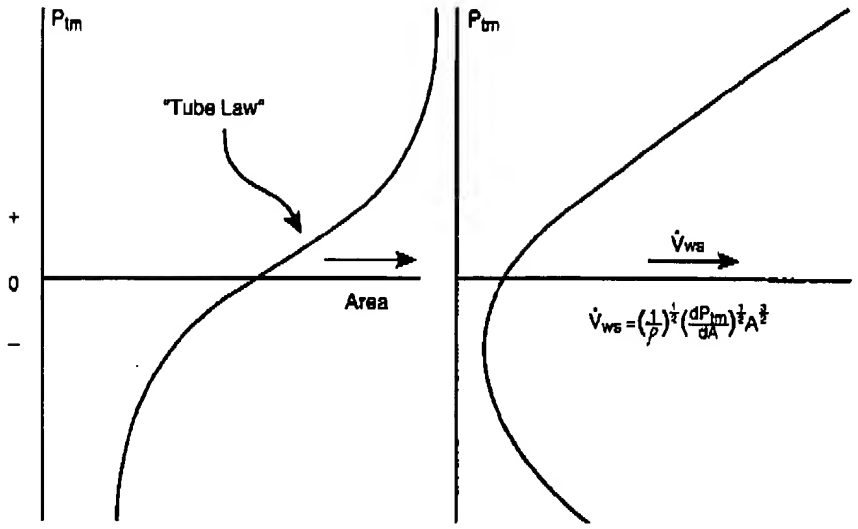

Figure 2–19. *Left,* Typical relationship between the cross-sectional area of an airway (A) and the transmural pressure across it (P_{tm}). When the transmural pressure across an airway is negative, the airway area decreases to a minimum level as the tube is squeezed shut. As P_{tm} increases, the airway assumes a more normal shape and its area increases. However, at high transmural pressures the airway elastic elements are stretched and further changes in area with increased transmural pressure are small. Flow limitation is more likely to occur in floppy airways because they tend to collapse more readily as their transmural pressure decreases. *Right,* The maximal flow that can develop in a floppy tube ($\dot{V}_{ws}$) depends on the stiffness of the tube: the more rigid the tube, the greater the maximal flow. (Redrawn from Mead J: Expiratory flow limitation: a physiologist's point of view. Fed Proc 39:2771, 1980.)

Restrictive diseases arising from decreases in chest wall compliance can reduce FRC because lung static recoil is unchanged while static chest wall recoil is increased. The increased chest wall recoil can also lead to a decrease in TLC because the maximal decrease in pleural pressure that can be developed by the respiratory muscles will not increase lung volume to a normal TLC.

Physics of Expiratory Flow Limitation

Effort-independent expiratory flow limitation occurs at points along the airways where the local transmural pressure is negative enough to cause the airway to narrow, causing the appearance of a choke point that limits the flow rate. If the airways were stiff, rigid tubes, then choke points would not occur because the caliber of the airways would remain fixed over a wide range of transmural pressures. Real airways are not rigid but can vary in their degree of stiffness at different locations (i.e., trachea vs. small bronchi), depending on how much cartilage is present, what surrounds the airway at that point, and other factors. Hence, some points along the airway are more likely to form choke points than others.

In floppy tubes such as airways, the maximum flow that can occur at any point is related to the product of the velocity of propagation of a pressure wave along the tube (the *tube wave speed*), and the cross-sectional area of the tube at that point. This theoretical maximum flow is called the *tube wave speed flow* ($\dot{V}ws$):

$$\dot{V}ws = \left[\frac{1}{\rho} \cdot \frac{dP_{tm}}{dA}\right]^{\frac{1}{2}} \cdot A^{\frac{1}{2}}$$

where ρ is the gas density, A is the tube cross-sectional area at that point, and dP_{tm}/dA is related to the elasticity of the tube. Figure 2–19 shows a typical relationship between the area of an airway (A) and the transmural pressure across it (P_{tm}). When the transmural pressure across an airway is

negative, the airway area decreases to a minimum level. As P_{tm} increases, the airway assumes a more normal shape and its area increases. However, at high transmural pressures, the airway elastic elements are stretched and further changes in area with increased transmural pressure are small. The dP_{tm}/dA term in the equation is the slope of this relationship at any given point. This curve is sometimes called the *tube law*, since it describes how the area of a specific tube will vary with transmural pressure. The above formula states that if the stiffness of an airway is known (i.e., the tube law) and if the density of the gas is known, then the maximum theoretical flow that can occur in that airway is known. Factors that tend to increase the area of an airway (i.e., parenchymal tethering at high lung volumes) or that make an airway wall less floppy (i.e., more cartilage) tend to increase the maximum theoretical flow that the airway can support ($\dot{V}ws$). As the actual flow in an airway increases, it reaches a maximum when it equals the wave speed flow. Above that maximum flow a choke point forms, and flow is limited to the maximum value. This approach to understanding the physical mechanisms underlying expiratory flow limitation is termed *wave speed theory*.

J Appl Physiol
89: 908–916, 2000.

Comparative respiratory system mechanics in rodents

R. F. M. GOMES,[1] X. SHEN,[2] R. RAMCHANDANI,[2] R. S. TEPPER,[2] AND J. H. T. BATES[1]
[1]*Meakins-Christie Laboratories, McGill University, Montreal, Quebec, Canada H2X 2P2; and*
[2]*Department of Pediatrics, Indiana University School of Medicine, Indianapolis, Indiana 46223*

Received 21 January 2000; accepted in final form 17 April 2000

Gomes, R. F. M., X. Shen, R. Ramchandani, R. S. Tepper, and J. H. T. Bates. Comparative respiratory system mechanics in rodents. *J Appl Physiol* 89: 908–916, 2000.—Because of the wide utilization of rodents as animal models in respiratory research and the limited data on measurements of respiratory input impedance (Zrs) in small animals, we measured Zrs between 0.25 and 9.125 Hz at different levels (0–7 hPa) of positive end-expiratory pressure (PEEP) in mice, rats, guinea pigs, and rabbits using a computer-controlled small-animal ventilator (Schuessler TF and Bates JHT, *IEEE Trans Biomed Eng* 42: 860–866, 1995). Zrs was fitted with a model, including a Newtonian resistance (R) and inertance in series with a constant-phase tissue compartment characterized by tissue damping (Gti) and elastance (Hti) parameters. Inertance was negligible in all cases. R, Gti, and Hti were normalized to body weight, yielding normalized R, Gti, and Hti (NHti), respectively. Normalized R tended to decrease slightly with PEEP and increased with animal size. Normalized Gti had a minimal dependence on PEEP. NHti decreased with increasing PEEP, reaching a minimum at ~5 hPa in all species except mice. NHti was also higher in mice and rabbits compared with guinea pigs and rats at low PEEPs, which we conclude is probably due to a relatively smaller air space volume in mice and rabbits. Our data also suggest that smaller rodents have proportionately wider airways than do larger animals. We conclude that a detailed, comparative study of respiratory system mechanics shows some evidence of structural differences among the lungs of various species but that, in general, rodent lungs obey scaling laws similar to those described in other species.

respiratory system impedance; forced oscillations; comparative physiology; small rodents

SMALL RODENTS ARE NOW WIDELY utilized as animal models of lung disease because they can be obtained easily in large numbers for a reasonable price, they grow rapidly, and pure-bred strains are available. Ultimately, of course, to apply results from such studies to human disease, we need to know how rodent lungs compare mechanically with human lungs. However, it is also important to understand how the respiratory mechanical properties of different rodents compare among species so that appropriate choices can be made as to which species to use when a particular disease state is modeled. A number of studies have attempted to characterize and compare respiratory mechanics in different mammalian species (4, 10, 21, 27), but most of them consisted of pooled data from different sources in the literature, and some even used recently killed animals. Furthermore, these comparative studies have not taken into account the well-known dependence of respiratory mechanics on frequency and volume. We thus identified a need for a comprehensive, comparative study of respiratory system impedance (Zrs) in a variety of small-animal species that are currently widely used in respiratory research.

Particular interest has been directed recently to the evaluation of the mechanisms that affect respiratory system properties under both healthy and abnormal conditions and whether the predominance of these effects is in the airways or the parenchymal and/or chest wall tissues (1, 3, 12, 15–17, 19, 25–31, 35). Respiratory system elastance is known to increase with frequency, and tissue resistance is known to decay hyperbolically over the range of physiological breathing frequencies, whereas airway resistance (Raw) remains fairly constant both in healthy and mildly constricted lungs (12–15, 22, 32, 37). Consequently, the relative contributions of airway and tissue resistances are highly dependent on the breathing frequency. Furthermore, these relative contributions can change with lung volume (17). This highlights the importance of measuring Zrs over a broad range of frequencies and volumes. Such an undertaking is not trivial because of the technical difficulties associated with measuring Zrs accurately in small animals. However, we now have at our disposal a computer-controlled, small-animal ventilator (SAV) (34) that has solved these difficulties and allows us to measure Zrs over a wide frequency range and at controlled lung inflation pressures in animals as small as a mouse.

The goal of the present study was, therefore, to make a comparative study of Zrs in normal mice, rats, guinea pigs, and rabbits over a broad range of frequencies and at different levels of lung inflation with the use of the SAV. We interpreted the measured Zrs in terms of a model proposed by Hantos et al. (15), which features a Newtonian resistance (R) connected to a constant-phase viscoelastic tissue compartment. The parameters of the model account extremely well for Zrs <20

Address for reprint requests and other correspondence: J. H. T. Bates, Colchester Research Facility of The Univ. of Vermont, 55A South Park Dr., Colchester, VT 05446 (E-mail: jhtbates@zoo.uvm.edu).

The costs of publication of this article were defrayed in part by the payment of page charges. The article must therefore be hereby marked "*advertisement*" in accordance with 18 U.S.C. Section 1734 solely to indicate this fact.

Hz and permit us to compare interspecies respiratory mechanics in a frequency-independent fashion.

MATERIALS AND METHODS

Experimental procedures. We studied four different species of rodents: A/J mice (n = 11; 20.5–24.7 g), Sprague-Dawley rats (n = 8; 260–290 g), Dunkin-Hartley guinea pigs (n = 5; 360–410 g), and New Zealand White rabbits (n = 6; 2.6–3.0 kg). Mice and rats were sedated with an intraperitoneal bolus of xylazine (7 and 14 mg/kg, respectively). All animals were anesthetized [pentobarbital sodium in mice (50 mg/kg ip), rats (35 mg/kg ip), and guinea pigs (65 mg/kg ip); sodium thiopental in rabbits (35 mg/kg iv)] and tracheostomized. Except for the rabbits, which had their trachea cannulated with a rigid plastic tube and which were ventilated with a commercial version of the SAV (flexiVent, SCIREQ, Scientific Respiratory Equipment, Montreal, Quebec), all of the other animals had a snug-fitting metal tracheal cannula connected to a SAV prototype (34). Mice, rats, guinea pigs, and rabbits were mechanically ventilated with sinusoidal inspiration and passive expiration with tidal volumes of 6, 8, 9, and 7 ml/kg and breathing frequencies of 150, 90, 70, and 60 breaths/min, respectively. Positive end-expiratory pressure (PEEP) was set at 3 hPa by connecting the expiratory line of the ventilator to a water trap. Mice and rabbits were paralyzed with pancuronium bromide (0.8 mg/kg ip and 0.1 mg/kg iv, respectively). Rats and guinea pigs were paralyzed with succinylcholine chloride (20 and 13 mg/kg ip, respectively).

Every 3 min, the animals were ventilated against one of five different levels of PEEP (0–7 hPa) chosen randomly. Three total lung capacity maneuvers were performed by closing the expiratory line until an airway opening pressure (Pao) of 30–35 hPa was obtained. We waited for 15 breathing cycles, the animals were allowed to expire passively to the relaxation volume as determined by PEEP (established by connecting the expiratory line of the ventilator to a water trap), and an 18-s small-amplitude, broad-band volume perturbation was applied to the airway opening. The volume perturbation waveform contained 12 discrete sinusoidal components having mutually prime frequencies from 0.25 to 9.125 Hz, and its peak-peak amplitude corresponded to 35% of the tidal volume of the animal. The individual amplitudes in flow had equal power at each frequency. The phases of the sinusoids were adjusted to minimize the peak-peak amplitude of the volume signal. The frequencies were chosen to be mutually prime to avoid harmonic distortion in the airway pressure (Paw) signal (6). Also, this range of frequencies was selected because it is suitable for the partition of Newtonian resistive and respiratory tissue viscoelastic properties. Once measurements at all of the five different levels of PEEP had been taken, the procedure was repeated.

The SAV is a computer-controlled ventilator in which a linear motor drives a piston in a cylinder of known diameter (34). Calculations of Zrs are made from measurements of piston volume displacement (Vcyl) and the pressure inside the cylinder (Pcyl). Vcyl and Pcyl were recorded at 1,024 Hz after being passed through low-pass filters with cutoff at 200 Hz. The data were then digitally low-passed filtered at 30 Hz and decimated to 128 Hz before being stored on a personal computer for subsequent analysis.

Data analysis. Corrections for gas compressibility within the system and resistive and accelerative losses in the connecting tubing and tracheal cannula were performed as described previously (3, 17). Briefly, we first obtained dynamic calibration signals of Pcyl and Vcyl from the SAV before connecting the animal by applying the volume perturbation through the tracheal cannula first when it was completely closed and then again when it was open to the atmosphere. Subsequently, when the animal was connected to the SAV, we used these calibration signals to remove the contribution of both the tracheal cannula and the SAV itself from the measured animal Zrs.

Zrs was calculated as the ratio between the cross-power spectrum of Pao with Vcyl and the autopower spectrum of Vcyl multiplied by $j2\pi f$, where j is the imaginary unit and f is frequency. The first 2 s of each 18-s data record were discarded to avoid initial transients, and the remaining 16 s were divided into five 8-s blocks that overlapped by 75%. The cross- and autopower spectra for all blocks were averaged before being divided to yield Zrs to reduce the effects of measurement noise (13).

Zrs consists of a real part known as respiratory system resistance (Rrs) and an imaginary part known as respiratory system reactance (Xrs). We normalized Rrs and Xrs by multiplying them by body weight (BW) to obtain normalized Rrs (NRrs) and Xrs (NXrs), respectively.

We also fit Zrs data to a model consisting of a R connected to a constant-phase tissue compartment. Thus

$$Zrs(f) = R + j2\pi fI + \frac{Gti - jHti}{(2\pi f)^{\alpha}} \quad (1)$$

where I is inertance, Gti and Hti embody energy dissipation and storage, respectively, within the tissues, and

$$\alpha = \left(\frac{2}{\pi}\right) \arctan\left(\frac{Hti}{Gti}\right) \quad (2)$$

The α determines the frequency dependence of both real and imaginary parts of Zrs and is related to the hysteresivity index (η) introduced by Fredberg and Stamenovic (9) where

$$\eta = \frac{Gti}{Hti} \quad (3)$$

To facilitate comparisons among species, we normalized the parameters R, I, Gti, and Hti by multiplying them by BW to obtain, respectively, NR, NI, NGti, and NHti.

We calculated the coherence between Pcyl and Vcyl at each of the frequencies used in the volume perturbation signal and fit the model to Zrs at only those frequencies for which the coherence was >0.9. On this basis, we discarded 0.15, 1.25, and 1.25% of the Zrs data in mice, rats, and rabbits, respectively. We also calculated the SD of the residuals between data and model fit and discarded those frequencies for which the real and/or imaginary parts of Zrs were more than two SDs away from the fit. All together, 1.97, 3.39, 0.41, and 2.78% of the Zrs data obtained in mice, rats, guinea pigs, and rabbits, respectively, were not used in the model fitting.

ANOVA was used to look for significant differences in the fitted model parameters due to the effects of species, PEEP, their interaction, and of a particular animal in one species. We found that the way in which the model parameter values depended on PEEP varied significantly among species; therefore, we used one-way ANOVA to investigate the effects of PEEP in each species. We also studied the differences in the parameter values among species for each PEEP. When appropriate, Tukey's honestly significant difference multiple pairwise comparisons were performed. Statistical significance was considered when $P < 0.05$.

RESULTS

Figures 1 and 2 show, respectively, NRrs and NXrs as functions of frequency for each of the species studied

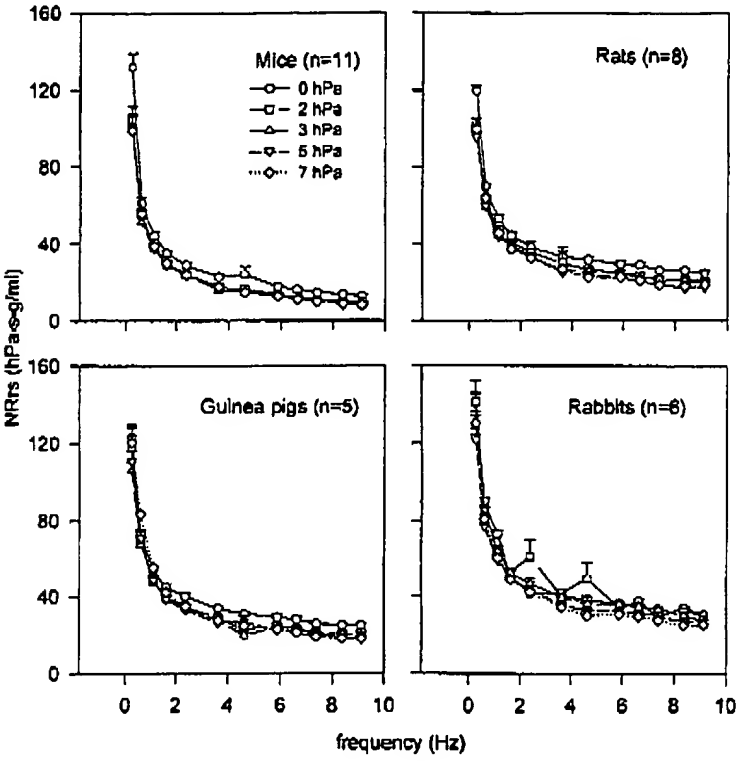

Fig. 1. Real parts of respiratory system impedance normalized to body weight (BW) (NRrs) in 4 different species. Values are means ± SE calculated for positive end-expiratory pressures (PEEPs) ranging between 0 and 7 hPa in each species.

at five different levels of PEEP. In each case, NRrs decreased monotonically, whereas NXrs increased monotonically with frequency. The resonant frequency was not attained in any of the animals by 9.125 Hz, as NXrs was always negative up to this frequency. Figure 1 also shows that mice had lower NRrs values at higher frequencies than did rats, guinea pigs, or rabbits. At the lowest frequency of 0.25 Hz and at 0-hPa PEEP, mice and rabbits had higher NRrs than did rats and guinea pigs. Above 6 Hz, NRrs decreased consistently with increasing PEEP. Figure 2 shows that mice and rabbits had lower NXrs at 0.25 Hz, in the absence of PEEP, than did rats and guinea pigs.

Figure 3 shows the PEEP dependence of the Zrs model parameters in the four species studied. NR tended to decrease with PEEP in all species and was very similar in rats and guinea pigs, lowest in mice, and highest in rabbits. NI was very small in magnitude and usually negative. Furthermore, when I was excluded from *Eq. 1* and the model was refitted to the Zrs data, there was essentially no change in the values of the remaining parameters. We, therefore, consider the influence of NI to be negligible over the frequency range studied. Mice and rats had higher values of NGti in the absence of PEEP than when PEEP was applied. NGti did not show any PEEP dependence in rabbits, and in guinea pigs NGti tended to increase at higher levels of PEEP. Differences in NGti among species were minor and occurred at a PEEP of 0 hPa between mice and rats and at PEEPs of 2 and 7 hPa between rats and rabbits. In all species, NHti tended to decrease with increasing PEEP until 5 hPa when there was an inflexion point, except in mice. At lower PEEPs, mice and rabbits had higher values of NHti than did rats and guinea pigs. The α and η were independent of PEEP in mice, but they showed a tendency to decrease and increase, respectively, with PEEP in rats and rabbits. In guinea pigs, the only difference noted was between PEEP levels of 0 and 2 hPa. Except when no PEEP was applied, mice showed values of α and η that were significantly different from those of other species.

The repeat set of measurements that was made in each animal was analyzed to establish the reproducibility of the results in time. The first and second measurements of R, Gti, Hti, α, and η at each of the five different levels of PEEP were compared. Paired t-test analysis showed no significant differences in almost all the parameters. Exceptions were found for Gti in guinea pigs at a PEEP of 7 hPa, for Hti in guinea pigs at PEEPs of 5 and 7 hPa, for Hti in rabbits at a PEEP of 0 hPa, and for α and η in mice at a PEEP of 2 hPa. However, the relative differences were always <9.1% for Hti and η, <3.1% for Gti, and <1% for α.

DISCUSSION

The present study was motivated by the wide utilization of rodents in the investigation of lung development and processes related to respiratory-system diseases. Although the species we used have been studied in the past (3, 4, 10, 14, 16, 17, 19, 21, 25–30, 32, 35–37, 39), very little has been reported about the Zrs

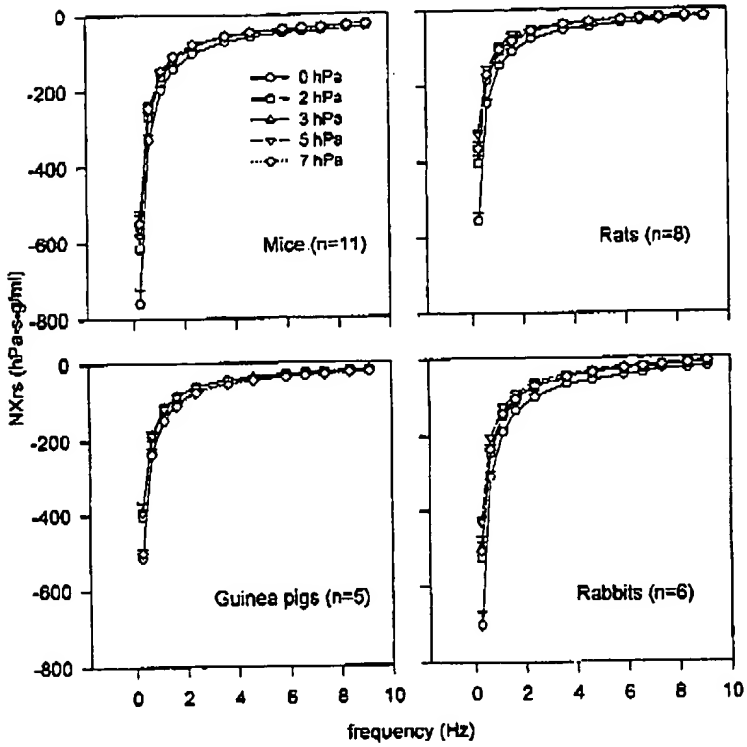

Fig. 2. Imaginary parts of respiratory system impedance normalized to BW (NXrs) in 4 different species. Values are means ± SE calculated for PEEPs ranging between 0 and 7 hPa in each species.

of mice, no doubt in part because of the technical difficulties associated with making the necessary measurements. Also, most of the comparative studies on mammalian respiratory mechanics have been performed during spontaneous tidal breathing, which allows animals to choose (and vary) their tidal volumes, breathing frequencies, and functional residual capacities. Furthermore, existing comparative data have been gathered from different sources in the literature; therefore, the methods used to assess mechanics were not always the same in the various species. Considering the present need to perform accurate measurements of Zrs in small rodents and the fact that Zrs depends markedly on frequency and lung volume (Figs. 1 and 2), there is clearly a need for comparative measurements of Zrs in various rodent species over a broad range of frequencies and at different levels of PEEP. This was the purpose of our study.

Zrs by itself can provide useful information regarding the state of the respiratory system, but the utilization of suitable models can greatly facilitate its interpretation. The model we used consists of an R and I leading to a constant-phase tissue compartment characterized by the dissipative parameter Gti and the elastic parameter Hti. It has been shown previously that this model provides extremely accurate fits to normal Zrs over the range of frequencies that we studied (12, 15, 17, 22, 31), despite having only four independent parameters. As in our laboratory's previous study in rats (17), we found I to make a negligible contribution to input impedance over the frequency range examined in the present study. Our laboratory's previous studies in dogs (2) and rats (17) have also shown that R contains contributions from both the chest wall tissues and the pulmonary airways, respectively, to varying degrees, depending on the species. Gti and Hti characterize the viscoelastic properties of the respiratory tissues.

To compare Zrs, R, I, Gti, and Hti among species, we multiplied them by BW. Alternatively, we could have normalized to lung volume. However, this can be misleading because lung volume at any particular inflation pressure depends on the elastic properties of the lungs and chest wall (23), and because respiratory elastance (Hti) is one of the parameters in which we are interested, we would be effectively normalizing it to itself. On the other hand, we could have normalized to lung weight. However, it is known that guinea pigs undergo marked bronchoconstriction after death, probably due to the release of substance P, which can increase vascular permeability and enhance edema formation (20). Therefore, the postmortem measurement of lung weight in guinea pigs would likely overestimate its value in vivo relative to the other species. Consequently, we decided that normalizing to BW was the most appropriate thing to do, especially as our mechanics parameters reflect not only the lungs but also chest wall properties (8). Also, the lungs of an animal serve its entire body and not just its lung tissue; therefore, it would seem to make sense to consider how our parameters relate to the entire body. Finally, normalizing a parameter with respect to BW allows it to be easily associated with metabolic rate,

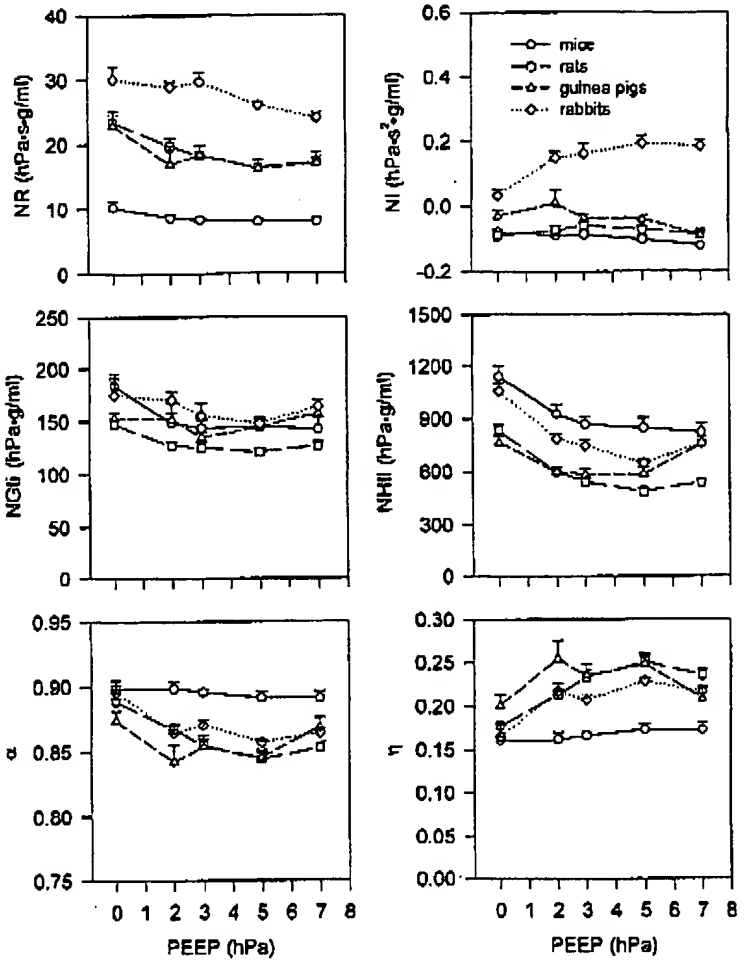

Fig. 3. Parameters of the constant-phase model fitted to respiratory system impedance data of mice (n = 11), rats (n = 8), guinea pigs (n = 5), and rabbits (n = 6) as a function of PEEP. Values are normalized to BW and represent means ± SE. NR, normalized Newtonian resistance; NI, normalized inertance; NGti, normalized tissue damping; NHti, normalized tissue elastance; $\alpha = (2/\pi)\arctan(Hti/Gti)$; η, hysteresivity.

which has been shown to follow BW to the 0.75 power in mammals (33).

NR and Raw. Our results show that NR tends to decrease with PEEP (Fig. 3), presumably due to increasing parenchymal tethering forces causing an increase in airway caliber. Moreover, NR increased from the smaller to the larger species. This appears to suggest that the airways of smaller species are relatively larger than those of larger species, although we must be careful in drawing such a conclusion because R contains contributions from both the airways and the chest wall tissues, although the relative amounts may vary with species. In dogs, for example, the chest wall and airways have been shown to make approximately equal contributions to the Newtonian resistive properties of the respiratory system (2), whereas in humans the chest wall has been reported to contribute 27% of R (5). Data collected by Rotger et al. (32) suggest that the chest wall contributes roughly one-third of R in rabbits. We have observed in mice that the lung contributes up to 50% of R over a range of lung volumes (unpublished observations), whereas in rats (17, 30) and cats (12) the chest wall contributes very little to the Newtonian properties of the respiratory system. Therefore, it is possible that the rank ordering of NR that we found in the present study (Fig. 3) may not be the same rank ordering of actual normalized Raw.

However, the notion that the rank orderings are indeed the same comes from a comparative respiratory mechanics review by Leith (21), who showed that Raw is related to BW over a wide range of species by

$$\text{Raw} = a(\text{BW})^b \qquad (4)$$

where a and b were determined by linear regression analysis, and the value of b varied between −0.86 and −0.70, depending on the source. The R data from our present study obtained at 0-hPa PEEP concur, insofar as R is an accurate reflection of Raw, giving an intermediate value of −0.75 (Fig. 4). These relationships again lead to the conclusion that relative Raw (i.e., normalized by the inverse of BW) increases with increasing animal size. Further support comes from Valerius (38), who studied silicone rubber lung casts of four species of myomorphic rodents and found that the volume of the conducting bronchial tree as a percentage of total lung volume was much smaller in the ~1.5-kg African giant pouched rat (*Cricetomys gambianus*) than in the 6-g harvest mouse (*Micromys*

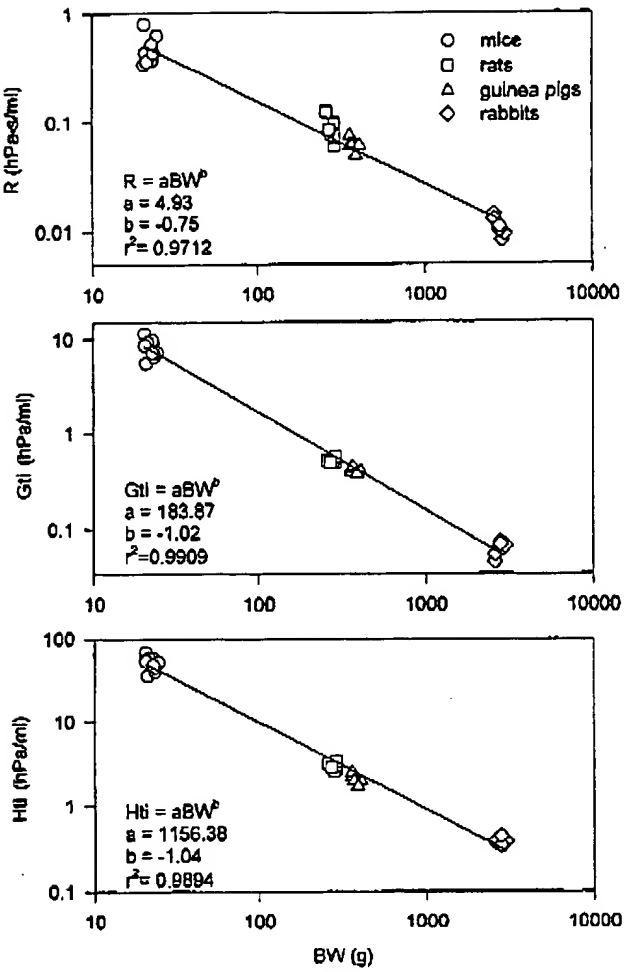

Fig. 4. Allometric relationships of the respiratory system model parameters obtained in normal mice (n = 11), rats (n = 8), guinea pigs (n = 5), and rabbits (n = 6) at 0-hPa PEEP. R, Newtonian resistance; Gti, tissue damping; Hti, tissue elastance. Solid line corresponds to the linear regression analysis of each parameter with BW on a log-log scale. r^2, Coefficient of determination; a and b, variables.

minutus). Valerius also noted a progressive decline with animal size in the relative diameter of the left main bronchus.

Resonant frequency. The resonance frequency was not reached by 9.125 Hz in any of the species we investigated (Fig. 2). This agrees with data obtained from studies on low-frequency forced oscillations in rats (14, 17), guinea pigs (39), and rabbits (37) and from studies on high-frequency oscillatory ventilation in rabbits (36). Petak et al. (30) were able to detect an inertive component in the respiratory system properties of rats using frequencies up to 21 Hz and concluded that the inertive component of Zrs is essentially determined by lung impedance, agreeing with data obtained from cats (12). The fact that our estimates of I were negligible for frequencies <9.125 Hz (Fig. 3) does not mean that there were no inertial elements in the airways but rather that inertial effects were minimal over the frequency range studied.

Effect of PEEP on tissue resistance. We found NGti in mice and rats to be higher at lower levels of PEEP (Fig. 3), agreeing with previous finding in rats (17). It has been shown in both rats and dogs that the chest wall resistance is independent of mean Pao (1, 17). Therefore, the negative dependence of Gti with lung volume is fully attributable to the lung and most likely reflects air space closure occurring at lower levels of PEEP. However, in rabbits, NGti was not dependent on end-expiratory volume, and in guinea pigs, there was a slight rise in NGti at the highest level of PEEP compared with intermediate lung volumes (Fig. 3). Because smaller animals are known to have more compliant chest walls, the relaxation volume normalized to lung size in these animals is usually lower than in larger animals (10). Therefore, the mice and rats in this study could have been ventilated at proportionately lower lung volumes at a given level of PEEP compared with other rodents, thus explaining the differences we found among species.

Nagase et al. (25, 26, 28, 29) used the alveolar capsule technique to partition lung resistance into its airway and tissue components in mice, rats, guinea pigs, and rabbits. They showed that lung tissue resistance increased significantly with PEEP. In rabbits this increase was compensated for by a decrease in Raw (29) so that total lung resistance was maintained. In mice, rats, and guinea pigs, total lung resistance increased with PEEP, despite a reduction in Raw (25, 26, 28). Other studies utilizing alveolar capsules in guinea pigs and rabbits confirm that lung tissue resistance increases substantially with lung volume (19, 35). Dogs also exhibit an increase in lung resistance as mean Paw increases, but the most striking increases in resistance occurred at levels of Paw corresponding to volumes below the relaxation volume (1). Dechman et al. (7) showed lung resistance in dogs to have a minimum at a PEEP of 3–4 hPa. They attributed the increase in resistance above this PEEP level to the nonlinear viscoelastic properties of lung tissue, whereas the increase in resistance at low PEEP levels was attributed to air space closure. The differences between our results and the previous ones by Nagase et al. (25, 26, 28, 29) in rodents are probably due to the considerably different volume amplitudes utilized for the assessment of respiratory mechanics.

Effects of PEEP on Hti. The dependence of respiratory system elastance on PEEP was marked by a decline in NHti at lower levels of lung inflation in all species followed by an increase at 5 hPa, except in mice (Fig. 3). These results confirm a previous study in rats (17), in which Hti as a function of lung volume for both the lung and chest wall exhibited minima. Presumably the increasing values of NHti at low levels of PEEP reflect alveolar collapse and/or airway closure resulting from reduced airway-parenchymal interdependence forces, although nonlinear chest wall elastic properties may also have contributed to this phenomenon. The increase in NHti at higher levels of lung

inflation was probably due to the nonlinear elastic tissue properties of both chest wall and lungs. The absence of a clear minimum in the NHti curve for mice may reflect the fact that smaller animals with comparatively floppier chest walls have relatively lower lung volumes at a given PEEP. The range of PEEPs studied would then not have been sufficient to push the lungs and chest wall into the upper nonlinear portions of their respective pressure-volume curves. Another possibility is that an increase in NHti for the lung may have been compensated for by a decrease in NHti for the chest wall, because we know that in rats the minima in these two quantities occur at different inflation volumes (17). The lung volume dependence of pulmonary elastance has been previously studied in small rodents with the use of the alveolar capsule technique (19, 25, 26, 28, 29, 35), and in all animals a sharp increase in dynamic elastance with lung inflation has been reported. Nagase et al. (25, 26, 28, 29) studied lung mechanics at transpulmonary pressures as low as 3 hPa in mice, rats, guinea pigs, and rabbits but could not detect a fall in elastance at very low lung volumes, confirming the results of Shardonofsky et al. (35) in rabbits ventilated against PEEPs of 2–4.6 hPa. Most probably, the difference between our results and theirs is due to the fact that we used very-small-amplitude volume oscillations, whereas the alveolar capsule technique was performed during tidal ventilation.

Tissue mechanics among species. Leith (21) showed that chest wall compliance increases with BW to the 0.86 power, whereas lung compliance increases with BW to a power between 1.08 and 1.20. When Leith used respiratory system elastance in the equivalent of *Eq. 4*, he found a value for b of -1.04, which is the exact value we found for Hti (Fig. 4). However, mice and rabbits had relatively more rigid respiratory systems at low PEEPs than did rats and guinea pigs (Fig. 3). This may have been due to differences in the relative compliances of the lung and chest wall among species. However, the chest wall contribution to respiratory system elastance is ~35% in mice (16) and 20% in rabbits (32). Therefore, it seems unlikely that a relatively increased chest wall elastance in rabbits would solely account for a higher NHti in rabbits than in rats or guinea pigs.

Alternatively, Haber et al. (11) showed that surface forces have a predominant influence on the elastic properties of the lung at volumes higher than functional residual capacity, which implicates alveolar size as the major determinant of specific pulmonary elastance for a constant number of alveoli. We used the data of Mercer et al. (24) to calculate lung volume in various species as the product of the number of alveoli per lung and the mean alveolar volume. We then assumed elastance to be inversely proportional to lung volume and calculated lung elastance normalized to BW relative to that of the mouse (Fig. 5). Although the normalized lung elastances decreased with size for most species, rabbits and mice had very similar pulmonary distensibilities because of the unusually small alveoli in the rabbit (24). We compared these values

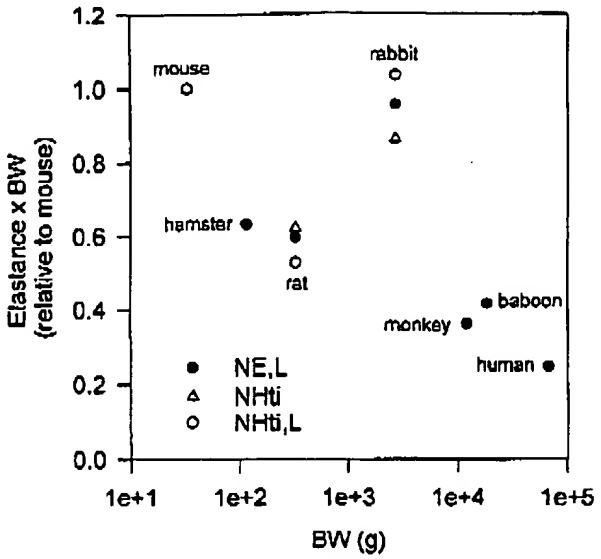

Fig. 5. Elastances normalized to BW and relative to the mouse values as a function of BW in different species. NE,L, normalized pulmonary elastance estimated from total alveolar volume obtained from Mercer et al. (24); NHti,L, normalized pulmonary tissue elastance.

with estimates of NHti for the lung in mice, rats, and rabbits by assuming that the lung accounted for 65% of respiratory system NHti in the mouse, 55% in the rat, and 80% in the rabbit (16, 17, 30, 32). Figure 5 shows that our estimates of normalized pulmonary NHti agree well with the literature-derived values of lung elastance. It thus seems likely that mice and rabbits have relatively higher NHti compared with rats and guinea pigs because of proportionately smaller total air space volumes.

We found Gti to vary with BW to the -1.02 power, which is very similar to the relationship we found for Hti (Fig. 4). This means that Gti and Hti should have a constant ratio; therefore, η should be independent of animal size. Although η was essentially constant in mice over the PEEP range studied, rats, guinea pigs, and rabbits showed values of η that varied with PEEP (Fig. 3). Hirai et al. (17) reported a modest variation in η with lung volume for the respiratory system in rats that was due to only a slight variation in η for the lung but a marked variation in η for the chest wall. Lung η has also been shown not to be affected by transpulmonary pressures between 3 and 11 hPa in mice (28) and between 2 and 4.6 hPa in rabbits (35), whereas hyperinflated guinea pig lungs ventilated with normal tidal volume had reduced η (19). This suggests that the observed PEEP dependence of respiratory system η that we found was due to the chest wall.

Finally, we must consider some potential shortcomings of our study. In making a comparison among species, it is important to keep experimental conditions and protocols as similar as possible for the different animals. It is impossible to do this perfectly, especially when animals of different sizes are examined. In our

study, for example, we had to ventilate the different rodents with tidal volumes and frequencies pertaining to their respective breathing patterns. However, the actual measurements of respiratory mechanics were made by using the same volume perturbation waveform in each animal, scaled in amplitude according to the various animals' tidal volumes. In this way, we hoped to avoid the confounding effects of frequency, amplitude, and PEEP that are known to affect the mechanical behavior of the respiratory system to a significant degree (1, 12–17, 30–32, 35). Another potential source of variability in our measurements was the fact that we did not use the same anesthetic and paralyzing agents in all species. Our experience is that different species are best treated with different drugs, especially in terms of the paralyzing agent used (complete paralysis is essential for the accurate determination of respiratory impedance). This raises the question as to whether our results could have been affected by these differences in drug treatment. We cannot know for sure. However, we suspect that the effects were negligible because the results we obtained in the different species scaled generally with animal size, with those departures being interpretable in terms of the previously reported differences in relative airway size between large and small animals.

In summary, we performed a comparative study of Zrs in mice, rats, guinea pigs, and rabbits using a computer-controlled SAV. We interpreted Zrs in terms of a constant-phase tissue model in series with a R and I. We documented the PEEP dependencies of airway and tissue properties in these animals and interpreted our observations in terms of various physiological phenomena, such as air space recruitment and airway-parenchymal interdependence. We also showed that R is proportionately higher in larger animals, probably due to the relatively smaller increase in airway caliber as size increases. We also argued that a relatively smaller total air space volume could explain the higher values of Hti that we found in mice and rabbits. We thus conclude that a detailed, comparative study of respiratory system mechanics shows evidence of some structural differences among the lungs of various species, although, overall, the rodents that we studied had respiratory mechanics that scaled according to BW in a similar fashion to that reported in other species (21). This suggests that the lungs of the rodents that we studied differ from those of larger species essentially only in terms of scale, which supports their validity as general-purpose models of the human lung.

We acknowledge the Medical Research Council of Canada; the Fonds de la Recherche en Santé du Québec, Inspiraplex; the JT Costello Memorial Research Fund; and the National Heart, Lung, and Blood Institute (Grant HL-48522).

REFERENCES

1. **Barnas GM and Sprung J.** Effects of mean airway pressure and tidal volume on lung and chest wall mechanics in the dog. *J Appl Physiol* 74: 2286–2293, 1993.
2. **Bates JHT, Abe T, Romero PV, and Sato J.** Measurement of alveolar pressure in closed-chest dogs during flow interruption. *J Appl Physiol* 67: 488–492, 1989.
3. **Bates JHT, Schuessler TF, Dolman C, and Eidelman DH.** Temporal dynamics of acute isovolume bronchoconstriction in the rat. *J Appl Physiol* 82: 55–62, 1997.
4. **Bennet FM and Tenney SM.** Comparative mechanics of mammalian respiratory system. *Respir Physiol* 49: 131–140, 1982.
5. **D'Angelo E, Prandi E, Tavola M, Calderini E, and Milic-Emili J.** Chest wall interrupter resistance in anesthetized paralyzed humans. *J Appl Physiol* 77: 883–887, 1994.
6. **Daroczy B and Hantos Z.** Generation of optimum pseudorandom signals for respiratory impedance measurements. *Int J Biomed Comput* 25: 21–31, 1990.
7. **Dechman G, Lauzon A-M, and Bates JHT.** Mechanical behavior of the canine respiratory system at very low lung volumes. *Respir Physiol* 95: 119–129, 1994.
8. **Fisher JT and Mortola JP.** Statics of the respiratory system in newborn mammals. *Respir Physiol* 41: 155–172, 1980.
9. **Fredberg JJ and Stamenovic D.** On the imperfect elasticity of lung tissue. *J Appl Physiol* 67: 2408–2419, 1989.
10. **Gillespie JR.** Mechanisms that determine functional residual capacity in different mammalian species. *Am Rev Respir Dis* 128: S74–S77, 1983.
11. **Haber PS, Colebatch HJH, Ng CKY, and Greaves IA.** Alveolar size as a determinant of pulmonary distensibility in mammalian lungs. *J Appl Physiol* 54: 837–845, 1983.
12. **Hantos Z, Adamicza A, Govaerts E, and Daroczy B.** Mechanical impedances of lungs and chest wall in the cat. *J Appl Physiol* 73: 427–433, 1992.
13. **Hantos Z, Daroczy B, Csendes T, Suki B, and Nagy S.** Modeling of low-frequency pulmonary impedance in dogs. *J Appl Physiol* 68: 849–860, 1990.
14. **Hantos Z, Daroczy B, Suki B, and Nagy S.** Low-frequency respiratory mechanical impedance in the rat. *J Appl Physiol* 63: 36–43, 1987.
15. **Hantos Z, Daroczy B, Suki B, Nagy S, and Fredberg JJ.** Input impedance and peripheral inhomogeneity of dog lungs. *J Appl Physiol* 72: 168–178, 1992.
16. **Hirai T and Bates JHT.** Lung and chest wall mechanics in relation to lung volume in the mouse (Abstract). *Am J Respir Crit Care Med* 159: A833, 1999.
17. **Hirai T, McKeown KA, Gomes RFM, and Bates JHT.** Effects of lung volume on lung and chest wall mechanics in rats. *J Appl Physiol* 86: 16–21, 1999.
18. **Horsfield K.** Some mathematical properties of branching trees with application to the respiratory system. *Bull Math Biol* 38: 305–315, 1976.
19. **Ingenito EP, Davison B, and Fredberg JJ.** Tissue resistance in the guinea pig at baseline and during methacholine constriction. *J Appl Physiol* 75: 2541–2548, 1993.
20. **Lai Y-L and Cornett AF.** Substance P-inducing massive postmortem bronchoconstriction in guinea pig lungs. *J Appl Physiol* 62: 746–751, 1987.
21. **Leith DE.** Comparative mammalian respiratory mechanics. *Am Rev Respir Dis* 128: S77–S82, 1983.
22. **Lutchen KR, Suki B, Zhang Q, Petak F, Daroczy B, and Hantos Z.** Airway and tissue mechanics during physiological breathing and bronchoconstriction in dogs. *J Appl Physiol* 77: 373–385, 1994.
23. **Mead J.** Mechanical properties of lungs. *Physiol Rev* 41: 281–330, 1961.
24. **Mercer RR, Russel ML, and Capro JD.** Alveolar septal structure in different species. *J Appl Physiol* 77: 1060–1066, 1994.
25. **Nagase T, Fukuchi Y, Teramoto S, Matsuse T, and Orimo H.** Mechanical interdependence in relation to age: effects of lung volume on airway resistance in rats. *J Appl Physiol* 77: 1172–1177, 1994.
26. **Nagase T, Ito T, Yanai M, Martin JG, and Ludwig MS.** Responsiveness of and interactions between airways and tissue in guinea pigs during induced constriction. *J Appl Physiol* 74: 2848–2854, 1993.
27. **Nagase T, Martin JG, and Ludwig MS.** Comparative study of mechanical interdependence: effect of lung volume on Raw during induced constriction. *J Appl Physiol* 75: 2500–2505, 1993.

28. **Nagase T, Matsui H, Aoki T, Ouchi Y, and Fukuchi Y.** Lung tissue behavior in the mouse during constriction induced by methacholine and endothelin-1. *J Appl Physiol* 81: 2373–2378, 1996.
29. **Nagase T, Matsui H, Sudo E, Matsuse T, Ludwig MS, and Fukuchi Y.** Effects of lung volume on airway resistance during induced constriction in papain-treated rabbits. *J Appl Physiol* 80: 1872–1879, 1996.
30. **Petak F, Hall GL, and Sly PD.** Repeated measurements of airway and parenchymal mechanics in rats by using low-frequency oscillations. *J Appl Physiol* 84: 1680–1686, 1998.
31. **Petak F, Hantos Z, Adamicza A, and Daroczy B.** Partitioning of pulmonary impedance: modeling vs. alveolar capsule approach. *J Appl Physiol* 75: 513–521, 1993.
32. **Rotger M, Peslin R, Navajas D, and Farré R.** Lung and respiratory impedance at low frequency during mechanical ventilation in rabbits. *J Appl Physiol* 78: 2153–2160, 1995.
33. **Schmidt-Nielsen K.** Energy metabolism, body size, and problems of scaling. *Fed Proc* 29: 1524–1532, 1970.
34. **Schuessler TF and Bates JHT.** A computer-controlled research ventilator for small animals: design and evaluation. *IEEE Trans Biomed Eng* 42: 860–866, 1995.
35. **Shardonofsky FR, McDonough JM, and Grunstein MM.** Effects of positive end-expiratory pressure on lung tissue mechanics in rabbits. *J Appl Physiol* 75: 2506–2513, 1993.
36. **Sipinkova I, Koller EA, Buess C, and Kohl J.** Mechanical respiratory system input impedance during high-frequency oscillatory ventilation in rabbits. *Crit Care Med* 22: S66–S70, 1994.
37. **Tepper R, Sato J, Suki B, Martin JG, and Bates JHT.** Low-frequency pulmonary impedance in rabbits and its response to inhaled methacholine. *J Appl Physiol* 73: 290–295, 1992.
38. **Valerius K-P.** Size-dependent morphology of the conductive bronchial tree in four species of myomorph rodents. *J Morphol* 230: 291–297, 1996.
39. **Watson JW, Jackson AC, and Drazen JM.** Effect of lung volume on pulmonary mechanics in guinea pigs. *J Appl Physiol* 61: 304–311, 1986.

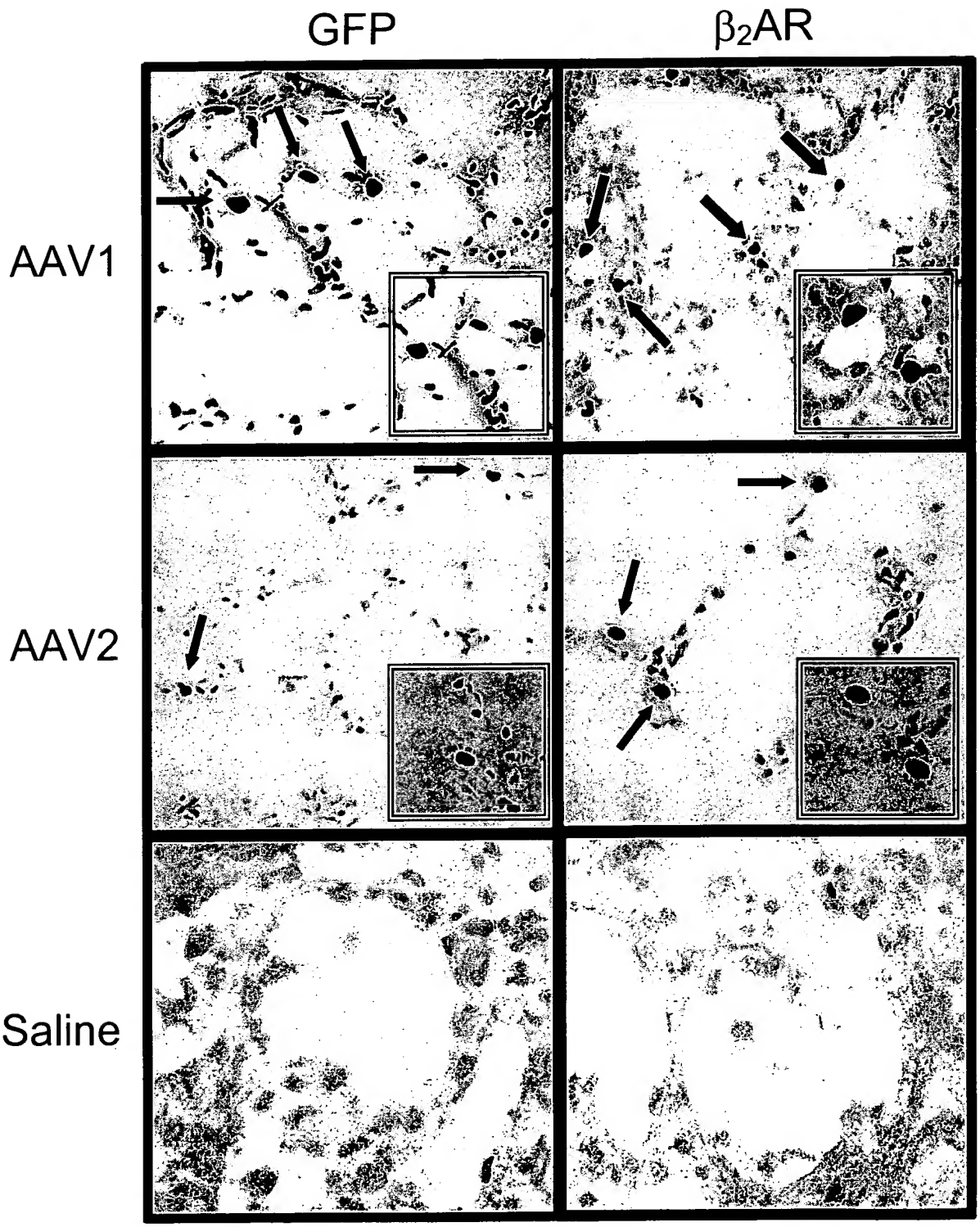

FIGURE 2

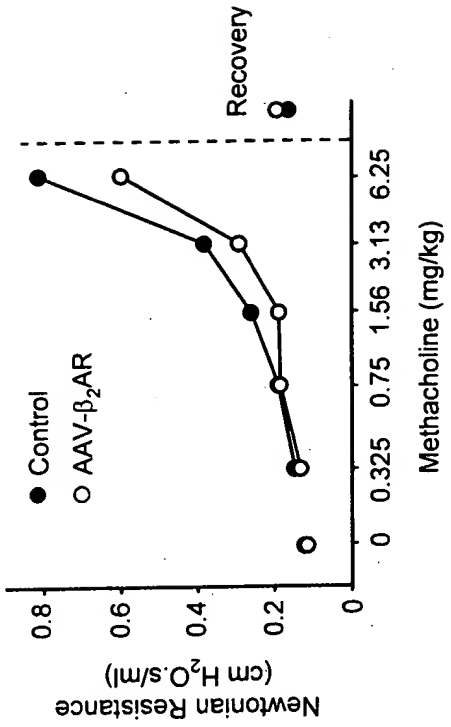
Newtonian Resistance
(cm H2O.s/ml)
0.8
0.6
0.4
0.2
0
Control
AAV-β2AR
Recovery
0
0.325
0.75
1.56
3.13
6.25
Methacholine (mg/kg)

FIGURE 3

Characterization of allergen-induced bronchial hyperresponsiveness and airway inflammation in actively sensitized Brown-Norway rats

Wayne Elwood, BSc, Jan O. Lötvall, MD, PhD, Peter J. Barnes, DSc, FRCP, and K. Fan Chung, MD, MRCP *London, England*

Bronchial responsiveness to inhaled acetylcholine (ACh) and inflammatory cell recruitment in bronchoalveolar lavage fluid (BALF) were studied in inbred Brown-Norway rats actively sensitized to, and later exposed to, ovalbumin (OA). We examined animals 21 days after initial sensitization at 18 to 24 hours, or 5 days after a single challenge, or after the last of seven repeated exposures administered every 3 days. BALF was examined as an index of inflammatory changes within the lung. Animals repeatedly exposed to OA aerosols had an increased baseline lung resistance and a significant increase in bronchial responsiveness to inhaled ACh compared to control animals at both 18 to 24 hours and 5 days after the last OA exposure. Sensitized animals receiving a single OA aerosol also demonstrated bronchial hyperresponsiveness (BHR) to inhaled ACh ($p < 0.01$) at 18 to 24 hours of a similar order as the multiple-exposed group. There was a significant increase in eosinophils, lymphocytes, and neutrophils in BALF at 18 to 24 hours but not at 5 days after single or multiple exposure to OA aerosol in the sensitized groups. Control animals demonstrated no changes in bronchial responsiveness, although a small but significant increase in inflammatory cells was observed compared to saline-only treated animals. There was a significant correlation between bronchial responsiveness and eosinophil counts in the BALF in the single allergen-exposed group ($R_s = 0.68$; $p < 0.05$). We conclude that (1) BHR after allergen exposure in sensitized rats is associated with the presence of pulmonary inflammation but persists despite the regression of inflammatory cells in BALF after multiple OA exposures, and (2) this rat model has many characteristics of human allergen-induced BHR. (J ALLERGY CLIN IMMUNOL 1991;88:951-60.)

Key words: Brown-Norway rats, bronchial hyperresponsiveness, active sensitization, ovalbumin, bronchoalveolar lavage

BHR to a wide variety of bronchoconstrictor stimuli is a characteristic feature of asthma[1, 2] and is closely related with the severity and frequency of asthma symptoms.[3] Although the precise mechanism(s) of this phenomenon have not been elucidated, considerable attention has been focused on the role of airway inflammation in the pathophysiology of BHR. Experimental studies in several animal models, including dog, rabbit, and sheep, have demonstrated a close temporal association between the degree of inflammatory cell infiltration in the airway wall and the development of BHR induced by several stimuli, in-

Abbreviations used

ACh:	Acetylcholine
BHR:	Bronchial hyperresponsiveness
BALF:	Bronchoalveolar lavage fluid
OA:	Ovalbumin
PC_{200}:	Provocative concentration producing 200% increase in lung resistance
R_L:	Lung resistance
R_s:	Spearman's rank-correlation coefficient
$Al(OH)_3$:	Aluminium hydroxide
ip:	Intraperitoneal
Ab:	Antibody
EOS:	Eosinophil

From the Department of Thoracic Medicine, National Heart and Lung Institute, and Royal Brompton National Heart and Lung Hospital, London, England.

Supported by the National Asthma Campaign (U.K.), and Medical Research Council (U.K.).
Received for publication March 14, 1991.
Revised June 25, 1991.
Accepted for publication July 5, 1991.

Reprint requests: K. F. Chung, MD, Department of Thoracic Medicine, National Heart and Lung Institute, Dovehouse St., London SW3 6LY, England.

1/1/32249

TABLE I. Characteristics of eight experimental groups and procedures performed for each group

Group	N	Body weight (g)	Ip Injection (× 3)	Aerosol exposure	Baseline R_L (cm H_2O $ml^{-1}s^{-1}$)	Challenge (time after last exposure)
A	9	265 ± 10	Saline	Saline (× 1)	0.44 ± 0.03	18-24 hr
B	8	248 ± 10	$Al(OH)_3$	—	0.46 ± 0.03	—
C	6	255 ± 8	OA plus $Al(OH)_3$	—	0.53 ± 0.01	—
D	5	243 ± 12	—	OA (× 1)	0.51 ± 0.03	18-24 hr
E	11	240 ± 14	OA plus $Al(OH)_3$	OA (× 1)	0.49 ± 0.05	18-24 hr
F	8	253 ± 11	OA plus $Al(OH)_3$	OA (× 7)	0.60 ± 0.05*	18-24 hr
G	5	260 ± 18	OA plus $Al(OH)_3$	OA (× 7)	0.53 ± 0.06	5 days
H	6	257 ± 14	OA plus $Al(OH)_3$	OA (× 1)	0.43 ± 0.03	5 days

*$p < 0.01$ compared to saline-exposed group.

cluding allergen and ozone.[4] In the sensitized dog, rabbit, and sheep,[5, 6] allergen exposure causes an increase in bronchial responsiveness associated with a neutrophilia in BALF. Allergen challenge in sensitized guinea pigs[7, 8] and monkeys,[9, 10] however, produces an EOS influx into the airways, and these animals have been proposed as better models for human asthma because the EOS, rather than the neutrophil, appears to be a more prominent cell in the airway submucosa of patients with asthma. Similar studies have been performed in sensitized rats that are known to develop specific Abs of the IgE class,[11, 12] in contrast to guinea pigs that usually demonstrate the presence of IgG Abs.[13] After allergen exposure, these rats develop both an acute and a late bronchoconstrictor response,[12] and increases in bronchial responsiveness to methacholine[14] similar to the responses observed in human subjects with asthma.[15]

We have characterized further this model by studying the effect of allergen challenge on bronchial responsiveness and on the influx of cells into the lungs and airways with BAL. We examined the duration of the induced BHR and determined whether repeated exposure to aerosolized allergen compared to a single allergen exposure could further enhance and prolong this BHR and its accompanying inflammatory response. In addition, we examined the effects of sensitization per se, of treatment with adjuvant only and of exposure of unsensitized animals to OA aerosol on bronchial responsiveness and cellular composition of BALF.

METHODS

Sensitization procedures and allergen exposure

We studied eight separate groups of inbred male Brown-Norway rats weighing 200 to 350 g. Seven of the eight groups were administered ip injections on days 1, 2, and 3. The object of the eight groups used was (1) to determine the effects of a single or multiple exposure to allergen after ip sensitization, (2) to compare the time course after the last allergen exposure between 18 to 24 hours and 5 days in the single- and multiple-exposure groups, (3) to determine the effect of ip sensitization per se and of adjuvant alone, and (4) to examine the effect of aerosolized allergen exposure in unsensitized animals. The groups are summarized in Table I and were as follows:

Group A (saline). One milliliter of saline was injected intraperitoneally, followed 21 days later by a single saline-aerosol exposure for 15 minutes. Animals were studied 18 to 24 hours later.

Group B (Al(OH)$_3$ only). One milliliter of a 100 mg $Al(OH)_3$ in 0.9% (wt/vol) saline suspension was injected intraperitoneally but no aerosol exposure.

Group C (sensitized; no allergen aerosol exposure). One milliliter of a 1 mg OA/100 mg $Al(OH)_3$ in 0.9% (wt/vol) saline suspension was injected intraperitoneally; this group was not exposed to allergen.

Group D (allergen aerosol exposure only). Naive animals were exposed to a 1% OA aerosol for 15 minutes; animals were studied 18 to 24 hours later.

Group E (single allergen aerosol exposure). One milliliter of a 1 mg OA/100 mg $Al(OH)_3$ in 0.9% (wt/vol) saline suspension was injected intraperitoneally, followed 21 days later by a single exposure to 1% OA aerosol for 15 minutes; animals were studied 18 to 24 hours later.

Group F (chronic allergen aerosol exposure). One milliliter of a 1 mg OA/100 mg $Al(OH)_3$ in 0.9% (wt/vol) saline suspension was injected intraperitoneally, followed by exposure to 1% OA aerosol for 15 minutes administered every third day for a 21-day period; animals were studied 18 to 24 hours after their last exposure.

Group G (5 days after chronic allergen aerosol exposure). One milliliter of a 1 mg OA/100 mg $Al(OH)_3$ in 0.9% (wt/vol) saline suspension was injected intraperitoneally, followed by exposure to 1% OA aerosol for 15 minutes administered every third day for a 21-day period; animals were studied 5 days after their last exposure.

Group H (5 days after single allergen aerosol exposure). One milliliter of a 1 mg OA/100 mg $Al(OH)_3$ in 0.9% (wt/vol) saline suspension was injected intraperitoneally,

followed 21 days later by a single exposure to 1% OA aerosol for 15 minutes; animals were studied 5 days later.

Aerosol exposure was accomplished by placing the rats in a 6.5 liter plexiglass chamber connected to a DeVilbiss PulmoSonic nebulizer (model No. 2512, DeVilbiss Health Care, U.K., Ltd., Feltham, Middlesex, U.K.) that generated an aerosol mist pumped into the exposure chamber by the airflow supplied by a small animal ventilator set at 60 strokes/min^{-1} with a pumping volume of 10 ml.

Measurement of lung function and airway responsiveness to ACh

For measurement of airway responsiveness, rats were anesthetized with an initial dose of 60 to 80 mg/kg of pentobarbitone injected intraperitoneally. Additional pentobarbitone was administered as required to maintain adequate anesthesia. A tracheal cannula (10 mm length and 1.3 mm internal diameter) was inserted into the lumen of the cervical trachea through a tracheostomy and tied snugly with suture material. A polyethylene catheter was inserted into the left carotid artery to monitor blood pressure and heart rate with a pressure transducer. The right external jugular vein was cannulated for administration of intravenous drugs and fluids. Animals were then connected to a small animal respirator (Harvard Apparatus, Ltd., Edenbridge, Kent, U.K.) and ventilated with 10 ml/kg^{-1} air at a rate of 90 strokes/min^{-1}. Transpulmonary pressure was measured with a pressure transducer (model FCO 40; ± 1000 mm of H_2O, Furness Controls, Ltd., Bexhill, Sussex, U.K.) with one side attached to an air-filled catheter inserted into the right pleural cavity and the other side attached to a catheter connected to a side port of the intratracheal cannula. The ventilatory circuit had a total volume of 20 ml. Airflow was measured with a pneumotachograph (model F1L; Mercury Electronics, Ltd., Glasgow, Scotland) connected to a transducer (model FCO 40; ± 20 mm of H_2O, Furness Controls, Ltd.). The signals from the transducers were digitalized with a 12-bit analog-digital board (NB-MIO-16, National Instruments, Austin, Texas) connected to a Macintosh II computer (Apple Computer Inc., Cupertino, Calif.) and analyzed with a software (LabView, National Instruments), which was programmed to instantaneously calculate R_L according to the method of von Neergard and Wirz.[16] Transpulmonary pressure and mean blood pressure were also monitored throughout the experiments. Aerosols were generated with an ultrasonic nebulizer (model 2511; PulmoSonic, DeVilbiss Co., Pa.) and were administered to the airways through a separate ventilatory system that bypassed the pneumotachograph. The volume of this circuit was 50 ml. The mean mass diameter of the aerosol was 3.8 μm, with a geometric standard deviation of 1.3, measured with a laser droplet and particle analyzer (model 2600C, Malvern Instruments, Derbyshire, U.K.).

Animals were initially injected with propranolol (1 mg/kg intravenously) to inhibit adrenergic effects. A dose of inhaled saline was administered for 45 breaths, and the subsequent R_L value was used as baseline. Starting 3 minutes after saline exposure, increasing half-log_{10} concentrations of ACh were administered by inhalation (45 breaths) with the initial concentration set at 10^{-4} mol/L. Increasing concentrations were administered at 5- to 7-minute intervals with one hyperinflation of twice the tidal volume applied between each ACh concentration, performed by manually blocking the outflow of the ventilator. The challenge was stopped when an increase in R_L exceeding 200% over the initial baseline was obtained. PC_{200} was calculated by log-linear interpolation of concentration-response curves from individual animals.

BAL and cell counting

After measurement of lung-function parameters, rats were administered an overdose of sodium pentobarbitone (100 mg/kg^{-1} intravenously), and lungs were lavaged with 10 × 2 ml aliquots of 0.9% wt/vol of sterile saline through a polyethylene tube introduced through the tracheostomy. Lavage fluid was centrifuged (500 *g* for 10 minutes at 4° C), and the cell pellet was resuspended in 0.5 ml of Hanks' balanced salt solution. Total cell counts were made by adding 10 μl of the cell suspension to 90 μl of Kimura stain and counted in a Neubauer (American Optical Corp., Southbridge, Mass.) chamber under a light microscope. Differential cell counts were made from cytospin preparations stained by May-Grünwald stain. Cells were identified as EOSs, lymphocytes, neutrophils, and macrophages by standard morphology and 500 cells counted under ×400 magnification, and the percentage and absolute number of each cell type were calculated.

Drugs

We used the following drugs: OA (grade V, salt free) and ACh (Sigma Chemical Co., Poole, Dorset, U.K.), aluminum hydroxide (BDH Chemicals Ltd., Dorset, Poole, U.K.), propranolol (Inderal, ICI, plc, Macclesfield, Cheshire, U.K.), and pentobarbitone sodium (Sagatal, May & Baker, Ltd., Dagenham, U.K.).

Data analysis

PC_{200} data have been log_{10} transformed and are reported as mean $-\log PC_{200}$ ± SEM. Nonparametric analysis of variance (Kruskal-Wallis method) was used to determine significant variance among the eight groups. If a significant variance was found, we used Mann-Whitney U test to analyze for significant difference between individual groups, and since more than one comparison was made, a p value of <0.01 was considered significant. Spearman rank-correlation coefficient (Rs) was used to analyze the relationship between variables. Data were analyzed with a Macintosh computer (Apple Computer Inc.) with standard statistical packages.

RESULTS

Baseline analysis

Baseline R_L and body weight are presented for each individual group in Table I. A single allergen exposure (group E) did not significantly increase the baseline R_L 18 to 24 hours later compared to the saline-exposed

group (group A). However, after repeated allergen exposure (group F), baseline R_L was significantly higher than after saline exposure only ($p < 0.01$) (Table I).

Aerosol exposure

Animals sensitized by ip injection of 1 ml of 1 mg OA/100 mg $Al(OH)_3$ responded when they were exposed to an aerosol of 1% OA solution by demonstrating obvious respiratory distress characterized by the development of a defensive posture and exaggerated labored breathing motions. This immediate response started within 3 to 5 minutes of aerosol administration, but its appearance did not result in the death of any animal nor did it necessitate the use of protective drug cover. All animals recovered spontaneously from aerosol exposure. Animals administered saline intraperitoneally and then exposed to a subsequent saline aerosol did not demonstrate this immediate response, nor did unsensitized animals exposed to aerosolized allergen.

Airway responsiveness

Inhaled ACh caused a concentration-dependent increase in R_L. Individual peak R_L responses at each challenge concentration for animals in groups A, E, and F are illustrated in Fig. 1. After inhalation of each concentration of ACh, peak R_L was reached within 45 seconds and recovered during 2 to 5 minutes. Mean $-\log PC_{200}$ values for all the groups are also illustrated in Fig. 2.

The airway responsiveness of the three groups that received the adjuvant $Al(OH)_3$ only (group B), OA with $Al(OH)_3$ without a subsequent allergen aerosol exposure (group C), and the group that only received an allergen aerosol exposure (group D) demonstrated a small but nonsignificant change in responsiveness compared to saline-only treated animals (group A) that had a $-\log PC_{200}$ value of 1.8 ± 0.12 mol/L of ACh.

The two groups that had been intraperitoneally sensitized and then exposed to either a single or a multiple allergen challenge and tested 18 to 24 hours after the last exposure (groups E and F) were significantly more responsive ($p < 0.01$) than the four control groups. Hyperresponsiveness to ACh was also present when the chronic allergen-exposed rats were tested 5 days after their last aerosol exposure (group G) with a mean $-\log PC_{200}$ value of 2.6 ± 0.12 mol/L of ACh ($p < 0.01$). The group of sensitized animals administered a single allergen exposure and tested 5 days later (group H) was not significantly more responsive than the control group A.

The greatest increase in responsiveness was observed in the chronic allergen-exposed group (group F) with a $-\log PC_{200}$ value of 2.9 ± 0.19 mol/L of ACh, which is approximately a tenfold increase in airway responsiveness compared to the saline-treated group ($p < 0.01$). However, the single allergen aerosol-exposed rats (group E) produced a similar increase in airway responsiveness to those chronically exposed, revealing a $-\log PC_{200}$ value of 2.6 ± 0.11 mol/L of ACh.

Cellular content of BALF

BALF recovered from sensitized animals that had been exposed to a 1% OA aerosol had significantly increased total cell numbers 18 to 24 hours later (group E, $4.33 \pm 0.55 \times 10^6$; group F, $4.29 \pm 0.92 \times 10^6$) ($p < 0.01$) compared both to saline-treated animals (group A, $2.18 \pm 0.39 \times 10^6$) or to animals not exposed to allergen aerosol (group B, $1.92 \pm 0.34 \times 10^6$; group C, $1.47 \pm 0.10 \times 10^6$) or to unsensitized animals exposed to 1% OA (group D, $1.91 \pm 0.48 \times 10^6$) (Fig. 3).

There was a significant preferential increase in the numbers of EOSs and lymphocytes in groups E and F when these groups were compared to all the other groups ($p < 0.01$) (Fig. 4): saline-treated animals (group A: EOSs, $0.013 \pm 0.01 \times 10^6$; lymphocytes, $0.01 \pm 0.02 \times 10^6$), single allergen-exposed animals (group E: EOSs, $1.34 \pm 0.31 \times 10^6$; lymphocytes, $0.57 \pm 0.12 \times 10^6$), and chronic allergen-exposed animals (group F: EOSs, $1.42 \pm 0.35 \times 10^6$; lymphocytes, $0.73 \pm 0.32 \times 10^6$). Total BAL cell counts from groups G and H were not significantly different from counts from control groups B, C, and D. The EOS and lymphocyte counts from groups G and H were significantly lower than counts from groups E and F, respectively. However, the animals from the chronically exposed group tested 5 days later (group G) were still hyperresponsive. There was a small, but significant, increase in inflammatory cell infiltration (i.e., EOSs, lymphocytes, and neutrophils) in animals from groups B, C, and D ($p < 0.01$) when compared to saline-only treated animals.

Relationship between BHR and cells in BALF

There was a significant correlation between bronchial responsiveness (PC_{200}) and the degree of EOS, lymphocyte, and neutrophil infiltration when these data from all the different experimental groups were analyzed together (for EOSs, $R_s = 0.78$; $p < 0.01$; for lymphocytes, $R_s = 0.36$; $p < 0.02$; for neutrophils, $R_s = 0.48$; $p < 0.01$). When the sensitized, single allergen-exposed group (group E) was analyzed alone, this significant relationship remained only between EOS count and the PC_{200} to ACh ($R_s = 0.68$; $p < 0.05$; Fig. 5).

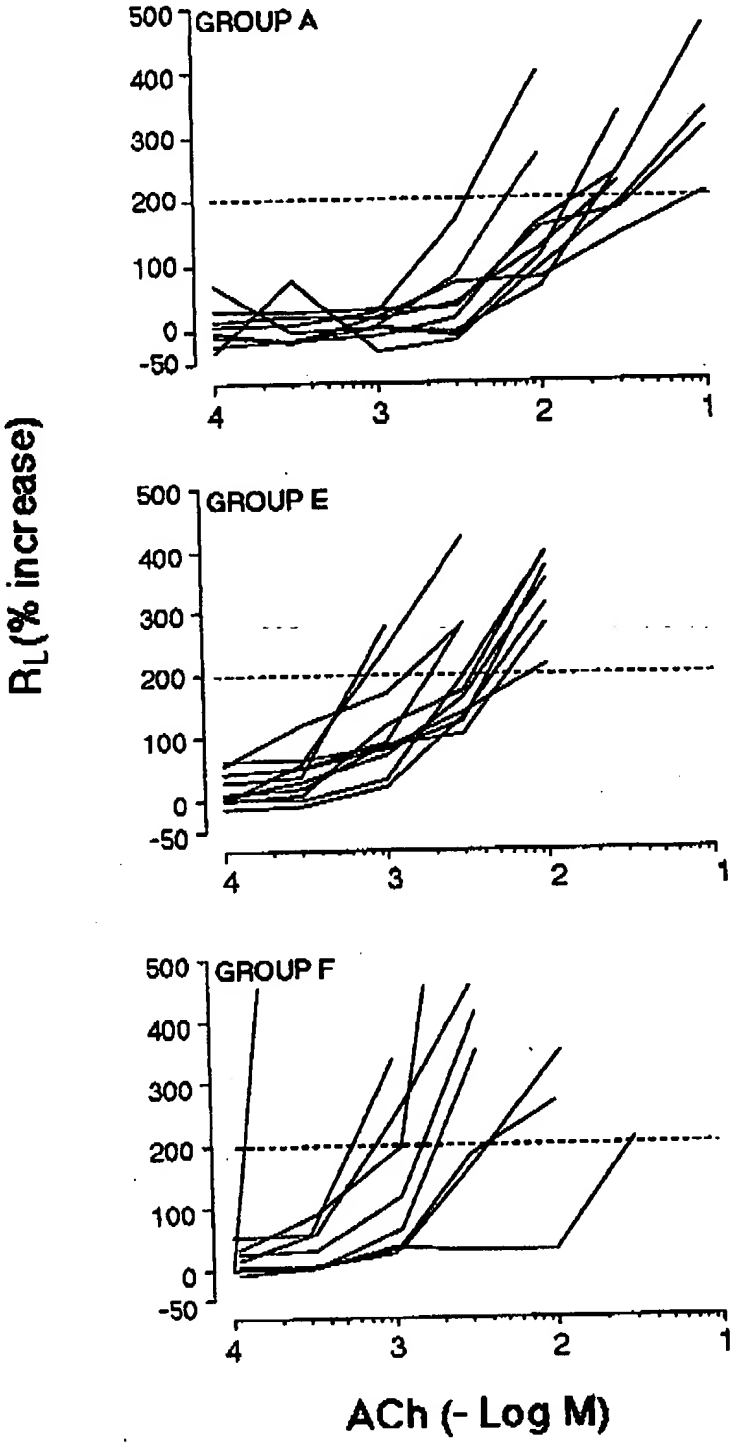

FIG. 1. Individual concentration R_L relationships for inhaled ACh for the individual rats from group A (nonsensitized, saline exposed), group E (sensitized, single allergen exposed), and group F (sensitized, chronic allergen exposed). R_L is expressed as percent increase above baseline. The *horizontal dotted line* represents the 200% increase above baseline and its intersection with the concentration-response curve and indicates the individual PC_{200} values.

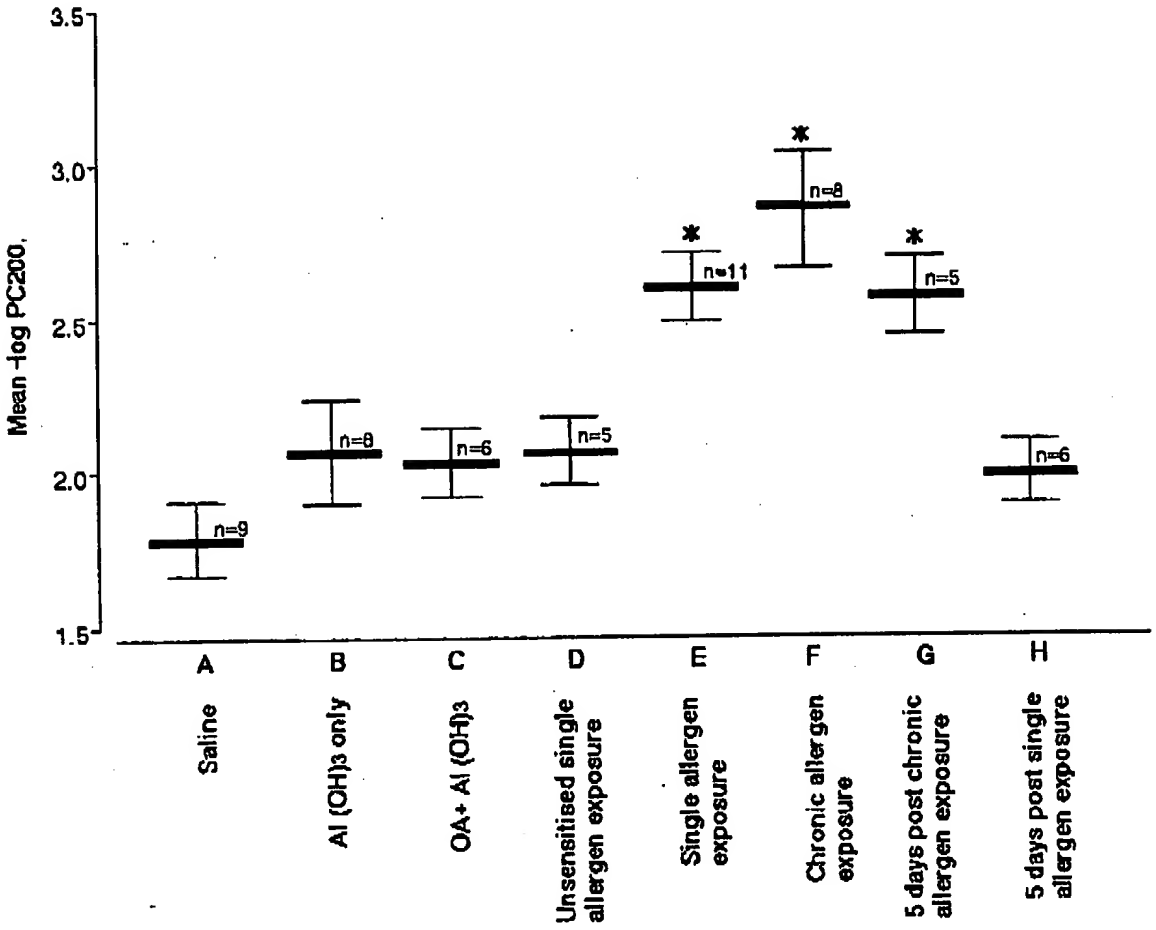

FIG. 2. Mean $-\log PC_{200}$ (± SEM) for groups A to H (see Table I for the individual groups). Only groups E, F, and G reveal a significant increase in bronchial responsiveness compared to that of control group A (*$p < 0.01$).

DISCUSSION

In this in vivo rat model, we have demonstrated that bronchial responsiveness to inhaled ACh was significantly increased at 18 to 24 hours in intraperitoneally sensitized rats after exposure to OA aerosol compared to bronchial responsiveness of unsensitized or unexposed groups. The increase in responsiveness observed was of a similar order of sevenfold to tenfold in rats exposed either to a single allergen aerosol or to multiple aerosols. BHR observed after a single OA aerosol was detectable at 18 to 24 hours after exposure but was not present 5 days later. However, in animals exposed repeatedly to OA aerosols, there was a more persistent BHR that was also observed 5 days after the last exposure. In this respect, our results are similar to results of Eidelman et al.[12] who were unable to demonstrate a change in airway responsiveness to inhaled methacholine in sensitized rats, despite the development of an identifiable late response after a single exposure to OA aerosol measured 1 week after a single exposure. Bellofiore and Martin[14] also demonstrated an increase in methacholine responsiveness in sensitized rats after multiple OA aerosol exposures lasting for up to 17 days after the last challenge.

Brown-Norway rats are good producers of IgE Ab and almost uniformly respond to sensitization with the development of increased titers of specific IgE Ab.[17] As an index of the allergic inflammatory changes within the lungs, we used cell counts obtained by BAL. We demonstrated an increase in the total cells recovered in all groups that were sensitized and then exposed to aerosolized allergen. The biggest increases in EOS, lymphocyte, and neutrophil counts occurred 18 to 24 hours after allergen exposure in the sensitized

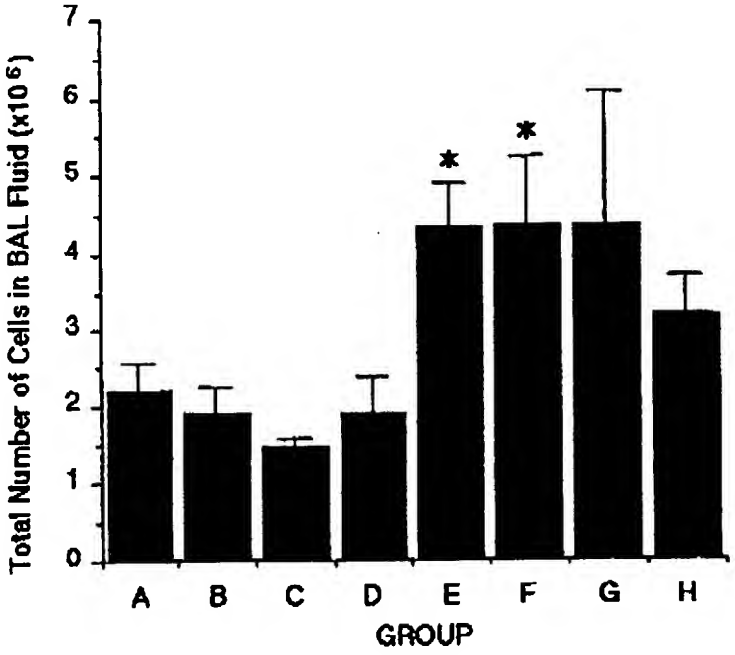

FIG. 3. Mean total cell counts (± SEM) in BALF from groups A to H (see Table I for the individual group treatments). There was a significant increase in total cells in groups E and F compared to that of control groups A to D ($*p < 0.01$).

animals, with a reduction in these cell types after 5 days to levels not significantly different from that of the control groups. A more variable increase in macrophage recovery in BALF by day 5 after the last allergen challenge was observed in the group of rats that demonstrated persistently increased responsiveness to inhaled ACh (group G). Unlike the ragweed sensitized dog model,[5] we found a slight, but nonsignificant, increase in neutrophils in BALF after allergen challenge compared to the intraperitoneally sensitized-only group (group C). The increase in EOS counts that we have demonstrated were transient and were not present 5 days after allergen exposure, unlike the sustained increase in EOS counts recently demonstrated in monkeys sensitized to *Ascaris suum*.[10] Interestingly, our data appear similar to data reported after allergen challenge in human subjects with asthma in whom EOSs were the predominant inflammatory cell type in BALF.[18]

Our studies reveal additional light on the relationship between the inflammatory process induced by allergen challenge and the increase in bronchial responsiveness to inhaled ACh. The BHR observed at 18 to 24 hours after allergen challenge coincided with the largest increases in inflammatory cell types in the BALF. We found a significant relationship between EOS count and PC_{200} when data from all groups were pooled. This significant relationship remained when results from rats in the single OA aerosol-exposed group only were analyzed (group 5). However, in our model, persistence of BHR at 5 days after the last allergen exposure was not accompanied by significant changes in cellular content of BALF. Our data therefore suggest that BHR may persist in the absence of inflammatory cells and that it is possible that the recruitment of inflammatory cells may only be a transient event that initiates mechanisms for BHR that may persist for longer than the inflammatory response itself. BHR that persists for weeks after a single exposure has been described in allergic dogs after allergen challenge, but in this model, no data on the BAL cell content at later time points were obtained.[5] Since we have not examined the histology of the airways in the present study, it is not possible to state whether the profile of cells recovered from the BAL represents a true reflection of submucosal airway inflammation. It is also possible that the persistent BHR that we observed may result from thickening of the airway submucosa from either persistent edema or connective-tissue fibrosis.[19]

We performed control studies in four separate groups of rats to determine whether the adjuvant used, $Al(OH)_3$, or sensitization per se, or exposure of unsensitized rats to OA aerosol had any effect on airway

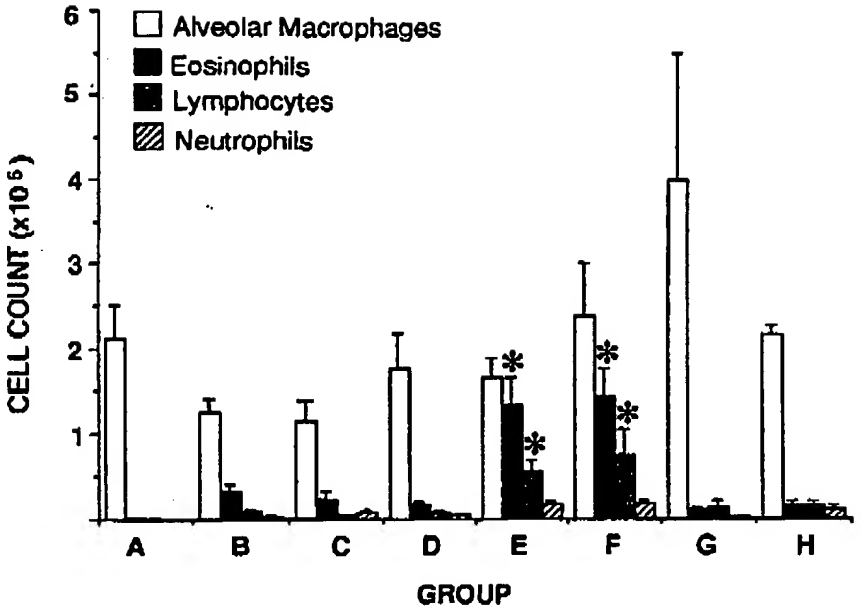

FIG. 4. Mean cell counts (± SEM) for macrophages, EOSs, lymphocytes, and neutrophils (*left to right*) from BALF obtained from groups A to H (see Table I for the individual groups). Groups E and F had a significant preferential increase in EOSs and lymphocytes compared to that of all other groups (*$p < 0.01$).

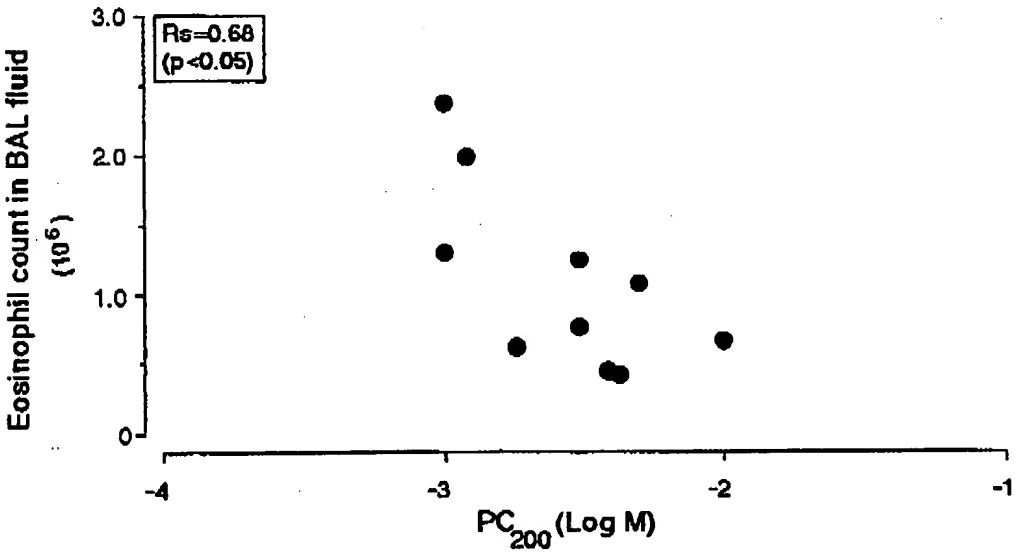

FIG. 5. Relationship between PC_{200} and total number of EOSs in BALF from sensitized, single allergen-exposed animals (group E). There is a significant correlation ($r_s = 0.68$; $p < 0.05$).

responsiveness or inflammatory changes within the lung compared to a saline-only treated group. These procedures caused no significant change in bronchial responsiveness consistent with previous studies in rats, guinea pigs, and dogs,[20-22] and although there were small changes in the relative proportions of cells recovered by BAL, the total cell counts were not affected. These observations suggest that ip sensitiza-

tion itself is not responsible for the large increase in inflammatory cell recovery found in the BALF after allergen exposure and may represent a nonspecific response of the immune system or of the lungs to $Al(OH)_3$ or to aerosolized allergen exposure, respectively. In the saline-only treated group, there were very few EOSs, lymphocytes, or neutrophils, and alveolar macrophages usually accounted for 95% of all recovered cells.

Repeated exposure to OA in sensitized rats did not induce additional increases in airway responsiveness or in total cell recovery compared to those found after a single exposure. This raises the possibility that there may be a process of desensitization to prevent ongoing and increasing inflammation and the attendant BHR, as has been described in guinea pigs sensitized to OA[23, 24] and sheep sensitized to *A. suum*,[25] and as was observed in the rat to some extent by Bellofiore and Martin.[14] The mechanisms for this limitation of BHR and inflammation are not clear, but one possibility is that this could be due to T suppressor cell generation after repeated aerosol challenge that would reduce the amount of chemoattractant lymphokine generation, as has been described in the rat.[26] It is also possible that repeated exposure to OA via the respiratory tract may eventually lead to diminution of IgE titers.[27] Nevertheless, repeated exposure appears to lead to a more persistent increase in airway responsiveness compared to the effect of a single OA exposure.

Of great prominence is the presence of increased numbers of lymphocytes and EOSs in the BALF of the sensitized rats challenged with OA. Current evidence suggests that lymphocytes may be involved in regulating both EOS influx[28] and activation in the airways of patients with asthma[29] through the release of various lymphokines, such as interleukin-5.[30, 31] EOS recruitment and activation in the airways may be an important step in the pathogenesis of BHR.[32] It is also possible that lymphocytes may be important both in enhancing and limiting the degree of BHR in our model, and it is therefore important to investigate further the role of these cells in this animal model of BHR.

In summary, this in vivo model in the sensitized rat demonstrates several features that bear similarities to features of human asthma, including an immediate response after allergen exposure, followed 18 to 24 hours later by a significant increase in EOS and lymphocyte counts in BALF associated with BHR to inhaled ACh after a single allergen exposure, and more sustained BHR after repeated allergen exposure. Our findings in this rat model are therefore of relevance to bronchial asthma in humans, and our model may be used to elucidate the roles of the EOS and lymphocyte in the pathogenesis of human allergic airway inflammatory responses and BHR.

We thank Dr. I. M. Richards (The Upjohn Co., Kalamazoo, Mich.) for his help and advice, and Dr. Anders Ullman (Sahlgrarn Hospital, Gothenburg, Sweden) for substantial help with the development of software for data acquisition.

REFERENCES

1. Boushey HA, Holtzman MJ, Sheller JR, Nadel JA. Bronchial hyperreactivity. Am Rev Respir Dis 1980;121:389-413.
2. Cockcroft DW, Ruffin RE, Dolovich J, Hargreave FE. Allergen-induced increase in non-allergic bronchial reactivity. Clin Allergy 1977;7:503-13.
3. Juniper EF, Frith PA, Hargreave FE. Airway responsiveness to histamine and methacholine: relationship to minimum treatment to control symptoms of asthma. Thorax 1981;36:575-9.
4. Chung KF. Role played by inflammation in the hyperreactivity of the airways in asthma. Thorax 1986;41:657-62.
5. Chung KF, Becker AB, Lazarus SC, Frick OL, Nadel JA, Gold WM. Antigen-induced airway hyperresponsiveness and pulmonary inflammation in allergic dogs. J Appl Physiol 1985;558:1347-53.
6. Lanes S, Stevenson JS, Codias E, Hernandez A, Sielczak MW, Wanner A, Abraham WM. Indomethacin and FPL-57231 inhibit antigen-induced airway hyperresponsiveness in sheep. J Appl Physiol 1986;61:864-72.
7. Kallos P, Kallos L. Experimental asthma in guinea pigs revisited. Int Arch Allergy Appl Immunol 1984;73:77-85.
8. Dunn CJ, Elliott GA, Oosteven JA, Richards IM. Development of a prolonged eosinophil-rich inflammatory leucocyte infiltration in the guinea pig asthmatic response to ovalbumin inhalation. Am Rev Respir Dis 1988;137:541-7.
9. Wegner CD, Torcellini CA, Clarke CC, Letts LG, Gundel RH. Effects of single and multiple inhalations of antigen on airway responsiveness in monkeys. J ALLERGY CLIN IMMUNOL 1991;87:835-41.
10. Gundel RH, Gerritsen ME, Gleich GJ, Wegner CD. Repeated antigen inhalation results in a prolonged airway eosinophilia and airway hyperresponsiveness in primates. J Appl Physiol 1990;68:779-86.
11. Blythe S, England D, Esser B, Junk P, Lemanske RF Jr. IgE antibody-mediated inflammation of rat lung: histologic and bronchoalveolar lavage assessment. Am Rev Respir Dis 1986;134:1246-51.
12. Eidelman DH, Bellofiore S, Martin JG. Late airway responses to antigen challenge in sensitised inbred rats. Am Rev Respir Dis 1988;137:1033-7.
13. Andersson P. Antigen-induced bronchial anaphylaxis in actively sensitised guinea pigs. Allergy 1980;35:65-71.
14. Bellofiore S, Martin JG. Antigen challenge of sensitised rats increases airway responsiveness to methacholine. J Appl Physiol 1988;65:1642-6.
15. Boulet LP, Cartier A, Thomson NC, Roberts RS, Dolovich J, Hargreave FE. Asthma and increases in nonallergic bronchial responsiveness from seasonal pollen exposure. J ALLERGY CLIN IMMUNOL 1983;71:399-406.
16. von Neergard K, Wirz K. Die messung der stromungswiderstande in den atemwegen des menschen, insbesondere bei asthma und emphysem. Z Klin Med 1927;105:51-8.
17. Pauwels R, Bazen H, Platteau B, van der Straeten M. The influence of antigen dose on IgE production in different rat strains. Immunology 1979;36:151-7.

18. de Monchy JG, Kauffman HF, Venge P, Koeter GH, Jansen HM, Sluiter HJ, De Vries K. Bronchoalveolar eosinophilia during allergen-induced late asthmatic reactions. Am Rev Respir Dis 1988;131:373-6.
19. Moreno RH, Hogg JC, Pare PD. Mechanics of airway narrowing. Am Rev Respir Dis 1986;133:1171-80.
20. Church MK. Response of the rat lung to humoral mediators of anaphylaxis and its modification by drugs and sensitisation. Br J Pharmacol 1975;55:423-30.
21. Popa V, Douglas JS, Bouhuys A. Airway responses to histamine, acetylcholine, and propranolol in allergic hypersensitivity in guinea pigs. J ALLERGY CLIN IMMUNOL 1973;51:344-56.
22. Hirschman LA, Downes H. Antigen sensitisation and methacholine responses in dogs with hyperreactive airways. J Appl Physiol 1985;58:485-91.
23. Andrew KK, Schellenberg RR, Hogg JC, Hanna CJ, Pare PD. Physiological and immunological effects of chronic antigen exposure in immunised guinea pigs. Int Arch Allergy Appl Immunol 1984;75:208-13.
24. Broder I, Rogers S. Model of allergic bronchoconstriction in the guinea pig: recurrent reactions in individual animals. Clin Immunol Immunopathol 1982;14:211-21.
25. Kleeberger SR, Wagner EM, Adams GK, Dannebert AM, Spannhake EW. Effect of repeated antigen exposure on antigen and mediator-induced bronchoconstriction in sheep. J Appl Physiol 1985;59:1866-73.
26. Sedgwick JD, Holt PG. Down regulation of immune responses to inhaled antigen: studies on the mechanism of induced suppression. Immunology 1985;56:635-42.
27. Holt PG, Batty JE, Turner KJ. Inhibition of specific IgE responses in mice by preexposure to inhaled antigen. Immunology 1981;42:409-17.
28. Frew AJ, Moqbel R, Azzawi M, et al. T-lymphocytes and eosinophils in allergen-induced late-phase asthmatic reactions in the guinea pig. Am Rev Respir Dis 1990;141:407-13.
29. Azzawi M, Bradley B, Jeffrey PK, et al. Identification of activated T-lymphocytes and eosinophils in bronchial biopsies in stable atopic asthma. Am Rev Respir Dis 1990;142:1407-13.
30. Silberstein DS, David JR. The regulation of human eosinophil function by cytokines. Immunology Today 1987;8:380-6.
31. Miyajima A, Miyatake S, Schreurs J, et al. Co-ordinate regulation of immune and inflammatory responses by T cell-derived lymphokines. Faseb J 1988;2:2462-73.
32. Frigas E, Gleich G. The eosinophil and the pathology of asthma [Postgrad course]. J ALLERGY CLIN IMMUNOL 1986;77:527-37.

Am J Physiol Lung Cell Mol Physiol
279: L379–L389, 2000.

Transgenic overexpression of β_2-adrenergic receptors in airway epithelial cells decreases bronchoconstriction

DENNIS W. McGRAW,[1] SUSAN L. FORBES,[1] JUDITH C. W. MAK,[2] DAVID P. WITTE,[3] PATRICIA E. CARRIGAN,[4] GEORGE D. LEIKAUF,[3] AND STEPHEN B. LIGGETT[1,5]

Departments of [1]Medicine, [5]Molecular Genetics, and [4]Environmental Health, University of Cincinnati College of Medicine, Cincinnati 45267; [3]Department of Pathology, Children's Hospital Medical Center, Cincinnati, Ohio 45229; and [2]Department of Thoracic Medicine, National Heart and Lung Institute, London SW3 6LY, United Kingdom

Received 24 September 1999; accepted in final form 20 March 2000

McGraw, Dennis W., Susan L. Forbes, Judith C. W. Mak, David P. Witte, Patricia E. Carrigan, George D. Leikauf, and Stephen B. Liggett. Transgenic overexpression of β_2-adrenergic receptors in airway epithelial cells decreases bronchoconstriction. *Am J Physiol Lung Cell Mol Physiol* 279: L379–L389, 2000.—Airway epithelial cells express β_2-adrenergic receptors (β_2-ARs), but their role in regulating airway responsiveness is unclear. With the Clara cell secretory protein (CCSP) promoter, we targeted expression of β_2-ARs to airway epithelium of transgenic (CCSP-β_2-AR) mice, thereby mimicking agonist activation of receptors only in these cells. In situ hybridization confirmed that transgene expression was confined to airway epithelium, and autoradiography showed that β_2-AR density in CCSP-β_2-AR mice was approximately twofold that of nontransgenic (NTG) mice. Airway responsiveness measured by whole body plethysmography showed that the methacholine dose required to increase enhanced pause to 200% of baseline (ED_{200}) was greater for CCSP-β_2-AR than for NTG mice (345 ± 34 vs. 157 ± 14 mg/ml; $P < 0.01$). CCSP-β_2-AR mice were also less responsive to ozone (0.75 ppm for 4 h) because enhanced pause in NTG mice acutely increased to 77% over baseline ($P < 0.05$) but remained unchanged in the CCSP-β_2-AR mice. Although both groups were hyperreactive to methacholine 6 h after ozone exposure, the ED_{200} for ozone-exposed CCSP-β_2-AR mice was equivalent to that for unexposed NTG mice. These findings show that epithelial cell β_2-ARs regulate airway responsiveness in vivo and that the bronchodilating effect of β-agonists results from activation of receptors on both epithelial and smooth muscle cells.

G protein-coupled receptor; adenosine 3′,5′-cyclic monophosphate; adenylyl cyclase; ozone

THE AIRWAY EPITHELIUM represents a critical interface between the bronchial smooth muscle and the external environment. As such, the epithelium can be a significant regulator of airway responsiveness (reviewed in Ref. 58). First, the epithelium forms a mechanical barrier that protects the underlying bronchial structures from exposure to environmental spasmogens (19, 42). Second, the epithelium has enzymatic activity that can degrade a variety of bronchospastic substances (12, 47, 53). Third, mucociliary clearance is regulated by the ciliary activity of the epithelium (10), as is the production and content of the epithelial lining fluid (4). These functions of the epithelium affect airway responsiveness indirectly by limiting the exposure of airway smooth muscle to luminal spasmogens.

In addition to these indirect effects, airway epithelial cells may regulate bronchial tone directly through the release of substances that either relax or contract airway smooth muscle. Known epithelium-derived substances that relax airway smooth muscle include PGE_2 (22, 59) and nitric oxide (NO) (26). Some studies (3, 14) have also suggested the presence of a nonprostanoid epithelium-derived factor that inhibits contraction. However, the presence of such a factor has not been a consistent finding, and its significance remains speculative (24). Contractile factors produced by the bronchial epithelium include leukotrienes (23), $PGF_{2\alpha}$ (22), and endothelin-1 (29). Airway epithelial cells produce a number of different cytokines and adhesion molecules that could affect smooth muscle responsiveness as well (8).

This notion that the epithelium is an important regulator of airway tone is further supported by clinical observations in asthma. Asthma is a chronic inflammatory disorder of the airways characterized by bronchial hyperresponsiveness to a variety of nonspecific stimuli. The pathogenesis of bronchial hyperresponsiveness in asthma is unclear, but there is evidence that disruption of the bronchial epithelium may be a contributing factor. Indeed, alteration of the epithelium may be present even in mild asthma (27, 28). Furthermore, the amount of epithelial damage can be correlated to the degree of airway hyperreactivity (5).

Results of several studies suggest that these inhibitory functions of the bronchial epithelium are modulated by β_2-adrenergic receptors (β_2-ARs). The β_2-AR is a G protein-coupled membrane receptor that acts to raise intracellular cAMP levels via stimulation of ad-

Address for reprint requests and other correspondence: S. B. Liggett, University of Cincinnati College of Medicine, 231 Bethesda Ave., Cincinnati, OH 45267-0564 (E-mail: Stephen.Liggett@uc.edu).

The costs of publication of this article were defrayed in part by the payment of page charges. The article must therefore be hereby marked "*advertisement*" in accordance with 18 U.S.C. Section 1734 solely to indicate this fact.

enylyl cyclase (18). The receptor is expressed on airway smooth muscle cells where it acts to relax the muscle and promote bronchodilation (reviewed in Ref. 2). However, the airway epithelium contains a high density of β_2-ARs as well (6, 9, 21, 49). Although neither receptor autoradiography nor in situ hybridization have localized the β_2-ARs to specific epithelial cell types, these receptors have been shown to regulate ion transport (7, 38), mucus secretion (33), ciliary beat frequency (10), and Clara cell secretory activity (36, 37). The regulatory role of the epithelial cell β_2-AR is further supported by the observation that mechanical removal of the epithelium from tracheal rings decreases the bronchodilator effect of isoproterenol in vitro (14, 16, 51). This finding has been interpreted to indicate that β-agonists stimulate the epithelial release of relaxant factors that act directly on smooth muscle. However, this effect has not been consistently observed (1, 3), leaving the concept of a physiologically relevant β_2-AR-regulated, epithelium-derived relaxant factor in some doubt. The physiological and pathophysiological significance of epithelial cell β_2-ARs therefore remains unclear, primarily because the effects of epithelial cell β_2-ARs in vivo cannot be easily differentiated from the direct bronchodilator effects of β_2-ARs on airway smooth muscle.

In the current study, we selectively overexpressed the β_2-AR in the airway epithelium of transgenic (TG) mice and examined the role that these receptors play in the regulation of airway tone. The use of such a targeted strategy permitted the epithelial β_2-AR signaling pathway to be selectively enhanced without directly affecting the density or activity of smooth muscle β_2-ARs. Because the receptor is not a secreted product, we reasoned that the effects of epithelial cell β_2-AR activation could be distinguished in vivo from those of other cells by comparing airway responsiveness of nontransgenic (NTG) mice to that of TG Clara cell secretory protein (CCSP)-β_2-AR mice. Our results showed that overexpression of the β_2-AR in the airway epithelium of TG mice reduced airway responsiveness, thereby supporting a role for this population of receptors in the regulation of airway tone.

METHODS

TG mice. Targeted expression of the human β_2-AR to the airway epithelium was achieved with the use of the rat CCSP promoter (50). The CCSP-β_2-AR transgene was composed of a 2.4-kb *Hind* III-*Hind* III fragment from the rat CCSP promoter, a 1.5-kb *Hind* III-*Psh*A I fragment from the human β_2-AR [1.2 kb of open reading frame (ORF) and 0.3 kb of 3′-untranslated region (UTR)], and a 0.85-kb *Xho* I-*Bam*H I fragment encoding the SV40 small T intron and polyadenylation [poly(A)] signal. The fragments were ligated together in the vector pUC18, with the orientation of each fragment confirmed by sequence analysis and restriction enzyme digestion. A 4.75-kb *Not* I fragment (Fig. 1) was then isolated for injection. The DNA was gel purified and dialyzed against 5 mM Tris·HCl (pH 7.4) and 0.1 mM EDTA. Transgene DNA was injected into fertilized eggs of FVB/N mice and implanted into pseudopregnant females as previously described (54). Three founder mice were identified by Southern blot analysis of genomic DNA prepared from tail clips. Independent lines of heterozygous CCSP-β_2-AR mice were maintained by mating TG mice with NTG FVB/N mice. Subsequent screening for the heterozygous progeny was by PCR analysis of the genomic DNA with a forward primer from the β_2-AR ORF (5′-GGAGCAGAGTGGATATCACG-3′) and a reverse primer from the SV40 poly(A) region (5′-GTCACACCACAGAAGTAAGG-3′). Heterozygous mice from *generations 2* to *4* between the ages of 10 and 14 wk were used for all studies.

Transgene expression and localization. Screening for CCSP-β_2-AR transgene expression in the lung was initially done by RT-PCR. Total RNA was extracted from freshly isolated lungs with Tri-Reagent (Molecular Research Center, Cincinnati, OH). An aliquot of RNA was reverse transcribed with random hexamers with murine leukemia virus reverse transcriptase (PerkinElmer) as previously described (19). Transgene cDNA was amplified with 150 nM each of a sense primer from the CCSP promoter (5′-CATCAGCCCACATCTACAGACAGC-3′) and an antisense primer from the β_2-AR ORF (5′-GACCAGCACATTGCCAAACAC-3′). The

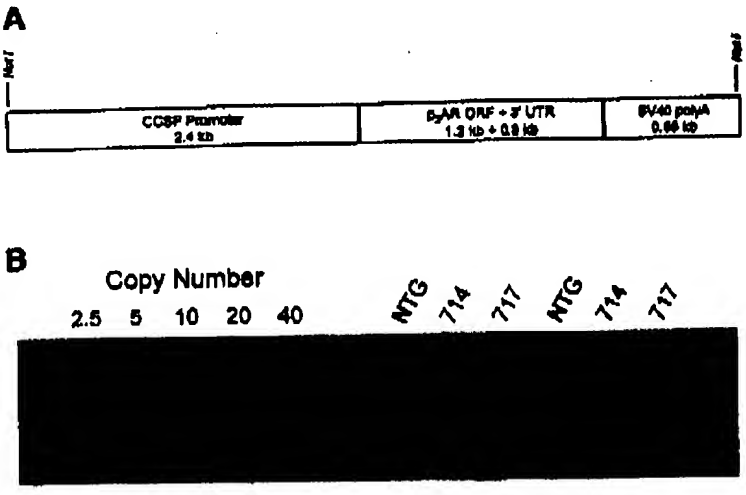

Fig. 1. *A*: Clara cell secretory protein (CCSP)-β_2-adrenergic receptor (AR; CCSP-β_2-AR) transgene was composed of the rat CCSP promoter, the human β_2-AR open reading frame (ORF), and the SV40 small T intron and polyadenylation [poly(A)] site. UTR, untranslated region. *B*: Southern blot analysis of genomic DNA from tail clips showed that the 2 founder mice (*lines 714* and *717*) used to establish transgenic (TG) lines each had >40 copies of the transgene DNA. NTG, nontransgenic.

PCR was started at 95°C for 120 s, followed by amplification for 35 cycles at 95°C for 60 s and 60°C for 60 s, followed by a final extension at 72°C for 7 min. The PCR products were detected in agarose gels stained with ethidium bromide. To quantitatively assess transgene expression among the independent TG lines, ribonuclease protection assays were performed as previously reported (40) with a ^{32}P-labeled antisense riboprobe corresponding to the distal 500 bp of the human β_2-AR ORF (40). Lung RNA (20 μg) and β_2-AR riboprobe were hybridized overnight, digested with RNase, and subjected to denatured PAGE analysis. The gels were visualized with a PhosphorImager (Molecular Dynamics, Sunnyvale, CA) and analyzed with the ImageQuant software package (Molecular Dynamics).

The distribution of transgene expression within the lung was assessed by in situ hybridization as previously reported (57). Tracheae and lungs were rapidly dissected, fixed in 4% paraformaldehyde, cryoprotected with 30% sucrose in PBS, and frozen in optimum cutting temperature compound. Cryostat sections (7 μm) were then mounted on silane-coated slides. An antisense cRNA probe for the human β_2-AR was prepared as described above for the ribonuclease protection assays except that the probe was labeled with ^{35}S-UTP. A sense cRNA probe was prepared with SP6 polymerase for use as a negative control. Hybridization was performed with $0.5–1.0 \times 10^6$ counts/min of labeled probe in a final volume of 30 μl/slide. After overnight incubation at 42°C, the sections were treated with 50 μg/ml of RNase A and 100 U/ml of RNase T1 for 30 min at 37°C and washed to a final stringency with 0.1× saline-sodium citrate at 50°C. Slides were dipped in NTB2 emulsion (Eastman Kodak) diluted 1:1 with 0.6 M ammonium acetate and exposed for 2 wk, after which they were developed with D19 developer (Eastman Kodak) and counterstained with hematoxylin and eosin.

Receptor density and function. Lung membranes were prepared from individual mice by homogenizing the entire lung or trachea in 10 ml of hypotonic lysis buffer (5 mM Tris, pH 7.4, and 2 mM EDTA) containing the protease inhibitors leupeptin, aprotinin, benzamidine, and soybean trypsin inhibitor (10 μg/ml each). Homogenates were centrifuged at 40,000 *g* for 10 min at 4°C. The supernatant was removed, and the pellets containing the crude membrane particulates were suspended in assay buffer (75 mM Tris, pH 7.4, 12.5 mM $MgCl_2$, and 2 mM EDTA). Receptor expression was determined by radioligand binding with [^{125}I]iodocyanopindolol (ICYP) as described (40). Adenylyl cyclase activity in these membrane preparations was assessed by a column chromatography method as previously reported (39).

Receptor localization. The distribution of β_2-AR expression within the lung was assessed by receptor autoradiography (35). The tracheae of anesthetized mice were cannulated, and the lungs were inflated with tissue embedding fluid diluted 1:4 with PBS. The tracheae and lungs were removed as a block, snap-frozen in isopentane cooled with liquid nitrogen, and stored at −80°C until further use. The tissues were subsequently sectioned (10 μm) on a cryostat at −30°C and thaw mounted onto slides coated with gelatin. Slides were stored at −80°C and showed no loss of binding capacity under these conditions. For autoradiography, the slides were allowed to warm to room temperature, after which they were washed for 15 min in incubation buffer (25 mM Tris·HCl, pH 7.4, 154 mM $NaCl_2$, 1.1 mM ascorbic acid, and 0.25% polypep). Binding reactions were then carried out at 37°C for 120 min in incubation buffer containing 25 pM ^{125}ICYP. Specific binding of β_2-ARs was determined in the presence of 100 μM CGP-20712A, a selective β_1-AR antagonist. Nonspecific binding was determined by incubation of adjacent tissue sections with ^{125}ICYP in the presence of 200 μM (−)-isoproterenol. After the incubation period, the slides were washed twice for 15 min in ice-cold 25 mM Tris·HCl (pH 7.4), rinsed in cold distilled water to remove buffer salts, and dried rapidly under a stream of cold air. The slides were postfixed in paraformaldehyde vapor at 60°C for 30 min and then dipped directly in Ilford K-5 emulsion. After 3 days at 4°C, the emulsion was developed and fixed. Sections were stained with hematoxylin and examined under a Zeiss microscope equipped with dark- and bright-field illumination. Grain counts, assessed as optical density, were measured with the Image Analysis System (Seescan, Cambridge, UK) with a constant magnification (×200) and corrected for background and nonspecific binding. The results represent the means of nine separate fields (300 μm^2/field) taken from three different mice, each within the NTG and TG groups (27 fields total/group).

Pulmonary function. Airway responsiveness (i.e., bronchoconstriction) was assessed noninvasively in conscious, unrestrained mice with a whole body plethysmograph (Buxco Electronics, Troy, NY) as previously described (31). With this system, the volume changes that occur during a normal respiratory cycle are recorded as the pressure difference between an animal-containing chamber and a reference chamber. The resulting signal is used to calculate respiratory frequency, minute volume, tidal volume, and enhanced pause (P_{enh}). P_{enh} was used as the measure of bronchoconstriction and was calculated from the formula: P_{enh} = pause × (peak expiratory pressure/peak inspiratory pressure), where pause is the ratio of time required to exhale the last 30% of tidal volume relative to the total time of expiration (20). Mice were placed in the plethysmograph and the chamber was equilibrated for 10 min. They were exposed to aerosolized PBS (to establish baseline) followed by incremental doses of methacholine (1–640 mg/ml). Each dose of methacholine was aerosolized for 2 min, and respiratory measurements were recorded for 2 min afterward. During the recording period, an average of each variable was derived from every 30 breaths (or 30 s, whichever occurred first). The maximum P_{enh} value after each dose was used to measure the extent of bronchoconstriction. On a separate day, the mice were submitted to the same protocol except that they were first treated with aerosolized albuterol (1 mg/ml) for 20 min. The concentration-response data for each mouse were fit to a curve by an iterative least squares technique, and the dose of methacholine required to increase P_{enh} to 200% of baseline (ED_{200}) was derived.

Ozone exposure. Mice were exposed for 4 h to filtered room air containing 0.75 ppm ozone in a 0.32-m^3 stainless steel inhalation chamber that was capable of complete air exchange every 2 min. Zhao et al. (60) have previously shown that this level of exposure does not result in inflammation or structural lesions. Ozone was generated from 100% extra-dry oxygen (Matheson, Columbus, OH) with a model V1-0 ultraviolet ozonator (OREC, Phoenix, AZ), and its concentration was measured continuously with an ultraviolet photometric ozone analyzer (model 1008-PC, Dasibi Environmental, Glendale, CA). This instrument has an internal calibration system and was routinely checked and calibrated against a US Environmental Protection Agency transfer standard. The status of the mice and the concentration of ozone were checked hourly throughout the exposure period. P_{enh} was measured by whole body plethysmography for 2-min intervals at 5, 15, 30, 45, 60, 90, and 120 min after ozone exposure. Methacholine challenge testing was performed 6 and 24 h postozone exposure with the protocol described in *Pulmonary function*. In studies carried out to characterize the increase in

P_{enh} that we observed in NTG mice after ozone exposure, mice were pretreated with either aerosolized albuterol or atropine. Albuterol (1 mg/ml) markedly reduced the increase in P_{enh} induced by ozone (2.47 ± 0.41 without albuterol, 1.26 ± 0.07 with albuterol; $n = 4$ animals; $P < 0.03$). These results confirmed that bronchospasm accounted for most, although not all, of the increase in P_{enh} that occurred acutely after exposure to ozone. In contrast, atropine (0.6 mg/ml) had little or no effect (<20% reduction, which was not significant) on the ozone response of NTG mice, consistent with a minimal role for cholinergic mechanisms in mediating the acute ozone-induced bronchospasm.

Bronchoalveolar lavage studies. To perform bronchoalveolar lavage (BAL), mice were killed by a lethal injection of pentobarbital sodium and exsanguinated via transection of the abdominal aorta. The trachea were then exposed and cannulated with a polyethylene catheter. BAL was performed by instilling 1 ml of PBS warmed to 37°C. The lavage fluid was allowed to dwell for 5 min, after which it was withdrawn by gentle aspiration. The typical fluid return was ~0.8 ml, with no difference observed between the TG and NTG mice. The BAL fluid was centrifuged at 1,000 *g* for 10 min at 4°C to remove cells, and the resulting supernatant was frozen and stored at −80°C until further use. Levels of PGE_2 in BAL fluid were measured by a colorimetric enzyme immunoassay from a commercial kit (Amersham Pharmacia Biotech, Piscataway, NJ). Duplicate samples (60 μl) from each BAL specimen were assayed directly in a 96-well plate. Optical density was read at 450 nm. The PGE_2 content of each sample, measured in triplicate, was determined from a reference curve of known PGE_2 standards. NO content in BAL fluid was determined by a spectrophotometric method based on the Griess reaction to measure nitrite (55). To enzymatically reduce BAL fluid nitrate to nitrite, samples were first incubated with 80 U/l of nitrate reductase, 1 μM NADPH, 0.5 mM glucose 6-phospbate, and 160 U/l of glucose-6-phosphate dehydrogenase for 3 h at 25°C. The sample (50 μl) was mixed with 50 μl of 1% sulfanilamide in 5% H_3PO_4 and 50 μl of 0.1% *N*-(1-napthyl)ethylenediamine. After incubation for 10 min, absorbance was read at 550 nm. The nitrite content of BAL samples was subsequently calculated from a reference curve that was generated from the absorbance values of sodium nitrite standards. The nitrite concentration for each sample was determined from the mean of duplicate measurements. To standardize BAL recovery, the urea content of BAL fluid was determined with a colorimetric assay (Sigma, St. Louis, MO). The manufacturer's protocol was followed except that sample size was increased to 50 μl, and the total reaction volume was reduced to 1 ml. These conditions provided for a linear calibration curve. Aliquots from each BAL sample were measured in duplicate.

Statistical analysis. Data are reported as means ± SE. Statistical comparisons between NTG and TG groups were performed with a two-tailed Student's *t*-test. For the whole body plethysmography studies, the effect of a given treatment within the NTG or TG group was assessed by paired analysis when appropriate. Differences were considered significant at the $P < 0.05$ probability level.

RESULTS

CCSP-β_2-AR founder mice were identified by Southern blot analysis of genomic DNA with a cDNA probe corresponding to the SV40 poly(A) fragment of the transgene. The transgene was detected in 3 of 36 mice initially screened. These founder mice, designated *lines 714, 717,* and *721,* were mated with NTG FVB/N mice to generate heterozygous offspring. Genotypic analysis of the progeny showed that the transgene was inherited in ~50% of the progeny, with equal distribution between males and females. Quantitative Southern blotting showed that heterozygous mice from *lines 714* and *717* contained ~40 copies of the transgene (Fig. 1), whereas *line 721* contained <5 copies (data not shown).

Expression of the CCSP-β_2-AR transgene was initially confirmed by RT-PCR. Total RNA prepared from whole lung homogenates was reverse transcribed and subjected to PCR with a forward primer from the CCSP promoter and a reverse primer from the β_2-AR ORF. As shown in Fig. 2*A*, only mice with positive genomic screens were found to express the transgene mRNA. No PCR products were detected in the absence of reverse transcriptase. CCSP-β_2-AR transgene expression was quantitated by ribonuclease protection assays (Fig. 2*B*). For these studies, total cellular RNA pre-

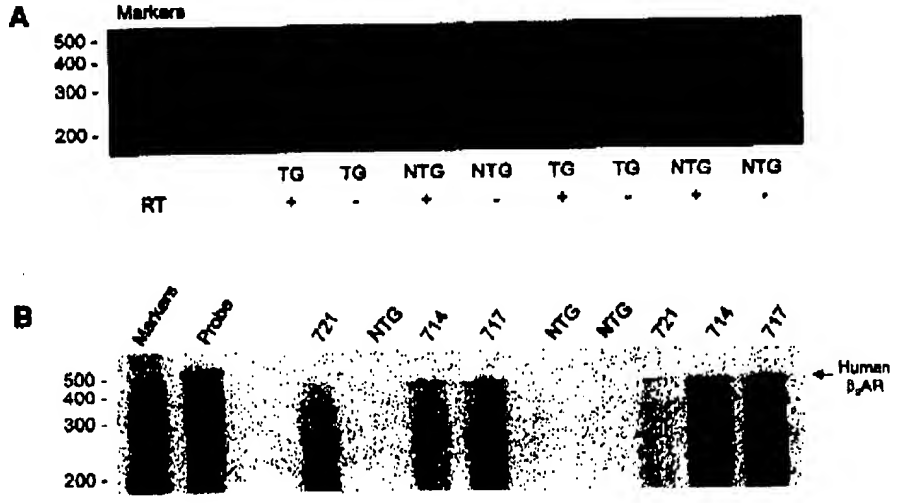

Fig. 2. Transgene expression in CCSP-β_2-AR mice. *A*: expression of the transgene was screened for by RT-PCR with a sense primer from the CCSP promoter and an antisense primer from the β_2-AR ORF. PCR products were detected in the presence (+) but not in the absence (−) of RT. *B*: quantitation of transgene expression was done by ribonuclease protection assays with an antisense riboprobe specific for the human β_2-AR. Phosphorimage analysis of the gels showed that transgene expression between *lines 714* and *717* was not different and was greater than expression in *line 721*. No signal was present in lung RNA from NTG mice. Nos. at *left*, no. of bp.

pared from whole lung homogenates was hybridized with an antisense riboprobe corresponding to the distal 500 bp of the human β_2-AR ORF. Because this region has only ~70% homology with the mouse gene, the riboprobe does not protect the endogenous mouse transcript from RNase digestion. Therefore, the full-length protected fragment (Fig. 2*B*, arrow) was only detected in mice expressing the CCSP-β_2-AR transgene. With this technique, we found that transgene expression in the lungs of mice from *lines 714* and *717* was equivalent and much greater than that of *line 721*. The two higher expressing lines were subsequently propagated for further studies.

After confirming that the β_2-AR transgene could be detected in whole lung RNA, we next used in situ hybridization to assess its distribution within the lung. With the human-specific β_2-AR riboprobe, we found that transgene expression in the CCSP-β_2-AR mice was limited to the airway epithelium (Fig. 3*A*). No specific binding was observed in lung sections from NTG mice (Fig. 3*B*). Similarly, no specific binding occurred in either CCSP-β_2-AR (Fig. 3*C*) or NTG (data not shown) mice when probed with the sense riboprobe.

A previous study (6) has demonstrated that >90% of all β_2-ARs in the lung are localized to the alveolar wall. Because the human TG receptor cannot be differentiated from the endogenous mouse receptor with β-AR radioligands, we anticipated that receptor overexpression in one population of cells (i.e., those of the bronchial epithelium) might go undetected in receptor binding studies with membranes prepared from whole lung homogenates. Indeed, our initial radioligand assays with ^{125}ICYP showed no difference in β_2-AR density of membranes prepared from CCSP-β_2-AR lungs or tracheae versus those prepared from NTG mice. Analysis of adenylyl cyclase activities in these membranes also showed no difference. We therefore used receptor autoradiography with ^{125}ICYP to establish that the receptor protein was overexpressed in the airway epithelium. To specifically assess β_2-AR density, CGP-20712A was included to inhibit ^{125}ICYP binding to the β_1-AR. Compared with NTG mice, CCSP-β_2-AR mice had increased grain density over the bronchial epithelium (Fig. 4, *A* and *D*). Grain counts over the airway epithelium of the TG mice were approximately twofold greater than those of the NTG mice (1.07 ± 0.07 vs. 0.59 ± 0.04 optical density, respectively, $P < 0.05$). No difference in grain density was observed for other lung structures (bronchial smooth muscle, alveoli, and vessels), indicating that receptor overexpression was confined to the airway epithelium. (−)-Isoproterenol inhibited ^{125}ICYP binding in both NTG and CCSP-β_2-AR mice (Fig. 4, *C* and *D*, respectively), confirming that binding was due to the β_2-AR.

Long-term observation of CCSP-β_2-AR TG mice (up to 20 mo) showed that epithelial cell overexpression of the β_2-AR was not associated with increased morbidity or mortality. CCSP-β_2-AR mice develop and grow normally compared with their NTG littermates. The gross structural anatomy of the lungs of CCSP-β_2-AR mice was unremarkable. Examination of hematoxylin and eosin-stained lung sections showed no histological abnormalities (Fig. 5, *A* and *D*). Additional staining with Masson's trichrome showed no evidence of increased collagen deposition (Fig. 5, *B* and *E*), and staining with Alcian blue showed no differences in the number of mucus-secreting cells (Fig. 5, *C* and *F*). Remodeling of the lung, at least as detected by these techniques, did not occur in CCSP-β_2-AR mice.

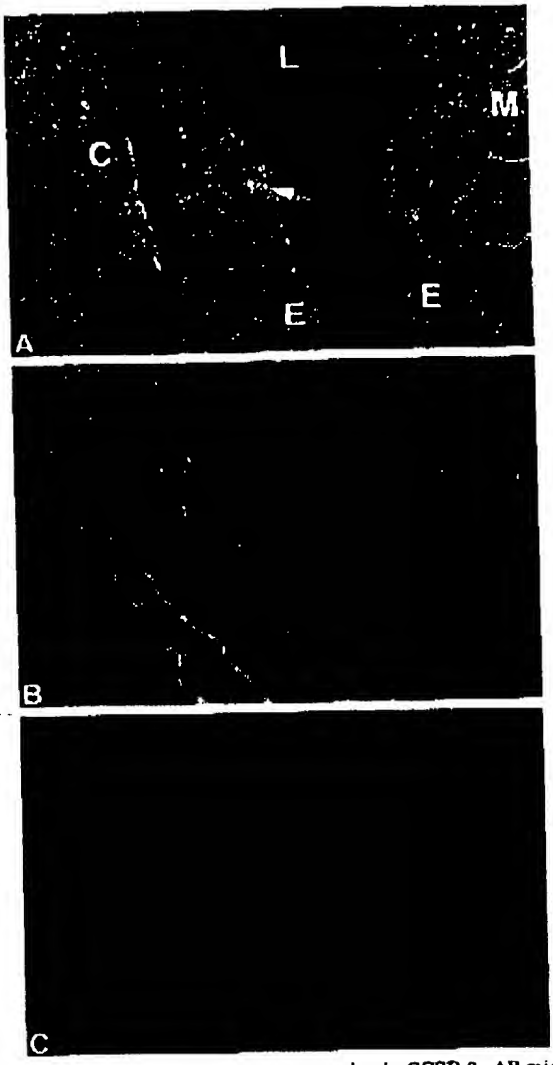

Fig. 3. Distribution of transgene expression in CCSP-β_2-AR mice. In situ hybridization of frozen lung sections was performed with a ^{35}S-UTP-labeled human β_2-AR riboprobe. Dark-field photographs of sections counterstained with hematoxylin and eosin are shown. *A*: section of a bronchus from a CCSP-β_2-AR TG mouse hybridized with the antisense riboprobe. L, lumen. Specific hybridization (arrow) was present over the airway epithelium (E) but not over the underlying cartilage (C) or smooth muscle (M). *B*: no specific signal was observed in NTG lung sections hybridized with the same probe. *C*: similarly, no signal was present when CCSP-β_2-AR lung sections were hybridized with a β_2-AR sense probe.

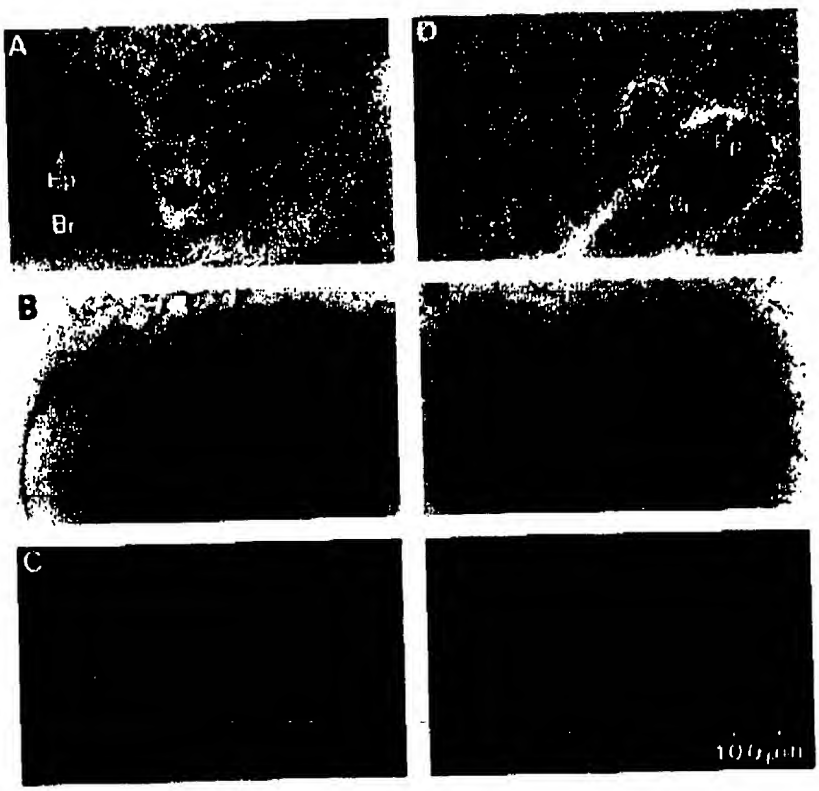

Fig. 4. Localization of β_2-AR expression by receptor autoradiography. Frozen lung sections from NTG (*A–C*) and CCSP-β_2-AR (*D–F*) mice were incubated with [^{125}I]iodocyanopindolol (ICYP) in the presence of 100 μM CGP-20712A. Dark-field examination showed that grain density over the airway epithelium (Ep) of CCSP-β_2-AR mice (*D*) was greater than that of NTG mice (*A*). However, no differences were observed for smooth muscle, bronchial vessels (Bv), or alveoli (A). Bronchi (Br) and surrounding lung structures are shown in bright-field photomicrographs of sections counterstained with hematoxylin (*B* and *E*). Addition of 200 μM (−)-isoproterenol inhibited ^{125}ICYP binding to lung sections from both NTG (*C*) and CCSP-β_2-AR (*F*) mice.

To examine the potential effects of targeted epithelial cell β_2-AR overexpression on airway responsiveness, we measured methacholine-induced bronchoconstriction in vivo so that the integrity and function of the epithelium could be maintained. For these experiments, we used whole body plethysmography to measure P_{enh}, a derived parameter that has been shown to correlate highly with airway resistance as measured by invasive methods (20). Conscious, unrestrained NTG and CCSP-β_2-AR mice were exposed to incremental doses of aerosolized methacholine for 2 min followed by recording of respiratory parameters for 2 min. As shown in Fig. 6, the CCSP-β_2-AR mice required higher doses of methacholine to induce a change in P_{enh} compared with the NTG mice. The ED_{200} for methacholine in CCSP-β_2-AR mice was approximately twice that of NTG mice (345 ± 34 vs. 157 ± 14 mg/ml, respectively; $P < 0.01$; $n = 10$). These results therefore indicated that overexpression of the β_2-AR in bronchial epithelial cells afforded protection against cholinergic-mediated bronchoconstriction in vivo. To confirm that this effect was the result of β_2-AR activation, NTG and CCSP-β_2-AR mice were treated with the β-antagonist propranolol (0.5 g/l in the drinking water) for 6 days. Afterward, the mice were exposed to 160 mg/ml (the ED_{200} for NTG mice) of aerosolized methacholine. The P_{enh} value for the 160 mg/ml concentration before propranolol treatment was then compared with that after treatment. For NTG mice, the P_{enh} value before propranolol treatment (1.55 ± 0.12; $n = 10$) was not different from that after treatment (1.49 ± 0.35; $n = 9$). In contrast, the P_{enh} of untreated CCSP-β_2-AR mice increased significantly after treatment with propranolol (0.99 ± 0.10 vs. 1.72 ± 0.33; $P < 0.03$; $n = 10$ and 7, respectively).

The results of the aforementioned experiments indicated that the CCSP-β_2-AR TG mice were hyporesponsive to methacholine and that this effect was specifically mediated rather than an artifact of transgene insertion in the genome. Our next goal was to assess whether the in vivo response of CCSP-β_2-AR mice to β-agonists was also different from that of NTG mice. For these experiments, NTG and CCSP-β_2-AR mice were pretreated with aerosolized albuterol (1 mg/ml) for 20 min before methacholine challenge. Figure 7 shows that albuterol caused a rightward shift in the methacholine dose response of NTG mice, increasing the ED_{200} from 157 ± 14 to 388 ± 68 mg/ml ($P < 0.01$; $n = 10$). Of note, the ED_{200} value for the albuterol-treated NTG mice was not statistically different from that of the untreated CCSP-β_2-AR mice. In CCSP-β_2-AR mice, pretreatment with albuterol also raised the ED_{200} for methacholine (345 ± 34 to 455 ± 62 mg/ml; $n = 10$), but this difference was small and did not reach significance. Thus in these mice, epithelial cell overexpression of the β_2-AR was as effective as inhaled albuterol that acts on both epithelial cell and smooth muscle cell receptors.

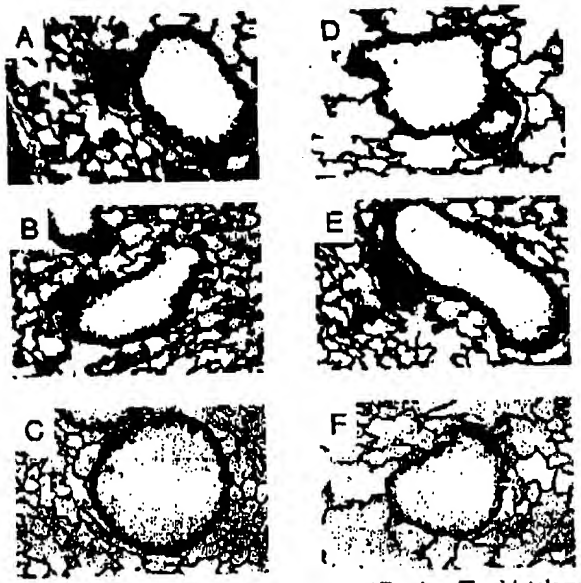

Fig. 5. Histological analysis of CCSP-β_2-AR mice. The histology of NTG mice (*A–C*) was compared with that of TG mice (*D–F*). Staining with hematoxylin and eosin (*A* and *D*), Masson's trichrome (*B* and *E*), and Alcian blue (*C* and *F*) showed no differences between NTG and CCSP-β_2-AR mice.

We next examined whether the acute response to ozone was altered in CCSP-β_2-AR mice. For these experiments, NTG and CCSP-β_2-AR mice were exposed to 0.75 ppm ozone for 4 h. P_{enh} was measured at frequent intervals during the initial 2-h postexposure period. As shown in Fig. 8, P_{enh} immediately increased to 77% over baseline in NTG mice and then remained significantly elevated for 1 h after exposure ($P < 0.05$).

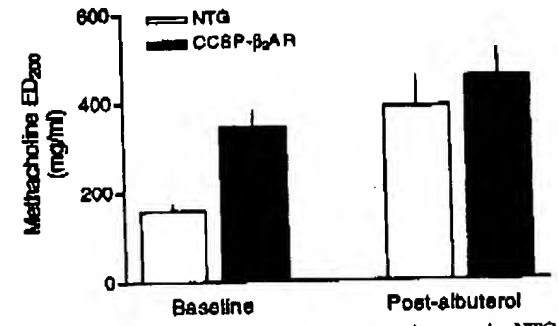

Fig. 7. Effect of β-agonists on airway responsiveness in NTG and CCSP-β_2-AR mice. Mice were pretreated with aerosolized albuterol (1 mg/ml) for 20 min before methacholine challenge. Data are means ± SE from 10 mice/group. Compared with baseline, albuterol increased the methacholine ED_{200} in NTG mice to 886 ± 68 mg/ml ($P < 0.01$). In CCSP-β_2-AR, the methacholine ED_{200} increased to 455 ± 62 mg/ml, but the difference was not significant. The postalbuterol methacholine ED_{200} values for NTG and CCSP-β_2-AR mice were not significantly different.

In contrast, CCSP-β_2-AR mice showed no increase in P_{enh} during the same time period.

To assess whether the extent of ozone-induced hyperresponsiveness was also affected in CCSP-β_2-AR mice, methacholine challenge testing was performed 6 and 24 h after ozone exposure. Ozone-induced airway hyperresponsiveness was observed for both NTG and CCSP-β_2-AR mice (Fig. 9). Compared with the preozone values, the ED_{200} for methacholine 6 h after ozone exposure decreased from 157 ± 14 to 56 ± 12 mg/ml ($P < 0.01$) in NTG mice and from 345 ± 34 to 143 ± 35 mg/ml ($P < 0.05$) in CCSP-β_2-AR mice. The postexposure ED_{200} for methacholine for the CCSP-β_2-AR mice remained significantly greater than that of the exposed NTG mice ($P < 0.05$) and, in fact, was not

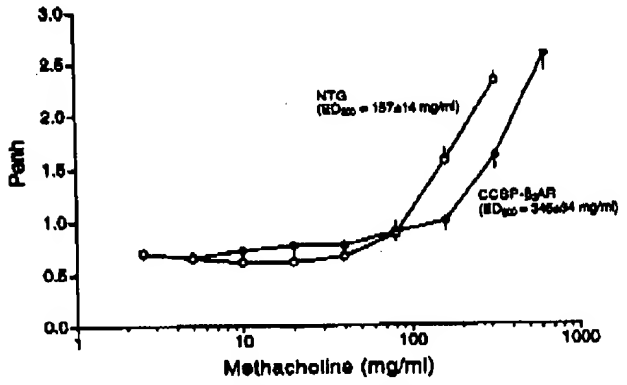

Fig. 6. In vivo assessment of airway responsiveness to methacholine. Methacholine-induced bronchoconstriction was assessed in conscious NTG and CCSP-β_2-AR mice with the use of whole body plethysmography to measure enhanced pause (P_{enh}). ED_{200}, dose required to increase P_{enh} to 200% of baseline. The methacholine dose-response curve of the CCSP-β_2-AR mice was shifted significantly to the right compared with that of the NTG mice. Values are means ± SE of measurements from 10 mice/group. $P < 0.01$ for ED_{200} values.

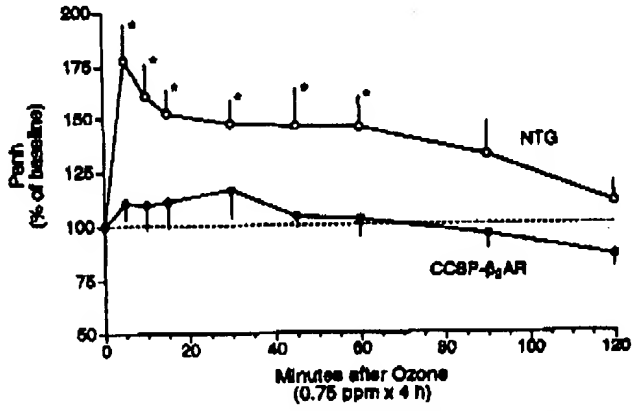

Fig. 8. In vivo assessment of airway responsiveness to ozone. NTG and CCSP-β_2-AR mice were exposed to ozone as described in METHODS, and P_{enh} was measured by whole body plethysmography at the indicated time points after exposure. Data for each time point are means ± SE of measurements from 10 mice. Compared with baseline, P_{enh} increased acutely in NTG mice (5 min) and remained elevated up to 1 h (*$P < 0.05$). In contrast, no increase in P_{enh} occurred in the CCSP-β_2-AR mice.

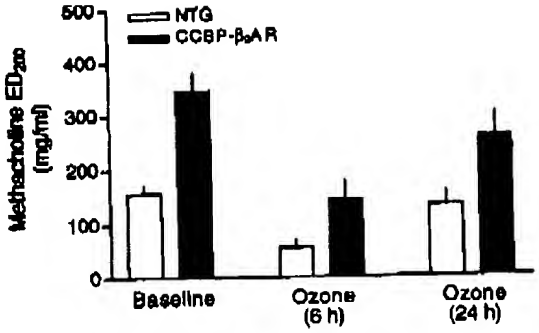

Fig. 9. Airway reactivity after ozone. Methacholine challenge was performed in NTG and CCSP-β_2-AR mice 6 and 24 h after ozone exposure, and an ED_{200} was calculated for each mouse. Data are means ± SE of 10 mice/group. The methacholine ED_{200} measured 6 h after ozone decreased from 157 ± 14 to 56 ± 12 mg/ml ($P < 0.01$) in NTG mice and from 345 ± 34 to 143 ± 35 ($P < 0.05$) in CCSP-β_2-AR mice. The ED_{200} for ozone-treated CCSP-β_2-AR was not significantly different from that of nonexposed NTG mice. At 24 h postexposure, hyperresponsiveness to methacholine had resolved in both groups.

different from that of unexposed NTG mice. However, this may have been due to the differences in baseline P_{enh} rather than differences in hyperreactivity per se. Ozone-induced hyperresponsiveness was transient in both groups of mice (Fig. 9). By 24 h postexposure, the ED_{200} for methacholine increased to 133 ± 26 mg/ml in the NTG mice and to 255 ± 45 mg/ml in the CCSP-β_2-AR mice.

The results of the whole body plethysmography studies showed that CCSP-β_2-AR mice were less responsive to methacholine and ozone than were NTG mice. To address the possibility that these effects were due to the release of bronchodilator substances by the bronchial epithelial cells, we measured the concentration of two candidates, PGE_2 and NO, in BAL fluid. For these measurements, mice were lavaged with 1 ml of PBS that was allowed to dwell for 5 min. In another group of mice, 10^{-6} M isoproterenol was added to the lavage fluid so that the response to β-agonists could be assessed. PGE_2 levels in the BAL fluid from NTG (0.56 ± 0.15 ng/ml) and CCSP-β_2-AR (0.66 ± 0.07 ng/ml) mice were not different (Fig. 10*A*). Addition of 1 μM isoproterenol to the lavage fluid had no effect on PGE_2 levels in BAL fluid from either group even though cAMP content in the BAL fluid was approximately four times greater than that in the untreated samples (data not shown). Likewise, basal levels of nitrite in BAL fluid, as measured by the Griess reaction, in NTG (1.05 ± 0.16 μM) and CCSP-β_2-AR (1.35 ± 0.11 μM) mice were not different (Fig. 10*B*). Exposure to isoproterenol had no effect on nitrite content in the BAL fluid from either CCSP-β_2-AR or NTG mice. Normalization of PGE_2 and NO measurements to either urea or protein had no impact on the results.

DISCUSSION

The β_2-AR is present on many different cell types within the lung, including airway epithelial cells. In vitro studies (14, 16, 51) have demonstrated that the airway epithelium can modulate bronchial tone and that this interaction may be at least partly regulated by the β_2-AR signal transduction pathway. However, the physiological and potential pharmacological significance of epithelial cell β_2-ARs have remained questionable, largely because of the inability to differentiate their effects in complex in vivo models from those of β_2-ARs on other cell types such as airway smooth muscle. In the current study, we have attempted to address this issue by overexpressing the β_2-AR specifically in epithelial cells, but not in smooth muscle cells, in the airways of TG mice. Increasing the expression of β_2-ARs has been shown in both cell (17) and TG (41, 54) models to increase basal signaling in a manner identical to that evoked by agonists. In transfected Chinese hamster fibroblasts, Green et al. (17) observed a direct correlation between receptor density and basal adenylyl cyclase activity. Furthermore, a mutant β_2-AR that exhibited decreased agonist-stimulated adenylyl cyclase activation had proportionately decreased basal levels of activation as well (17). Similarly, Turki et al. (54) and others (41) have shown that TG mice overexpressing the β_2-AR in the heart have increased basal adenylyl cyclase activities relative to their NTG litter-

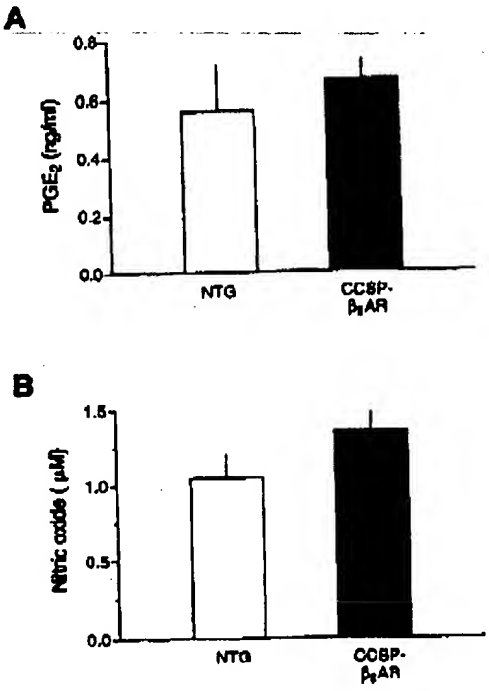

Fig. 10. PGE_2 and nitric oxide (NO) content in bronchoalveolar (BAL) fluid from NTG and CCSP-β_2-AR mice. *A*: PGE_2 content was measured with an enzyme immunoassay. Data are means ± SE of duplicate measurements from 4 different mice/group. PGE_2 levels in BAL fluid from NTG and CCSP-β_2-AR mice were not different. *B*: total nitrite content was measured by the Griess reaction after enzymatic conversion of nitrates (see RESULTS). Data are means ± SE of duplicate measurements from 4 different mice/group. Nitrite content in BAL fluid from NTG and CCSP-β_2-AR mice was not different.

mates. Various modeling techniques have shown that the increased basal signaling that occurs with β_2-AR overexpression is due to spontaneous conversion of receptors to the active (R^*) conformation (46). Thus by selectively targeting expression to a specific cell type, one has the capability to distinguish the effect(s) of β_2-AR activation in cell types that are anatomically in close proximity and otherwise not amenable to selective activation by agonists.

With the use of this strategy, our results revealed that β_2-AR activation in Clara cells had a striking effect on bronchomotor tone as assessed in vivo by whole body plethysmography. In response to the inhaled bronchoconstrictor methacholine, CCSP-β_2-AR mice were significantly less reactive than their NTG littermates. Remarkably, the degree of protection afforded to the CCSP-β_2-AR mice was the same as that achieved by inhalation of the β-agonist albuterol in NTG mice. Although there was a trend toward increased protection in CCSP-β_2-AR mice treated with albuterol, suggesting that epithelial β_2-ARs act in an additive fashion with smooth muscle β_2-ARs to bronchodilate, the difference did not reach significance. These data suggest, then, that epithelial cell β_2-ARs can have a substantial impact on airway smooth muscle responsiveness and are thus indicative of a response not previously quantifiable.

The protective effect of β_2-AR overexpression was not limited to methacholine because the acute response to ozone was also reduced. Unlike methacholine, ozone does not pass beyond the epithelial layer (45) and therefore does not act directly on airway smooth muscle. Instead, the effects of ozone are due to ozonation and oxidation of proteins and lipids in the epithelium and epithelial lining fluid that either act directly as bronchoconstrictors or lead to the production of other bronchospastic substances (reviewed in Ref. 32). Ozone caused an acute increase in P_{enh} of NTG mice that persisted up to 1 h after exposure. In contrast, P_{enh} was unchanged in the CCSP-β_2-AR mice over the same time period. Because P_{enh} parallels measures of airway resistance, the acute response in ozone-exposed NTG mice could conceivably be due to edema from inflammation, mucosal damage, or frank mucus plugging. However, several lines of evidence indicate that bronchospasm was the primary component. First, spontaneous resolution was rapid (<2 h). Second, the response was markedly attenuated by the β-agonist bronchodilator albuterol. Third, mice exposed to these concentrations of ozone showed no evidence of cellular inflammation, edema, or plugging for up to 4 h after exposure (60). Furthermore, it would not be expected that edema and mucus plugging would be readily reversed by a smooth muscle relaxant. Taken together, these findings indicate that smooth muscle contraction is the major contributing factor that accounts for the postozone increase in P_{enh}. The protection afforded to CCSP-β_2-AR mice was therefore effective against two different bronchoconstrictors (i.e., methacholine and ozone). These bronchospastic agents appear to act through different mechanisms because the anticholinergic agent atropine had little effect on the P_{enh} response after ozone.

Epithelial cell β_2-AR overexpression did not, however, prevent the development of ozone-induced airway hyperresponsiveness. The ED_{200} for methacholine measured 6 h after ozone was 36% of basal level in NTG mice and 41% of basal level in CCSP-β_2-AR mice. The relative protective effect of β_2-AR overexpression was maintained, though, because the ED_{200} for the ozone-exposed TG mice was still significantly less than that for the treated NTG mice. In fact, the ED_{200} of ozone-exposed CCSP-β_2-AR mice was not different from that for unexposed NTG mice. CCSP-β_2-AR mice were therefore protected in the sense that their response to methacholine after ozone was submaximal.

As mentioned earlier, airway epithelial cells could regulate airway responsiveness through one or more of several different mechanisms. Overexpression of the β_2-AR in airway epithelial cells could have caused chronic remodeling of the airways. However, histological analysis showed no structural alterations in the airways of the CCSP-β_2-AR mice, and the protection afforded to the TG mice was inhibited by short-term treatment with propranolol. Clara cells also have enzymatic activity (e.g., acetylcholinesterase) that could potentially be upregulated by β_2-AR activation and thus limit the response to an agent such as methacholine. However, the observation that CCSP-β_2-AR mice were also protected against ozone-induced bronchospasm (which was noncholinergic) suggests the presence of a generalized pathway rather than one specific for a given agent.

The bronchial epithelium is the source of a number of substances that may directly affect airway smooth muscle tone. We therefore considered the possibility that activation of epithelial cell β_2-ARs stimulates the release of a relaxant factor. The two candidates we chose to consider were PGE_2 and NO because both are known to relax airway smooth muscle (11, 52) and both are produced by Clara cells (30, 48). To investigate whether either of these substances could account for the inhibition of bronchoconstriction in the CCSP-β_2-AR mice, we measured the content of PGE_2 and NO in BAL fluid from NTG and CCSP-β_2-AR mice. Evaluation of this fluid showed no differences in the levels of PGE_2 or NO, suggesting that neither agent was contributing to the protective effect of β_2-AR overexpression. However, epithelial release of these mediators may be primarily directed toward the serosal surface (25, 34) and therefore underestimated in BAL fluid. Thus we cannot conclusively exclude PGE_2, NO, or other factors as mediators of the epithelial cell β_2-AR-mediated relaxation at this time. It is also possible that overexpression altered the production and release of Clara cell secretory products that in some way modify airway compliance or reactivity. β-Agonists have previously been shown to increase the secretory activity of Clara cells (37). An increase in such a component of the epithelial lining fluid could thus potentially act to limit the effect of methacholine and ozone by stabilization of the airways, making them more resistant to closure.

Baseline lung function and histology, however, were not different in the CCSP-β_2-AR TG mice, suggesting that this scenario is unlikely.

Regardless of the mechanism, our findings clearly show that overexpression of the β_2-AR in epithelial cells modulatee airway responsiveness to contractile agents. Previous ex vivo studies that used airway ring preparations have been inconsistent in demonstrating a modulatory role for the epithelial cell β_2-ARs. This may be due to the fact that the bronchoactive substances have direct access to airway smooth muscle via the exposed serosal surface, thus potentially bypassing protective effects of the epithelium. Furthermore, mechanical removal of the epithelium may introduce artificial confounding variables caused by mast cell degranulation (15). Because our goal was to assess the physiological relevance of this pathway on airway responsiveness in vivo, we assessed bronchoconstriction with whole body plethysmography to measure P_{enh}. P_{enh} is a derived measure of bronchoconstriction that has been shown to strongly correlate with airway resistance as measured by traditional invasive methods (20). Whole body plethysmography also permits assessment of airways distal to the trachea (20). This is particularly relevant with regard to the CCSP-β_2-AR mouse because Clara cells comprise up to 50% of the epithelial cells lining the terminal bronchioles of murine airways (43, 44). Furthermore, at least two studies (51, 56) have demonstrated that the effect of epithelial cell β_2-ARs varied among different airway generations, with their effect being most pronounced in the smaller airways.

In summary, we have found that TG mice overexpressing β_2-ARs in airway epithelial cells exhibit decreased responsiveness to methacholine and ozone. Although the mechanism by which this protection is afforded is unclear, these findings show that the bronchial epithelium is capable of modulating airway tone and that this interaction is at least partly regulated by β_2-ARs present on these cells. Furthermore, the effect of epithelial cell β_2-AR activation is distinct from the effects of β_2-AR activation in other lung cell types. The inhibition of bronchoconstriction in TG mice overexpressing the β_2-AR in the airway epithelium suggests the intriguing possibility that delivery of this gene in vivo could be used in the management of bronchospastic lung disease.

This study was funded by National Heart, Lung, and Blood Institute Grants HL-48967, HL-41496, and HL-54829.

REFERENCES

1. **Aizawa H, Miyazaki N, Shigematsu N, and Tomooka M.** A possible role of airway epithelium in modulating hyperresponsiveness. *Br J Pharmacol* 93: 139–145, 1988.
2. **Barnes PJ.** Beta-adrenergic receptors and their regulation. *Am J Respir Crit Care Med* 152: 838–860, 1995.
3. **Barnes PJ, Cuss FM, and Palmer JB.** The effect of airway epithelium on smooth muscle contractility in bovine trachea. *Br J Pharmacol* 86: 685–691, 1985.
4. **Basbaum CB and Finkbeiner WE.** Mucous-producing cells of the airways. In: *Lung Cell Biology*, edited by D. Massaro. New York: Dekker, 1989, p. 37–79.
5. **Beasley R, Roche WR, Roberts JA, and Holgate ST.** Cellular events in the bronchi in mild asthma and after bronchial provocation. *Am Rev Respir Dis* 139: 806–817, 1989.
6. **Carstairs JR, Nimmo AJ, and Barnes PJ.** Autoradiographic visualization of β-adrenoreceptor subtypes in human lung. *Am Rev Respir Dis* 132: 541–547, 1985.
7. **Corrales RJ, Coleman DL, Jacoby DB, Leikauf GD, Hahn HL, Nadel JA, and Widdicombe JH.** Ion transport across cat and ferret tracheal epithelia. *J Appl Physiol* 61: 1065–1070, 1986.
8. **Davies RJ and Devalia JL.** Asthma. Epithelial cells. *Br Med Bull* 48: 86–96, 1992.
9. **Davis PB, Silski CL, Kercsmar CM, and Infeld M.** β-Adrenergic receptors on human tracheal epithelial cells in primary culture. *Am J Physiol Cell Physiol* 258: C71–C76, 1990.
10. **Devalia JL, Sapsford RJ, Rusznak C, Toumbis MJ, and Davies RJ.** The effects of salmeterol and salbutamol on ciliary beat frequency of cultured human bronchial epithelial cells, in vitro. *Pulm Pharmacol* 5: 257–263, 1992.
11. **Dupuy PM, Shore SA, Drazen JM, Frostell C, Hill WA, and Zapol WM.** Bronchodilator action of inhaled nitric oxide in guinea pigs. *J Clin Invest* 90: 421–428, 1992.
12. **Dusser DJ, Nadel JA, Sekizawa K, Graf PD, and Borson DB.** Neutral endopeptidase and angiotensin converting enzyme inhibitors potentiate kinin-induced contraction of ferret trachea. *J Pharmacol Exp Ther* 244: 531–536, 1988.
13. **Eason MG and Liggett SB.** Human α_2-adrenergic receptor subtype distribution: widespread and subtype-selective expression of α_2C10, α_2C4, and α_2C2 mRNA in multiple tissues. *Mol Pharmacol* 44: 70–75, 1993.
14. **Flavahan NA, Aarhus LL, Rimele TJ, and Vanhoutte PM.** Respiratory epithelium inhibits bronchial smooth muscle tone. *J Appl Physiol* 58: 834–838, 1985.
15. **Franconi GM, Rubinstein I, Levine EH, Ikeda S, and Nadel JA.** Mechanical removal of airway epithelium disrupts mast cells and releases granules. *Am J Physiol Lung Cell Mol Physiol* 259: L372–L377, 1990.
16. **Goldie RG, Papadimitriou JM, Paterson JW, Rigby PJ, Self HM, and Spina D.** Influence of the epithelium on responsiveness of guinea-pig isolated trachea to contractile and relaxant agonists. *Br J Pharmacol* 87: 5–14, 1986.
17. **Green SA, Cole G, Jacinto M, Innis M, and Liggett SB.** A polymorphism of the human β_2-adrenergic receptor within the fourth transmembrane domain alters ligand binding and functional properties of the receptor. *J Biol Chem* 268: 23116–23121, 1993.
18. **Green SA and Liggett SB.** Molecular basis of G-protein-coupled receptor signaling. In: *The Genetics of Asthma*, edited by Liggett SB and Meyers D. New York: Dekker, 1996, p. 67–90.
19. **Gumbiner B.** Structure, biochemistry, and assembly of epithelial tight junctions. *Am J Physiol Cell Physiol* 253: C749–C758, 1987.
20. **Hamelmann E, Schwarze J, Takeda K, Oshiba A, Larsen GL, Irvin CG, and Gelfand EW.** Noninvasive measurement of airway responsiveness in allergic mice using barometric plethysmography. *Am J Respir Crit Care Med* 156: 766–775, 1997.
21. **Henry PJ, Rigby PJ, and Goldie RG.** Distribution of beta 1- and beta 2-adrenoceptors in mouse trachea and lung: a quantitative autoradiographic study. *Br J Pharmacol* 99: 136–144, 1990.
22. **Holtzman MJ.** Arachidonic acid metabolism in airway epithelial cells. *Annu Rev Physiol* 54: 303–329, 1992.
23. **Holtzman MJ, Hansbrough JR, Rosen GD, and Turk J.** Uptake, release and novel species-dependent oxygenation of arachidonic acid in human and animal airway epithelial cells. *Biochim Biophys Acta* 963: 401–413, 1988.
24. **Jacoby DB.** Role of the respiratory epithelium in asthma. *Res Immunol* 148: 48–58, 1997.
25. **Jacoby DB, Ueki IF, Widdicombe JH, Loegering DA, Gleich GJ, and Nadel JA.** Effect of human eosinophil major basic protein on ion transport in dog tracheal epithelium. *Am Rev Respir Dis* 137: 13–16, 1988.
26. **Kobzik L, Bredt DS, Lowenstein CJ, Drazen J, Gaston B, Sugarbaker D, and Stamler JS.** Nitric oxide synthase in

human and rat lung: immunocytochemical and histochemical localization. *Am J Respir Cell Mol Biol* 9: 371–377, 1993.
27. **Laitinen LA, Heino M, Laitinen A, Kava T, and Haahtela T.** Damage of the airway epithelium and bronchial reactivity in patients with asthma. *Am Rev Respir Dis* 131: 599–606, 1985.
28. **Laitinen LA, Laitinen A, and Haahtela T.** Airway mucosal inflammation even in patients with newly diagnosed asthma. *Am Rev Respir Dis* 147: 697–704, 1993.
29. **Laporte J, D'Orleans-Juste P, and Sirois P.** Guinea pig Clara cells secrete endothelin 1 through a phosphoramidon-sensitive pathway. *Am J Respir Cell Mol Biol* 14: 356–362, 1996.
30. **Laporte J, Hallee A, Maghni K, Robidoux C, Borgeat P, and Sirois P.** Metabolism of arachidonic acid by guinea pig Clara cells. *Prostaglandins* 41: 263–281, 1991.
31. **Lee JJ, McGarry MP, Farmer SC, Denzler KL, Larson KA, Carrigan PE, Brenneise IE, Horton MA, Haczku A, Gelfand EW, Leikauf GD, and Lee NA.** Interleukin-5 expression in the lung epithelium of TG mice leads to pulmonary changes pathognomonic of asthma. *J Exp Med* 185: 2143–2156, 1997.
32. **Leikauf GD, Simpson LG, Santrock J, Zhao Q, Abbinante-Nissen J, Zhou S, and Driscoll KE.** Airway epithelial cell responses to ozone injury. *Environ Health Perspect* 103: 91–95, 1995.
33. **Leikauf GD, Ueki IF, and Nadel JA.** Autonomic regulation of viscoelasticity of cat tracheal gland secretions. *J Appl Physiol* 56: 428–430, 1984.
34. **Leikauf GD, Ueki IF, Nadel JA, and Widdicombe JH.** Bradykinin stimulates Cl secretion and prostaglandin E_2 release by canine tracheal epithelium. *Am J Physiol Renal Fluid Electrolyte Physiol* 248: F48–F55, 1985.
35. **Mak JC, Nishikawa M, Shirasaki H, Miyayasu K, and Barnes PJ.** Protective effects of a glucocorticoid on downregulation of pulmonary beta 2-adrenergic receptors in vivo. *J Clin Invest* 96: 99–106, 1995.
36. **Massaro GD and Davis LD.** Demonstration of beta-adrenergic receptors in rat bronchiolar epithelial cells employing 9-aminoacridyl propranolol fluorescent microscopy. *J Histochem Cytochem* 32: 122–123, 1984.
37. **Massaro GD, Fischman CM, Chiang MJ, Amado C, and Massaro D.** Regulation of secretion in Clara cells: studies using the isolated perfused rat lung. *J Clin Invest* 67: 346–351, 1981.
38. **McCann JD and Welsh MJ.** Regulation of Cl- and K+ channels in airway epithelium. *Annu Rev Physiol* 52: 115–135, 1990.
39. **McGraw DW, Donnelly ET, Eason MG, Green SA, and Liggett SB.** Role of βARK in long-term agonist-promoted desensitization of the β_2-adrenergic receptor. *Cell Signal* 10: 197–204, 1998.
40. **McGraw DW, Forbes SL, Kramer LA, and Liggett SB.** Polymorphisms of the 5′ leader cistron of the human β_2-adrenergic receptor regulate receptor expression. *J Clin Invest* 102: 1927–1932, 1998.
41. **Milano CA, Allen LF, Rockman HA, Dolber PC, McMinn TR, Chien KR, Johnson TD, Bond RA, and Lefkowitz RJ.** Enhanced myocardial function in TG mice overexpressing the β_2-adrenergic receptor. *Science* 264: 582–586, 1994.
42. **Munakata M, Huang I, Mitzner W, and Menkes H.** Protective role of epithelium in the guinea pig airway. *J Appl Physiol* 66: 1547–1552, 1989.
43. **Plopper CG.** Comparative morphologic features of bronchiolar epithelial cells. The Clara cell. *Am Rev Respir Dis* 128: S37–S41, 1983.
44. **Plopper CG, Mariassy AT, and Hill LH.** Ultrastructure of the nonciliated bronchiolar epithelial (Clara) cell of mammalian lung: I. A comparison of rabbit, guinea pig, rat, hamster, and mouse. *Exp Lung Res* 1: 139–154, 1980.
45. **Pryor WA, Squadrito GL, and Friedman M.** A new mechanism for the toxicity of ozone. *Toxicol Lett* 82-83: 287–293, 1995.
46. **Samama P, Cotecchia S, Costa T, and Lefkowitz RJ.** A mutation-induced activated state of the β_2-adrenergic receptor. Extending the ternary complex model. *J Biol Chem* 268: 4625–4636, 1993.
47. **Sekizawa K, Nakazawa H, Ohrui T, Yamauchi K, Ohkawara Y, Maeyama K, Watanabe T, Sasaki H, and Takishima T.** Histamine N-methyltransferase modulates histamine- and antigen-induced bronchoconstriction in guinea pigs in vivo. *Am Rev Respir Dis* 147: 92–96, 1993.
48. **Shaul PW, North AJ, Wu LC, Wells LB, Brannon TS, Lau KS, Michel T, Margraf LR, and Star RA.** Endothelial nitric oxide synthase is expressed in cultured human bronciolar epithelium. *J Clin Invest* 94: 2231–2236, 1994.
49. **Spina D, Rigby PJ, Paterson JW, and Goldie RG.** Autoradiogrphic localization of beta-adrenoceptors in asthmatic human lung. *Am Rev Respir Dis* 140: 1410–1415, 1989.
50. **Stripp BR, Sawaya PL, Luse DS, Wikenheiser KA, Wert SE, Huffman JA, Lattier DL, Singh G, Katyal SL, and Whitsett JA.** cis-acting elements that confer lung epithelial cell expression of the CC10 gene. *J Biol Chem* 267: 14703–14712, 1992.
51. **Stuart-Smith K and Vanhoutte PM.** Heterogeneity in the effects of epithelium removal in the canine bronchial tree. *J Appl Physiol* 63: 2510–2515, 1987.
52. **Sweatman WJ and Collier HO.** Effects of prostaglandins on human bronchial muscle. *Nature* 217: 69, 1968.
53. **Talme C, Norel X, Walch L, Labat C, Verriest C, Mazmanian GM, and Brink C.** Cholinesterase activity in pig airways and epithelial cells. *Fundam Clin Pharmacol* 11: 201–205, 1997.
54. **Turki J, Lorenz JN, Green SA, Donnelly ET, Jacinto M, and Liggett SB.** Myocardial signaling defects and impaired cardiac function of a human β_2-adrenergic receptor polymorphism expressed in TG mice. *Proc Natl Acad Sci USA* 93: 10483–10488, 1996.
55. **Verdon CP, Burton BA, and Prior RL.** Sample pretreatment with nitrate reductase and glucose-6-phosphate dehydrogenase quantitatively reduces nitrate while avoiding interference by NADP+ when the Griess reaction is used to assay for nitrite. *Anal Biochem* 224: 502–508, 1995.
56. **Vornanen M.** Adrenergic responses in different sections of rat airways. *Acta Physiol Scand* 114: 587–591, 1982.
57. **Wang J, Niu W, Nikiforov Y, Naito S, Chernausek S, Witte D, LeRoith D, Strauch A, and Fagin JA.** Targeted overexpression of IGF-I evokes distinct patterns of organ remodeling in smooth muscle cell tissue beds of TG mice. *J Clin Invest* 100: 1426–1439, 1997.
58. **Widdicombe JH.** Physiology of airway epithelia. In: *The Airway Epithelium*, edited by Farmer SG and Hay DWP. New York: Dekker, 1991, p. 41–64.
59. **Widdicombe JH, Ueki IF, Emery D, Margolskee D, Yergey J, and Nadel JA.** Release of cyclooxygenase products from primary cultures of tracheal epithelia of dog and human. *Am J Physiol Lung Cell Mol Physiol* 257: L361–L365, 1989.
60. **Zhao Q, Simpson LG, Driscoll KE, and Leikauf GD.** Chemokine regulation of ozone-induced neutrophil and monocyte inflammation. *Am J Physiol Lung Cell Mol Physiol* 274: L39–L46, 1998.

doi:10.1016/S1525-0016(03)00003-0

Gene Therapy for Asthma

Phillip Factor*

Section of Pulmonary and Critical Care Medicine, Evanston Northwestern Healthcare and Northwestern University Feinberg School of Medicine, 2650 Ridge Rd., Evanston, Illinois 60201, USA

**To whom correspondence and reprint requests should be addressed. Fax: (847) 733-5187. E-mail: pfactor@northwestern.edu.*

The accessibility of the airway epithelium and the limitations of current treatments for asthma make the disease a logical target for gene therapy. Study of the immunopathology of chronic airway inflammation has recently identified several pathways that lead to the maladaptive, antigen-induced polarization of CD4+ T cells to a type-2 phenotype. This polarization is thought to lead to IgE production and eosinophil recruitment and activation that is associated with epithelial cell injury and airway hyper-reactivity. Gene transfer to the bronchial epithelium has been used in experimental models to redirect these pathways toward a less injurious, type-1 phenotype. This mini-review highlights recent mechanism-based immunomodulatory and supportive gene transfer approaches to treat animal models of asthma. Although substantial hurdles to airway gene transfer remain, gene transfer offers the possibility of interrupting the pathophysiology of airway inflammation. Doing so can be expected to yield long-lasting protection from bronchospastic challenge and reduced dependence on inhaled and oral medications.

Key Words: gene therapy, asthma, IFN-γ, IL-12, β_2-adrenergic receptor, airway epithelium, Th1, Th2

Asthma is a global health problem that results from a complex interplay between genetic and environmental factors. Inhaled β-adrenergic agonists and steroid treatments are effective, but are costly, and require daily dosing and depend on patient compliance and coordination. Extensive studies of the pathophysiology of chronic airway inflammation and reversible increases in airway resistance have uncovered maladaptive immunologic pathways that might be countered by gene transfer. Such therapies could be long-lived and might overcome the limitations of oral and inhaled medications. Numerous studies of gene transfer to the lung for purposes of modulating the mechanisms responsible for asthma have both improved the understanding of asthma and have raised the possibility of effective human gene therapy for this disease.

The Pathophysiology of Allergic Asthma

Most of the data used to explain the phenotype of asthma have come from genetically engineered mice. These studies have produced a complex mechanistic model of allergic airway inflammation that has been reviewed in depth elsewhere [1]. Briefly, inhaled "aero-antigens" are taken up by airway dendritic cells that migrate to bronchial lymph nodes where they mature into immunostimulatory cells capable of efficiently presenting antigen to T-helper ($CD4^+$) cell precursors. The cytokine balance in the node determines the fate of these precursor cells. If IL-12 predominates, then precursor cells become type 1, T-helper cells (Th1) that produce IFN-γ, IL-2, TNFα, and lymphotoxin—collectively referred to as Th1 cytokines. Conversely, if IL-4 predominates, $CD4^+$ precursor cells become type 2, T-helper cells (Th2) that secrete IL-4, IL-5, IL-9, and Il-13. These Th2 cytokines cause recruitment of eosinophils to the airway. Binding and subsequent antigen-dependent cross-linking of IgE bound to FcεRI receptors on eosinophils results in eosinophil activation and degranulation. Local release of mediators from eosinophils such as Major Basic Protein (MBP) cause injury to the airway in the form of epithelial cell sloughing, increased mucous production, and airway hyper-reactivity (AHR). Long-standing inflammation leads to subepithelial fibrosis and smooth muscle hypertrophy and hyperplasia that exacerbate AHR and, in some cases, irreversible increases in airways resistance. Each of these steps may be amenable to interruption or modulation for therapeutic purposes. An unexplained aspect of this model is the nature of the genetic and/or environmental influences responsible for increased IL-4 levels and abnormal polarization of the immune response toward a Th2 phenotype. Recent explanations drawn from comparisons of the prevalence of asthma in industrialized and developing countries has led to the "hygiene hypothesis" which suggests that reduced exposure to environmental antigens and infections that cause Th1 responses early in life (due to immunization and urban residence) results in reduced ability to generate a Th1 response.

Interferon-γ (IFN-γ) can counter Th2 activity by inhibiting development and expansion of Th2 cells and reducing the production of cytokines, but it does not reverse the lineage of committed Th2 $CD4^+$ cells. IFN-γ may also inhibit production of IgE by B cells. IL-12 enhances IFN-γ production (especially in the presence of Il-18) and is primarily produced by antigen-presenting cells. Although Th1 responses are inflammatory, they do not lead to

eosinophil recruitment. Both IL-12 and IFN-γ have been used to attenuate or prevent airway inflammation in experimental models and limited studies in humans.

In general, two genetic approaches have been used to treat asthma: immunomodulation and supportive, nonimmune mechanisms. Both strategies include imaginative approaches based on newly described mechanisms of epithelial and smooth muscle cell inflammation.

Modulation of Immune Pathways

The idea that a Th1 response is preferable to the Th2-driven recruitment of eosinophils has stimulated interest in strategies to repress the activity of Th2 cells and cytokine production in the airway. Both IFN-γ and IL-12 induce Th1 cell differentiation and function and downregulate cytokine production by Th2 cells, thereby limiting eosinophil recruitment and activation and reducing AHR. Observations in murine models of allergic asthma represent the bulk of gene transfer studies involving modulation of airway immunobiology. These approaches are particularly relevant because reduced levels of IFN-γ have been noted in asthmatics and in mouse models of allergic asthma [2].

IL-12 is a heterodimer, composed of p35 and p40 subunits, that cause IFN-γ production, Th1-cell differentiation, and downregulation of Th2-cell function. IL-12 also promotes Th1 cell differentiation through transcription of IFN-γ mediated by the Signal Transducer and Activator of Transcription (STAT) 4. Lee and colleagues cleverly produced a single chain polypeptide that consisted of both subunits of IL-12 separated by a proteolytically resistant linker of 18 amino acids in length [3]. Liposomal-mediated transfer of a plasmid encoding this IL-12 variant to the airway epithelium of mice with allergic airway inflammation caused by sensitization to dust mite antigen led to reduced IL-5 levels, increased IFN-γ levels, and less eosinophil infiltration into the lung. Their findings included significant reductions in allergen-induced increases in AHR. Hogan *et al.* used a recombinant vaccinia virus to deliver both subunits of murine IL-12 into the lungs of ovalbumin-sensitized mouse lungs before and after aerosol re-challenge with ovalbumin. This approach suppressed Th2 cytokine production and prevented airway inflammation and AHR through an IFN-γ dependent pathway [2]. Also noted in the latter study were reduced levels of antigen-specific IgE and IgG_2. Impressively, reductions in AHR were sustained for up to 4 weeks following gene transfer. Other groups used adenoviral-mediated IL-12 gene transfer to counteract the effects of GM-CSF induced airway inflammation [4]. Downregulation of IL-5 has also been effected through plasmid-mediated transfer of Galectin-3—an IgE-binding protein that selectively inhibits IL-5 transcription—to the airways of ovalbumin sensitized and challenged Brown-Norway rats [5]. Localized delivery of a gene encoding IL-12 might be expected to overcome many of the systemic side effects of IL-12; however, the results of these studies must be interpreted in the context of human studies showing that IL-12 does not reduce airway hyper-reactivity or the late responses to allergen in mild asthmatics [6]. Further, mice with targeted deletions of IL-5 still develop eosinophilia in response to allergen challenge; thus; it is not yet clear if abrogation of Th2 cytokine production will be sufficient to effect clinically significant reductions in airway inflammation [7].

In a different approach, Behera and colleagues [8] transduced the airway epithelium of ovalbumin-sensitized mice with an adenovirus expressing murine IFN-γ and noted significant reduction of AHR and reduced IL-4, IL-5, and eosinophil numbers in BALF fluid. These effects were mediated through a STAT-4 dependent pathway. Similar effects using a liposomal delivery system and plasmids encoding either human or murine IFN-γ genes have been reported by other groups [9,10]. IL-12 stimulated IFN-γ production is enhanced 10 fold in the presence of IL-18. This combination of IL-12 and IL-18 reduces IgE synthesis and induces IFN-γ production by B cells [11]. Walter and colleagues administered a recombinant adenovirus expressing murine IL-18 intranasally to mice and examined its effects on ovalbumin-induced AHR. They noted increased production of IFN-γ and reduced IL-4 levels, consistent with a shift toward a Th1 response. Reduced airway eosinophilia and goblet cell hyperplasia were also noted. Importantly, IL-18 gene transfer obviated AHR in ovalbumin-sensitized and re-challenged mice, essentially reversing the phenotype of ovalbumin-induced allergic asthma. However, IL-18 in the absence of IL-12 accentuates airway inflammation and AHR, rendering the clinical utility of this approach difficult to forecast.

In this issue of *Molecular Therapy*, Zavorotinskaya and colleagues [12] report the effects of adeno-associated virus-mediated gene transfer of a competitive inhibitor of the common subunit of the IL-4 and IL-13 receptors, IL-4Rα. This approach, which is an extension of a clinical trial using an intravenously administered recombinant human IL-4R antagonist [13], attenuated IL-4 and IL-13 mediated inflammation, reduced airway mucous production, and prevented allergen-induced increases in AHR. The multi-faceted effects of this paracrine approach in terminally differentiated airway epithelial cells is an attractive idea, especially in light of the increased expression of the IL-4Rα chain in the airway epithelium and subepithelium of asthmatics [14].

IL-10 is both immunosuppressive (via inhibition of cytokine production by both Th1 and Th2 cells) and anti-inflammatory; IL-10 is thus an attractive target to prevent both Th1 and Th2 responses, rather than simply redirecting $CD4^+$ T-cell polarization from a Th2 to a Th1 phenotype. Adoptive transfer of antigen-specific Th cells retrovirally transduced with murine IL-10 led to decreased airway inflammation and AHR in ovalbumin-sensitized and aerosol-rechallenged BALB/c mice [15]. IL-10

doi:10.1016/S1525-0016(03)00003-0

also counteracts the proinflammatory effects of GM-CSF in an ovalbumin mouse model [16]. While IL-10 prevents inflammation, data from IL-10 knockout mice suggested that it might contribute to AHR in this model of asthma [17], suggesting that IL-10 in the presence of eosinophilic inflammation might act directly on airway smooth muscle cells or via an eosinophil-independent intermediary to increase AHR.

Several groups have reported that nonmethylated bacterial CpG motifs are immunomodulatory. Kline and colleagues have shown that CpG oligodeoxynucleotides induce Th1 responses that prevent and reverse ovalbumin-induced asthma in mice [18–20]. These effects might be mediated through decreased IL-5 production and increased production of the Th1 cytokines IL-10, IL-12, and IFN-γ [21]. Oligodeoxynucleotides or plasmids incorporating CpG motifs could be readily delivered to the airways and might have therapeutic potential.

Other investigators have identified intracellular targets of asthma therapy. For example, STAT-6 transduces IL-4Rα signals to the nucleus and could be targeted to prevent IL-4 mediated effects or enhancement of IFN-γ effects via upregulation of STAT-4. Recently, reduced levels of the Th1 transcription factor, T-bet, have been noted in T cells from humans with asthma. T-bet knockout mice develop an asthma phenotype independent of allergen exposure [22], suggesting that T-bet gene transfer might prove effective in regulating airway inflammation.

Transforming growth factor-β (TGF-β), like IL-10, is an immunosuppressive and anti-inflammatory cytokine. Hansen and colleagues used Th cells transduced with a retroviral vector that results in secretion of a latent TGF-β to show that TGF-β-secreting Th cells, but not antigen-specific Th1 cells, reduce AHR and airway inflammation in the ovalbumin mouse model [23]. These findings highlight the important role for TGF-β in regulating epithelial inflammation.

Many of the studies identified above used recombinant adenoviruses, a situation likely reflecting their ease of construction and their ability to accommodate large expression cassettes, as well as the natural tropism of these human viruses for airway epithelia. These viruses have been used in a variety of experimental systems and, in general, induce significant host responses in the form of capsid- and transgene-related inflammation. Interestingly, two groups have reported small decreases in AHR and Th2 cytokine levels in mice infected with recombinant adenoviruses [8,11]. These changes may be related to a Th1 response induced by viral capsids or perhaps CpG motifs incorporated into the recombinant viral genome.

Each of the studies outlined above represents a method to redirect $CD4^+$ polarization from a primarily Th2 to a Th1 phenotype. These studies are based on the hypothesis that Th1 responses are associated with less eosinophil recruitment and activation than are Th2 responses and were borne from recent data regarding the molecular pathogenesis of allergy and inflammation in experimental animals. It is likely that similar processes occur in the human airway, although whether they contribute to inflammation in humans to the same degree as they do in mice remains to be determined. It is important to highlight that abrogation of a single inflammatory pathway may not affect meaningful reductions of epithelial inflammation. Thus, it is reasonable to speculate that "reprogramming" $CD4^+$ responses with gene transfer may someday be part of a complex, multidimensional attack on allergen and inflammation-induced increases in airways resistance via attenuation of epithelial inflammation and perhaps modulation of airway smooth muscle cell function.

Supportive Approaches

Another avenue for genetic therapy of asthma includes the development of supportive approaches that reduce airway resistance via enhanced bronchodilation or reduced epithelial cell mucous production. Recently, a transgenic mouse with β_2-adrenergic receptor overexpression confined to Clara cells was shown to be highly resistant to ozone-induced changes in airway reactivity, suggesting that upregulation of this catecholamine receptor can accentuate β-agonist-mediated bronchodilation [24]. This same group has published the design of a reengineered β_2-receptor for use as a genetic pharmaceutical [25]. This "new and improved" β-receptor is resistant to desensitization and responds to a novel ligand that could be provided by aerosol to produce bronchodilation. Preliminary data from the author's laboratory indicates that adenoviral-mediated overexpression of a β_2-adrenergic receptor in the bronchial epithelium of normal mice attenuates methacholine-induced bronchospasm [26]. Recently, 21-mer phosphorothioate respirable antisense nucleotides (RASONs) directed against the type 1 adenosine receptor (A1) have been reported [27]. Limited peer-reviewed data describing the *in vivo* efficacy, absorption, distribution, metabolism, and excretion of these oligomers in animal models of allergic asthma suggest that RASONs can effect long-acting inhibition of airway epithelial A1 receptors. It is possible that RASONs may alter the balance of adenosine receptor function toward the A2a receptor, which, like the β_2AR, increases intracellular levels of cAMP and leads to bronchodilation and possibly decreased airway inflammation.

Gob-5 is a member of the Ca^{2+}-dependent chloride channel family that has been localized to the airway epithelium and identified as a key molecule in the induction of murine allergic asthma [28]. Adenoviral-mediated expression of antisense *Gob-5* RNA in the bronchial epithelium has been shown to reverse the asthma phenotype in allergen (ovalbumin) sensitized mice by decreasing AHR and mucous production. This adjunctive approach addresses an important part of the pathophysiology and symptom complex associated with asthma.

Glucocorticoid-resistant asthma, defined as persistent airway inflammation despite high doses of oral steroids, is a common, frustrating clinical problem with no therapeutic solution. Mathieu and colleagues have suggested that overexpression of a glucocorticoid receptor might overcome defects in receptor expression and function in steroid-insensitive asthmatics [29]. This group transduced human lung cancer cells (A549) with an adenovirus expressing a full-length mouse glucocorticoid receptor and observed significant repression of the pro-inflammatory transcriptional regulators, AP-1 and NF-κB, without the addition of glucocorticoids. Although *in vivo* data are not yet available, this approach offers the possibility of sustained, localized glucocorticoid-effects that could overcome the hypertension, hyperglycemia, weight gain, psychosis, and cataracts associated with systemic steroid use. VP22 is a herpes simplex virus protein that affects actin-dependent intracellular trafficking to the nucleus. When VP22 was fused to the amino-terminal end of a truncated glucocorticoid receptor, enhanced repression of NF-κB was observed.

Genomic Promises

Important asthma loci are thought to exist on chromosomes 5q (Th2 cytokines), 6q (TNFα), 11q (high affinity IgE receptor β subunit ([FceRIβ]), 12q (IL-4Rα chain), 14q (T cell receptor a/d complex), and 20p (ADAM33). Each of these gene products represents potential targets for genetic therapy. Further, polymorphisms of the coding and 5′ flanking regions of key asthma-related genes such as the β_2-adrenergic receptor, CTLA4, and CD28 have been identified that may affect disease severity and/or responsiveness to therapy.

The Hurdles Ahead

The airway epithelium is a heterogeneous organ that plays a key role in the immunobiology of asthma [30]. Its accessibility makes it a logical target for genetic anti-asthma therapies. Most currently available asthma medications are short-lived and mediate their effects through membrane-bound receptors. Gene transfer offers the opportunity to effect sustained modulation of the immunologic and non-immunologic processes of asthma.

Nevertheless, numerous hurdles remain before therapeutic gene transfer for asthma can be considered. The first obstacle will be affecting efficient gene transfer to the airway epithelium. The ability of adenovirus and adeno-associated viruses to transduce the airway epithelium is limited. This is the result of the abluminal location of receptors for these viruses [31] and the presence of physical and immunologic host defenses that have evolved to protect the airway from respiratory pathogens. For example, epithelial glycoproteins and mucous serve as filters that limit access to epithelial cells and likely participate in signal transduction pathways that activate epithelial defense mechanisms. Additionally, neutralizing antibodies and antigen specific phagocytes are prevalent in the adult population. Methods that overcome these defenses by eliminating barriers [32] and/or improving access of vector to their respective receptors have been successfully tested in experimental systems [33,34]. An additional significant obstacle to gene transfer for asthma includes inflammation-induced loss of epithelial cells, which can be expected to attenuate the duration of transgene expression. Likewise, increased mucous and edema formation in asthma could further limit transduction efficiency, although data from a model of acute lung injury shows that adenoviruses are capable of transducing edematous, severely injured lungs [35].

Current paradigms of asthma are based primarily on allergen induced airway epithelial inflammation. It is likely that asthma is a phenotype that reflects presently undefined polygenic mechanisms. Hence, the absence of a central pathophysiologic process responsible for increases in airway resistance and inflammation make asthma a yet formidable target for gene therapy. Continued growth in the understanding of asthma and the evolution of better gene transfer vehicles offer optimism that gene therapy may some day allow for long-lasting therapies that forestall the frequent use of inhaled medications.

References

1. Corry, D. B., and Kheradmand, F. (1999). Induction and regulation of the IgE response. *Nature* 402: 818–23.
2. Hogan, S. P., Foster, P. S., Tan, X., and Ramsay, A. J. (1998). Mucosal IL-12 gene delivery inhibits allergic airways disease and restores local antiviral immunity. *Eur. J. Immunol.* 28: 413–423.
3. Lee, Y. L., *et al.* (2001). Construction of single-chain interleukin-12 DNA plasmid to treat airway hyperresponsiveness in an animal model of asthma. *Hum. Gene Ther.* 12: 2065–2079.
4. Stampfli, M. R., *et al.* (1999). Regulation of allergic mucosal sensitization by interleukin-12 gene transfer to the airway. *Am. J. Respir. Cell Mol. Biol.* 21: 317–326.
5. del Pozo, V., *et al.* (2002). Gene therapy with galectin-3 inhibits bronchial obstruction and inflammation in antigen-challenged rats through interleukin-5 gene downregulation. *Am. J. Respir. Crit. Care Med.* 166: 732–737.
6. Bryan, S. A., *et al.* (2000). Effects of recombinant human interleukin-12 on eosinophils, airway hyper-responsiveness, and the late asthmatic response. *Lancet* 356: 2149–2153.
7. Foster, P. S., *et al.* (2001). Elemental signals regulating eosinophil accumulation in the lung. *Immunol. Rev.* 179: 173–181.
8. Behera, A. K., Kumar, M., Lockey, R. F., and Mohapatra, S. S. (2002). Adenovirus-mediated interferon gamma gene therapy for allergic asthma: involvement of interleukin 12 and STAT4 signaling. *Hum. Gene Ther.* 13: 1697–1709.
9. Li, X. M., *et al.* (1996). Mucosal IFN-gamma gene transfer inhibits pulmonary allergic responses in mice. *J. Immunol.* 157: 3216–3219.
10. Dow, S. W., Schwarze, J., Heath, T. D., Potter, T. A., and Gelfand, E. W. (1999). Systemic and local interferon gamma gene delivery to the lungs for treatment of allergen-induced airway hyperresponsiveness in mice. *Hum. Gene Ther.* 10: 1905–1914.
11. Walter, D. M., *et al.* (2001). Il-18 gene transfer by adenovirus prevents the development of and reverses established allergen-induced airway hyperreactivity. *J. Immunol.* 166: 6392–6398.
12. Zavorotinskaya, T., Tomkinson, A., and Murphy, J. E. (2003). Treatment of experimental asthma by long-term gene therapy directed against IL-4 and IL-13. *Journal* vol: pages.
13. Tomkinson, A., *et al.* (2001). A murine receptor antagonist that inhibits IL-4 and IL-13 -induced responses prevents antigen-induced airway eosinophilia and airway hyperresponsiveness. *J. Immunol.* 166: 5792–5800.
14. Kotsimbos, T. C., *et al.* (1998). Expression of the IL-4 receptor alpha-subunit is increased in bronchial biopsy specimens from atopic and nonatopic asthmatic subjects. *J. Allergy Clin. Immunol.* 102: 859–866.
15. Oh, J. W., *et al.* (2002). CD4 T-helper cells engineered to produce IL-10 prevent allergen-induced airway hyperreactivity and inflammation. *J. Allergy Clin. Immunol.* 110: 460–468.
16. Stampfli, M. R., *et al.* (1999). Interleukin-10 gene transfer to the airway regulates allergic mucosal sensitization in mice. *Am. J. Respir. Cell Mol. Biol.* 21: 586–596.

doi:10.1016/S1525-0016(03)00003-0

17. Makela, M. J., *et al.* (2000). IL-10 is necessary for the expression of airway hyperresponsiveness but not pulmonary inflammation after allergic sensitization. *Proc. Natl. Acad. Sci. USA* 97: 6007–6012.
18. Kline, J. N., Kitagaki, K., Businga, T. R., and Jain, V. V. (2002). Treatment of established asthma in a murine model using CpG oligodeoxynucleotides. *Am. J. Physiol. Lung Cell Mol. Physiol.* 283: L170–179.
19. Jain, V. V., *et al.* (2002). CpG-oligodeoxynucleotides inhibit airway remodeling in a murine model of chronic asthma. *J. Allergy Clin. Immunol.* 110: 867–872.
20. Kitagaki, K., Jain, V. V., Businga, T. R., Hussain, I., and Kline, J. N. (2002). Immunomodulatory effects of CpG oligodeoxynucleotides on established th2 responses. *Clin. Diagn. Lab Immunol.* 9: 1260–1269.
21. Broide, D., *et al.* (1998). Immunostimulatory DNA sequences inhibit IL-5, eosinophilic inflammation, and airway hyperresponsiveness in mice. *J. Immunol.* 161: 7054–7062.
22. Finotto, S., *et al.* (2002). Development of spontaneous airway changes consistent with human asthma in mice lacking T-bet. *Science* 295: 336–338.
23. Hansen, G., *et al.* (2000). CD4(+) T helper cells engineered to produce latent TGF-beta1 reverse allergen-induced airway hyperreactivity and inflammation. *J. Clin. Invest.* 105: 61–70.
24. McGraw, D. W., *et al.* (2001). Targeted transgenic expression of beta(2)-adrenergic receptors to type II cells increases alveolar fluid clearance. *Am. J. Physiol. Lung Cell Mol. Physiol.* 281: L895–903.
25. Small, K. M., Brown, K. M., Forbes, S. L., and Liggett, S. B. (2001). Modification of the beta 2-adrenergic receptor to engineer a receptor-effector complex for gene therapy. *J. Biol. Chem.* 276: 31596–31601.
26. Factor, P., Burhop, J., Syed, I., Chen, L., and Dumasius, V. (2002). Adenoviral-mediated overexpression of a β_2-adrenergic receptor attenuates airway reactivity in mice. *Mol. Ther.* 5: S162.
27. Nyce, J. W., and Metzger, W. J. (1997). DNA antisense therapy for asthma in an animal model. *Nature* 385: 721–725.
28. Nakanishi, A., *et al.* (2001). Role of gob-5 in mucus overproduction and airway hyperresponsiveness in asthma. *Proc. Natl. Acad. Sci. USA* 98: 5175–5180.
29. Mathieu, M., *et al.* (1999). The glucocorticoid receptor gene as a candidate for gene therapy in asthma. *Gene Ther.* 6: 245–252.
30. Folkerts, G., and Nijkamp, F. P. (1998). Airway epithelium: more than just a barrier! *Trends Pharmacol. Sci.* 19: 334–341.
31. Walters, R. W., *et al.* (1999). Basolateral localization of fiber receptors limits adenovirus infection from the apical surface of airway epithelia. *J. Biol. Chem.* 274: 10219–10226.
32. Seiler, M. P., *et al.* (2002). Thixotropic solutions enhance viral-mediated gene transfer to airway epithelia. *Am. J. Respir. Cell Mol. Biol.* 27: 133–140.
33. Fasbender, A., *et al.* (1998). Incorporation of adenovirus in calcium phosphate precipitates enhances gene transfer to airway epithelia *in vitro* and *in vivo*. *J. Clin. Invest.* 102: 184–193.
34. Gregory, L. G., *et al.* (2003). Enhancement of adenovirus-mediated gene transfer to the airways by DEAE dextran and sodium caprate in vivo. *Mol. Ther.* 7: pages.
35. Factor, P., Mendez, M., Mutlu, G. M., and Dumasius, V. (2002). Acute hyperoxic lung injury does not impede adenoviral-mediated alveolar gene transfer. *Am. J. Respir. Crit. Care Med.* 165: 521–526.